



Faculty of Information Technologies and Systems
Telecommunications and Traffic Control Systems

Diagnostics of Shortest Path in the Internet

Xiaoming Zhou
M.Sc Thesis

Supervisor: Prof.dr.ir. P.Van Mieghem
ir. Janic Milena
May, 2002

Acknowledgments

This project was carried out from July 2001 to April 2002 at the Telecommunications and Traffic Control Systems group (TVS) of the faculty Information Technology and Systems (ITS) of the Delft University of Technology (TU Delft, the Netherlands).

I would like to thank all the people who provided their help during this project. Here, I would specially like to thank Prof.dr.ir.P.Van.Mieghem for his supervision and suggestions during this project. Next, I would also like to express my regards to ir. Milena Janic for her help during the whole project.

Moreover, I would like to thank H.Uijterwaal (RIPE), C.J.Bovy (M.Sc student of TU Delft) and Harry Mertodimedjo (M.Sc student of TU Delft) for providing their huge RIPE data gathered with the Test Traffic Measurement project.

And my great thanks also go to my family: my grandmother, my father, my mother and my elder sister.

Copyright ©2002 by Xiaoming Zhou

All rights reserved. No part of the material protected by this copyright may be reproduced or utilized in any form or by any means, electronic or mechanical, including photocopying, recording or by any information storage and retrieval system, without the permission from the author and Delft University of Technology.

Abstract

With the Internet growing larger every year and continuously changing overtime, the measurement of large-scale dynamic behaviours of the Internet routing become much harder. While routing protocols have been a subject of a lot of study in the last years, considerably less work has been done on investigating properties of Internet path, say, understanding how current routing algorithms affect the behaviour of Internet path. However, this knowledge is very important to understand the properties of Internet path.

Our work is a measurement-based analysis. The figure 1 shows the idea of this study.

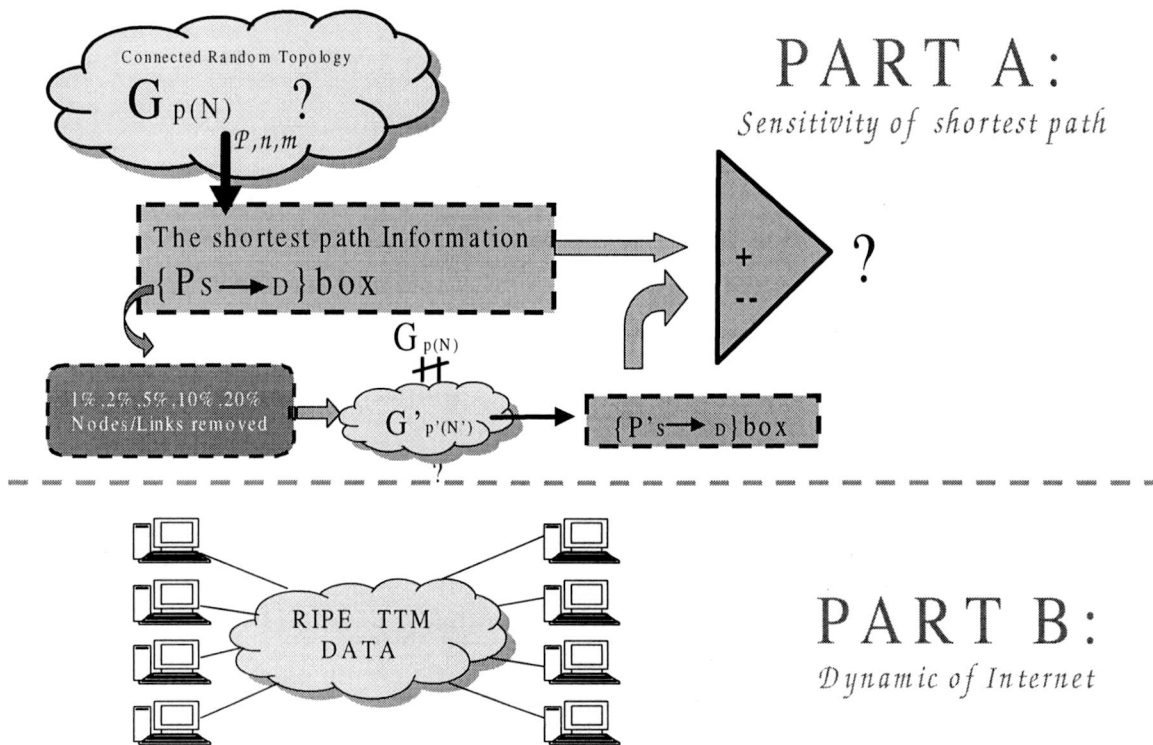


Figure 1. The schematic representation of the study

The first part of our study investigates the sensitivity of shortest path in the random topology (denoted by r.g. or $G_p(N)$, consisted all graphs which N nodes and links are chosen independently with connectivity density p), and the data is from the generated random

topologies. We are triggered to answer this question, “How does the shortest path change if the topology is changed”. In this study, a total of one million connected r.g.’s have been constructed for each simulation. For the comparison, we also constructed two different sub-graphs: $G_p'(N)$, which is obtained by randomly removing some links from the $G_p(N)$, and $G_p(N')$, which is obtained by randomly removing some nodes from the $G_p(N)$. Given a set of shortest paths in the classes $G_p(N)$, the special interest in this part lies in studying how those paths change if the topology is changed from $G_p(N)$ to $G_p'(N)$ or $G_p(N')$. The study found that the number of different paths between the different topologies is sensitive to some parameters of the topology; such as the total nodes number of nodes N in the topology and the number of the removed links/nodes. If the topology changes, there are 2 possibilities for the shortest path change. If there is a new different shortest path existed in the source-destination pairs compared with the original one, we called this new path a different path. In those different paths, we analysed how does each link changes. The study found that the figure of the probability density function of the number of changed links in the different random graphs shows an approximate Gaussian or triangle like shape.

The second part of our study is how current routing algorithms affect the behaviour of Internet paths and the data is returned by real networks. In this part, we used all the data returned from real Internet. We are triggered to conduct the measurement-based analysis, aiming at giving answers to these two questions:

1. Which types of errors do we observe in the current Internet routing?
2. Whether paths that packets following are shortest with respect to a link weight structure?

To answer these questions, we analyse the traceroutes returned by the RIPE Traffic Test Measurement [3]. For the 40 test boxes (both can be sources and destinations), 1,329,019 different routes have been obtained with in total 24,181,803 routes (the sum of the traceroute records for all source-destination pairs). After removing some test boxes whose paths often met error, 31 out of 40 test boxes are chosen in this study. The analysis of the different number of paths between a same source-destination pair has shown that (a) there are many paths and none of them dominates all the others and (b) most of the paths are asymmetric. The analysis also shows that when all link weights are equal to 1, 22% of the traceroutes correspond to shortest paths.

CONTENTS

ACKNOWLEDGMENTS	2
ABSTRACT	3

PART A: SENSITIVITY OF SHORTEST PATHS IN THE RANDOM TOPOLOGY

9

CHAPTER 1. INTRODUCTION	10
-------------------------------	----

CHAPTER 2. SIMULATION IN THE RANDOM GRAPH GP(N).....	11
--	----

CHAPTER 3. SIMULATION RESULTS	14
-------------------------------------	----

3.1 The probability density function of the number of changed paths in the shortest paths information matrix	14
--	----

3.2 The probability of the disconnected paths and the different paths	17
---	----

3.2.1 The probability density function of the number of links changed in the shortest paths	19
---	----

3.2.1.1 The probability density function of the number of changed links of the original shortest paths	20
--	----

3.2.1.2 The pdf of the number of links changed in new shortest paths of sub-graph---	22
--	----

3.3 The probability density function of a node ID being visited by the paths	24
--	----

3.4 Measurements of the Hopcount	27
--	----

3.4.1 The Mean and variance of the Hopcount	27
---	----

3.4.2 The probability density function of the hopcount H_n in the different paths	28
---	----

CHAPTER 4. CONCLUSION OF PART A	31
---------------------------------------	----

PART B: DYNAMIC OF THE INTERNET

32

CHAPTER 5. INTRODUCTION	33
-------------------------------	----

CHAPTER 6. METHODOLOGY	35
------------------------------	----

6.1 Introduction of RIPE & TTM Project	35
--	----

6.2 Participating sites	35
-------------------------------	----

6.3 The measurement configuration	38
---	----

6.4 Are the observations representative of Internet traffic?	40
--	----

CHAPTER 7. ROUTING PATHOLOGIES	41
--------------------------------------	----

7.1 Unresponsive routers	41
--------------------------------	----

7.2	Routing Loops -----	42
7.2.1	Persistent routing loops -----	42
7.2.2	Temporary routing loops-----	43
7.3	Infrastructure failure-----	44
7.4	Circuitous routing-----	45
7.5	Summary -----	46
 CHAPTER 8. GRAPH REPRESENTATION OF A PART OF INTERNET -----		47
8.1	Graph representation of a part of Internet -----	47
8.2	Collecting routes -----	48
8.3	Building graph from routes -----	51
8.4	Constructing the graph G_{10} based on the 10 most frequently occurring paths -----	55
 CHAPTER 9. THE LINK WEIGHT STRUCTURE -----		60
9.1	Simulation results -----	60
 CHAPTER 10. CORRELATION -----		67
10.1	Theory -----	67
10.2	Derivation of mathematical expression -----	68
10.3	RIPE NCC data-----	68
 CHAPTER 11. CONCLUSION AND RECOMMENDATION -----		71
 REFERENCES: -----		73
 APPENDIX A PATHOLOGIES IN THE INTERNET -----		75
A.1	Introduction -----	75
A.2	Sample nodes -----	76
A.3	The errors in the first 10 most frequently occurring paths -----	77
 APPENDIX B THE HIERARCHY OF RIPE TRACEROUTE -----		84
B.1	Introduction -----	84
B.2	Simulation results of the hierarchy of RIPE traceroute-----	84
 APPENDIX C THE OUTPUT DEGREE OF HIERARCHY LEVEL FROM RIPE TTM -----		88
C.1	Introduction -----	88
C.2	Simulation results -----	88

Part A: Sensitivity of Shortest paths in The Random Topology

Chapter 1. Introduction

Before going further the part A, it's better to show the motivation of this part. In order to check the diagnostic and error-correcting programs written at KPN, a random topology can be generated to simulate the Internet. Of course, Internet is not randomness, however, as illustrated in [1], Internet is chaotic and unstructured. Using randomness is a good way to simulate the Internet. As requirements, a set of shortest paths between source-destination pairs can be computed. These paths will be perturbed slightly, it is, errors will be included in this set of shortest paths. Using this way we simulate the topology changes in the measurement.

In the random graphs, the nodes represent the routers in the Internet, while the links represent the adjacencies between the routers. The answer of "How does the shortest path change if a number of nodes or links in a graph are removed?" is obtained from the random topology with Uniform link distribution. In the simulation, two modelling assumptions are made. (1) Packets are delivered along the shortest path to its destination in the graph with the Dijkstra's algorithm, (2) m nodes are chosen out of total number of the graph N as the source-destination pairs. Given a number of shortest paths in the classes $G_p(N)$, the special interest in this part lies in studying how those paths change if the topology is changed from $G_p(N)$ to $G_p'(N)$ or $G_p(N')$. The study found that the number of different paths between the different topologies is sensitive to some parameters of the topology; such as the total nodes number N in the topology and the number of the removed links/nodes. If the shortest path different in the sub-graphs, we analysed how the links change in that path. The study found that the figure of the probability density function of the number of changed links in the different random graphs shows an approximate Gaussian or triangle like shape.

First, we present the simulation methodology in the chapter 2. The results of the probability of the number of changed paths seen by the shortest paths information matrix (it will be clearer in the chapter 3), the probability of the number of links changed in the shortest path, The probability of a node ID being visited by the shortest path information matrix and the probability of the hopcount are discussed in chapter 3. Finally, a brief conclusion is given.

Chapter 2. Simulation in the random graph $G_p(N)$

There are a large amount of properties of random graphs, and the two most frequently occurring models for the random graphs are $G(N,E)$ and $G_p(N)$. The class $G(N,E)$ constitutes all the set of graphs with N nodes and E edges. As illustrated as first figure in figure 2, the class of $G_p(N)$ consists of all graphs with N nodes in which the edges are chosen independently and with probability p .

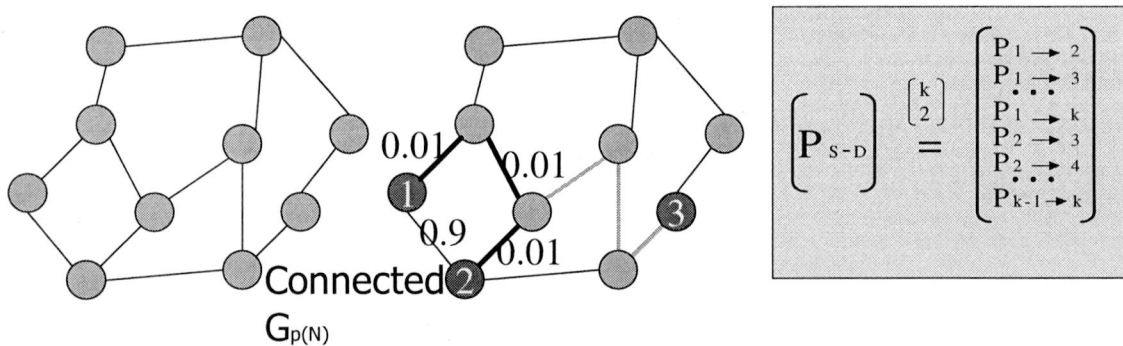


Figure 2. The way that Paths are perturbed

To better understand the problem, here is an example illustrated in the figure 2, first we used a connected random graph to simulate the Internet. A connected random graph is a graph that the IP packets in a node could be transferred to any other node in the graph. In the connected random graph, we randomly chose k nodes out of total N nodes of the random graph to be sampling nodes, as illustrated in red in the figures. The shortest paths are computed between any two sampling/red nodes by using Dijkstra's algorithm. In this way, we got a set of all the shortest paths among those k sampling/red nodes, with totally $\frac{k * (k - 1)}{2}$. We called this set a shortest path information box. As illustrated in the right of figure 2, the shortest path is that path which has the minimal sum of the links weight, so it is not necessary the shortest hop path.

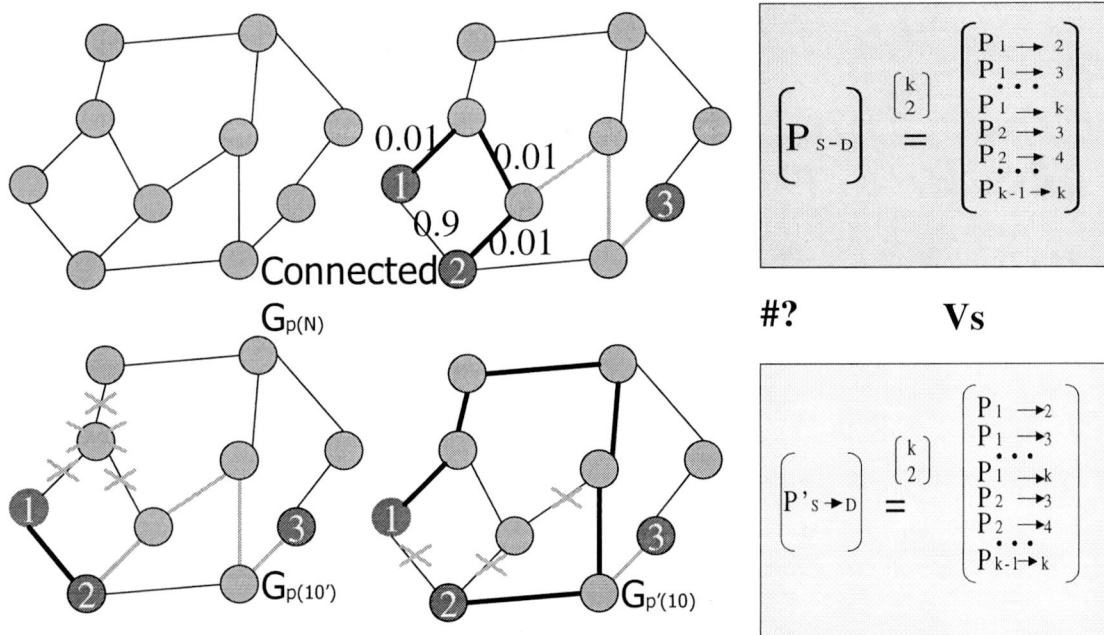


Figure 3. Simulate the topology changes

There are 2 ways to simulate the topology changes in the measurement. The first way is randomly removing some nodes from the random graph (excluding the sampling/red nodes). Another way is randomly removing some links from the random topology. In this way, we got two sub-graphs $G_p'(N)$ or $G_p(N')$. To any sub-graph, the same set of all the shortest paths are computed among those same k sampling nodes by using Dijkstra's algorithm and we also got another shortest paths information box.

After comparing each shortest path to the corresponding path in these two shortest paths information boxes, the answer of how many shortest paths have been different could be found. The value is stored in a histogram. After that, we regenerated a new connected random graph, and simulate the topology changes, etc.

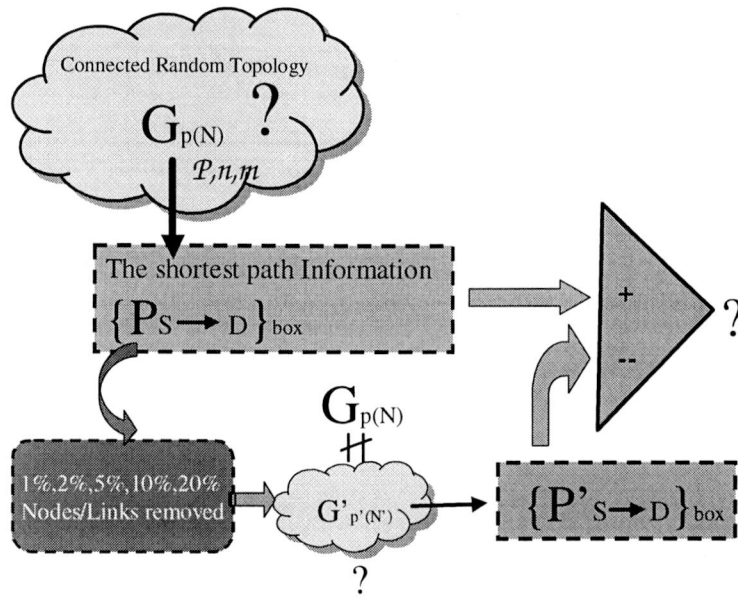


Figure 4. Set-up for the verification the sensitivity of shortest path

As illustrated in Figure 4, we start presenting results obtained for the class $G_{p(N)}$ with uniform link distribution. As illustrated in [16], the interconnection pattern of the $G_{p(N)}$ can be represented by a $N \times N$ connectivity matrix T consisting of element T_{ij} that are either random value X ($0 < X < 1$) or zero depending on whether there is a link between node i and j or not, but for any j , $T_{jj} = 0$. Using Prim's minimum spanning tree algorithm, every r.g. is first tested to assure that the r.g. is connected. Disconnected r.g.s are removed and totally one million connected r.g.s have been constructed for each simulation. For the comparison, we also constructed two different sub-graphs: $G_{p'(N')}$, which is obtained by randomly removing some links from the $G_{p(N)}$, and $G_{p(N')}$, which is obtained by randomly removing some nodes from the $G_{p(N)}$, excluding those source-destination pairs. In each $G_{p(N)}$, $G_{p'(N')}$ or $G_{p(N')}$, m out of total N nodes have been randomly chosen as source-destination pairs. The shortest paths among these k nodes are computed with Dijkstra's algorithm. In the simulations, we simulated the topology changes in the measurement by removing 1%, 2%, 5%, 10% and 20% links or nodes from each connected random graph, separately. Each hop of the shortest path has been stored in a histogram, from which a comparison of the corresponding shortest path of different graphs ($G_{p(N)}$ and $G_{p(N')}$) is done. Then the probability density function (pdf) of the number of different paths is deduced. Moreover, in the shortest paths, how the links change is also studied.

Chapter 3. Simulation results

The main goal of this simulation is to verify in which way the shortest paths change as the graph $G_p(N)$ is changed? Totally, one million connected r.g.s $G_p(N)$ have been constructed for each simulation. To each $G_p(N)$, two different sub-graphs were made: $G_p'(N)$ and $G_p(N')$.

Given a number of shortest paths in the classes $G_p(N)$, the special interest in this simulation lies in studying how those paths change if the topology is changed from $G_p(N)$ to $G_p'(N)$ or $G_p(N')$. As the change of the topology, the probability density function of the different paths seen by the shortest paths information box is analysed in chapter 3.1, the results indicate that the number of the different shortest paths seen by the shortest paths information box is sensitive to the total nodes number N of the topology and the number of the number of the removed links/nodes. The probability density function of the number of changed links of the shortest path is discussed in the chapter 3.2. The results indicate that the figure of the probability density function of the number of changed links shows an approximate Gaussian or triangle like shape. The probability density function of a node ID being visited by the shortest path information matrix is discussed in the chapter 3.3, the results indicate that since the topology is uniform link distributed, each node has the same probability appeared in the paths. In chapter 3.4, we show that the probability density function of the hopcount shows an approximate Gaussian or triangle like shape.

3.1 The probability density function of the number of changed paths in the shortest paths information matrix

For this study, we introduce some notation: in each simulation in the graph $G_p(N)$, we randomly chose the m nodes out of the total N nodes as the sampling source-destination pairs in the $G_p(N)$. This part studies how those paths change if the topology is changed from $G_p(N)$ to $G_p'(N)$ or $G_p(N')$. In the original graph $G_p(N)$, we use so-called the shortest paths information box (As illustrated in Figure3) to denote the set of all shortest paths

between node i and j , the path is further characterized by a vector $w(i \rightarrow j)$, where i is from 1 to $m-1$, while for each j , j is from $i+1$ to m . Totally, $[M]$ has $\frac{m(m-1)}{2}$ paths.

In the sub-graphs $G_p'(N)$ and $G_p(N')$, we respectively use $[M']$ and $[M'']$. Compared each corresponding shortest path in $[M']$ or $[M'']$ with that in $[M]$, the number of the different paths (represented by k) has been computed. The mean $E[k]$ and the variance $\text{var}[k]$ are shown in the table 1 for a same value of $p=0.08$, $m=10$, as a function of N and the removed percentage r .

Topologies after links removed				Topologies after nodes removed			
N=50	E[k]	Var[k]	Var[k]/E[k]	N=50	E[k]	Var[k]	Var[k]/E[k]
r=1%	0.961390	5.222781	5.432531	r=1%	2.601639	14.796216	5.687287
r=2%	2.627610	11.003718	4.187740	r=2%	2.614800	14.836997	5.67238
r=5%	7.311220	26.209927	3.584891	r=5%	7.393600	35.128279	4.751174
r=10%	14.019530	45.708265	3.260328	r=10%	11.684030	52.380919	4.483121
r=20%	24.527620	50.323956	2.051726	r=20%	20.267680	69.566268	3.432375
N=100	E[k]	Var[k]	Var[k]/E[k]	N=100	E[k]	Var[k]	Var[k]/E[k]
r=1%	1.638470	6.581785	4.017031	r=1%	1.483050	7.603784	5.127126
r=2%	3.42960	12.266187	3.531912	r=2%	2.903630	13.026849	4.486401
r=5%	8.47126	28.842414	3.404737	r=5%	6.905570	28.407545	4.113715
r=10%	15.59564	45.011576	2.886164	r=10%	12.735250	47.934186	3.763898
r=20%	26.22041	42.904334	1.636333	r=20%	21.913340	56.273903	2.568020

Table 1. Mean and Variance of the number of paths changed in the shortest paths information matrix

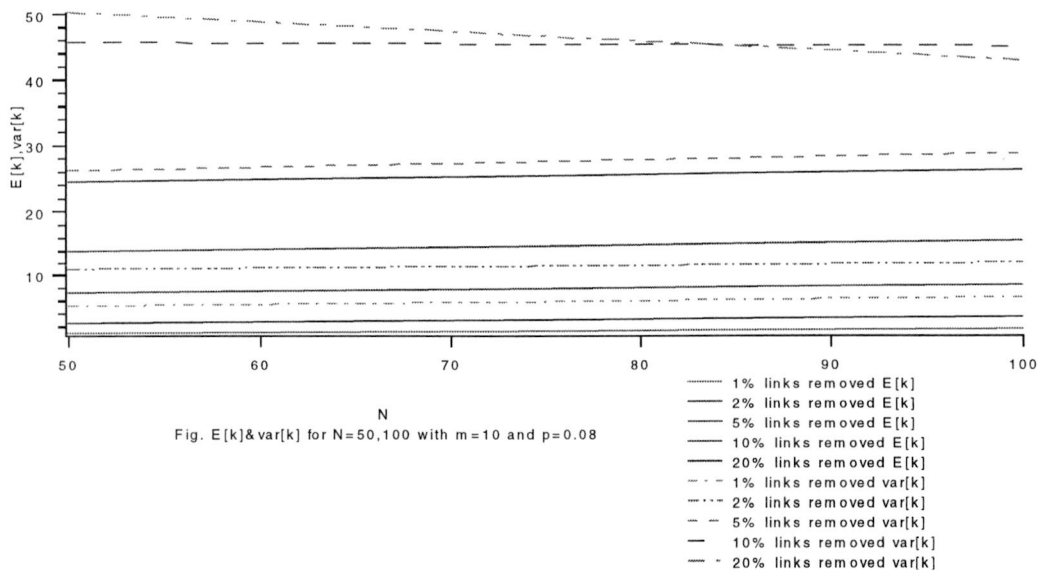


Fig. E[k]&var[k] for N=50,100 with m=10 and p=0.08

Figure 5. Mean and Variance of the number of paths changed in the shortest paths information matrix

Table 1 and Figure 5 show that with the removed percentage of links/nodes increasing, the mean values of the number of changed paths in the shortest paths information matrix increase. However, the value of Alfa ($\text{Alfa} = E[k]/\text{Var}[k]$) increasing. Table 1 also shows that larger N, smaller probability of the changed paths in the shortest path information matrixes. We also note that the values of the variance seem larger than expected.

The Figures 6-9 show the probability density function of the number of paths changed in the shortest paths information matrix.

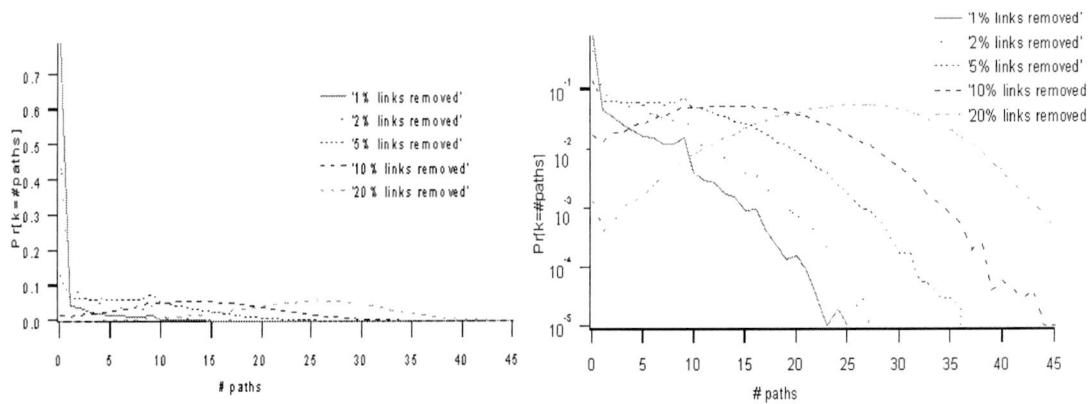


Figure 6. $\text{Pr}[k=\#\text{paths}]$ for $N=50, m=10$ and $p=0.08$

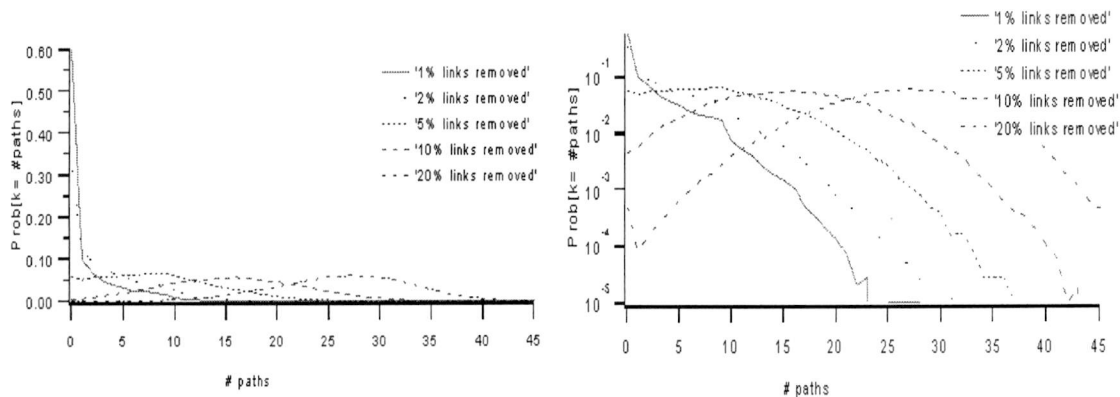


Figure 7. $\text{Pr}[k=\#\text{paths}]$ for $N=100, m=10$ and $p=0.08$

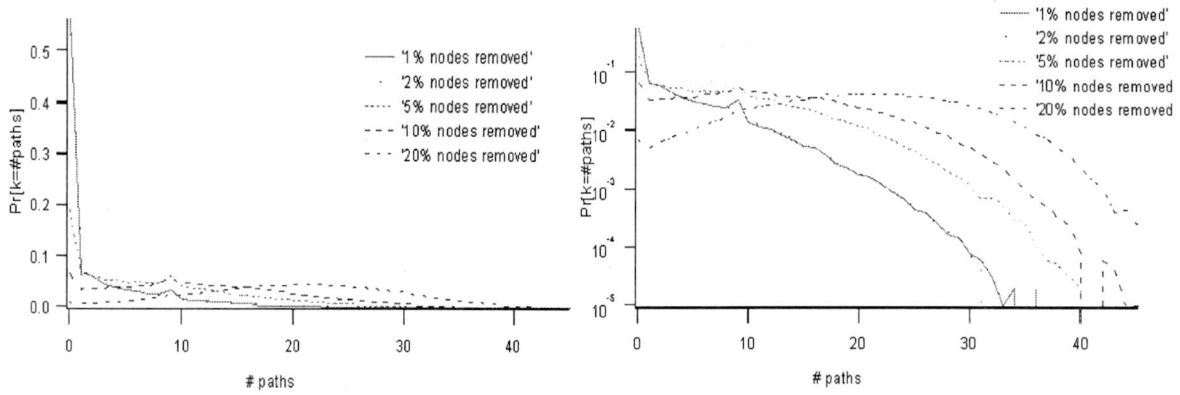


Figure 8. $\Pr[k=\#paths]$ for $N=50, m=10$ and $p=0.08$

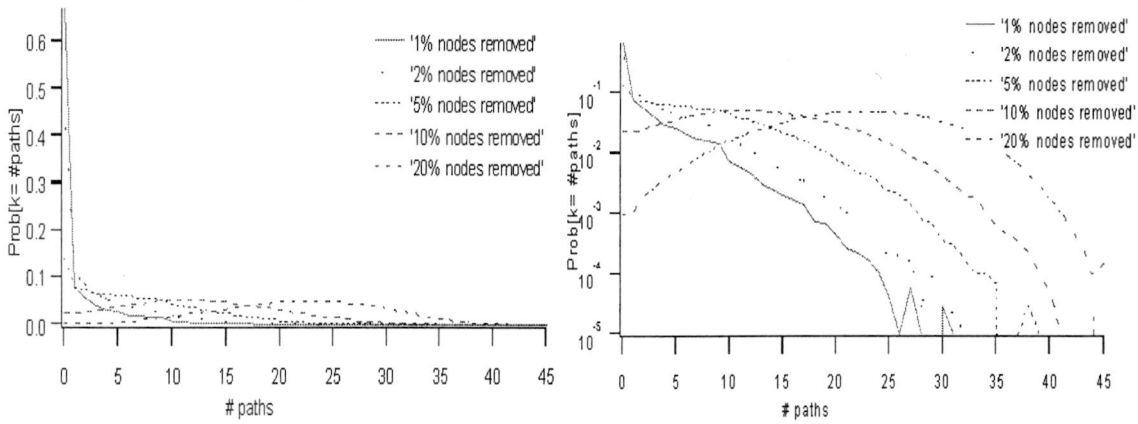


Figure 9. $\Pr[k=\#paths]$ for $N=100, m=10$ and $p=0.08$

There is no obvious conclusion could be made in these figures, such as why there are some peaks in the tails of some figures. However, in the special case where x axis is equal to 0, it means that there is no path change in the shortest path information box. The Figures above indicate that higher removed percentage; the less possibility of the there is no path change in the information box.

3.2 The probability of the disconnected paths and the different paths

In this part we consider the probability of the changed paths in the sub-graphs $[M']$ and the $[M'']$. If the topology changes in the measurement, to a shortest path, there are 2 possible ways be different.

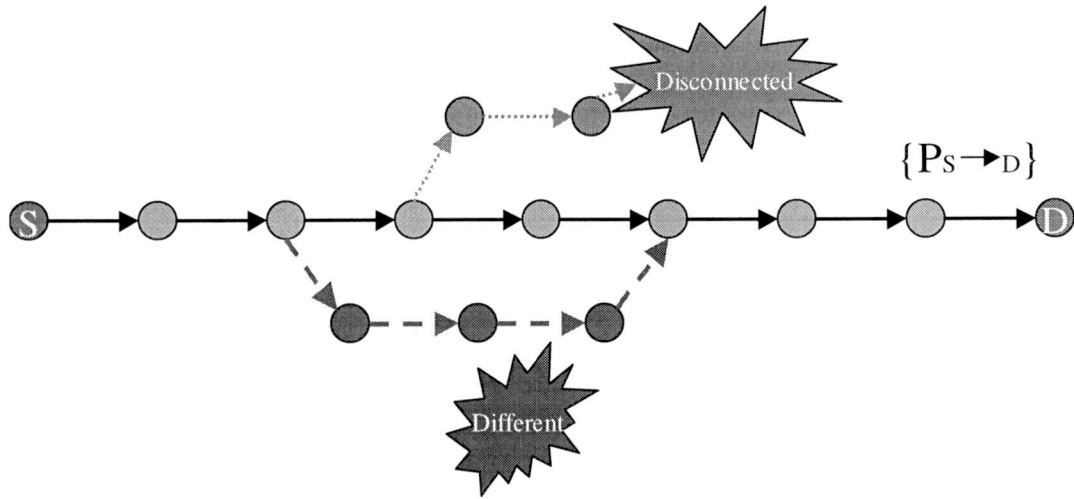


Figure 10. The disconnected path and the different path

As illustrated in Figure 10, in the $[M']$ and the $[M'']$, the path is called a disconnected path if there is no path connected between the source and the destination any more. $\text{Pr}[\text{dis}]$ represents the probability of the disconnected paths.

The path is called a different path if it is a different shortest path, compared with the corresponding one returned by the $[M]$. We used $\text{Pr}[\text{dif}]$ to represent the probability of the different paths.

Table 2 shows the results of some different cases, for a same value of $p=0.08, m=10$, as a function of N and the removed percentage r .

Topologies after nodes removed			Topologies after links removed		
N=50	Pr[dis]	Pr[dif]	N=50	Pr[dis]	Pr[dif]
r=1%	0.000713	0.020652	r=1%	0.003387	0.054427
r=2%	0.002394	0.055998	r=2%	0.003309	0.054798
r=5%	0.007673	0.154798	r=5%	0.010741	0.153562
r=10%	0.018586	0.292960	r=10%	0.019699	0.239968
r=20%	0.049315	0.496693	r=20%	0.051868	0.398790
N=100	Pr[dis]	Pr[dif]	N=100	Pr[dis]	Pr[dif]
r=1%	0.000036	0.036374	r=1%	0.000038	0.032919
r=2%	0.000074	0.077103	r=2%	0.000118	0.064407
r=5%	0.000266	0.187984	r=5%	0.000274	0.153183
r=10%	0.000682	0.345910	r=10%	0.000676	0.282330
r=20%	0.002279	0.580916	r=20%	0.002338	0.484730

Table 2. The percentages of disconnected paths and different paths

At the disconnectivity threshold, $P_c \sim \frac{\ln N}{N}$ for $N \rightarrow \infty$, the graph is with high probability disconnected. It can be shown in the table 2, though N is very small. The graph $G1$ with $N=50$ has $p_{c1} \approx 0.078$; and the graph $G2$ with $N=100$ has $p_{c2} \approx 0.064$. Given the same removed percentage $r=10\%$, $p_{c2} < (p^* (1-r)=0.07) < p_{c1}$. Table 2 does show the value of $\text{Pr}[\text{dis}]$ in the $G1$ is much larger than in the $G2$.

The table 2 also shows that more links/nodes removed, larger probability of the changed paths.

Removed the unchanged shortest paths and the disconnected paths from the record, we just investigated some characters of those different paths in the next parts. We analysed how do the links change in the different paths.

3.2.1 The probability density function of the number of links changed in the shortest paths

The sub-aim of this report is to show in which way the links changed in the corresponding different shortest paths. For this purpose, we removed all disconnected paths. Then we investigated the pdf of the number of different links among the $[M]$, the $[M']$ and the $[M'']$. The path between node i and j is characterized by a vector $w(i \rightarrow j)$, where $w(i \rightarrow j)$ characterizes $w(i \rightarrow j): (i \rightarrow n_1), (n_1 \rightarrow n_2), (n_2 \rightarrow n_3), (n_3 \rightarrow n_4) \dots (n_z \rightarrow j)$. In the $[M']$ and $[M'']$, we obtained the shortest path vector $w'(i \rightarrow j): (i \rightarrow n_1), (n_1 \rightarrow n_2), (n_2 \rightarrow n_3') \dots (n_z' \rightarrow B)$. As illustrated in Figure 10, compared $w(i \rightarrow i)$ and $w'(i \rightarrow j)$, we obtained one value on how many different links (the different links in the original path is represented by L_o) in $w(i \rightarrow i)$ compared with $w'(i \rightarrow i)$, and a value on how many different links (the different links in the $[M']$ or $[M'']$ is represented by L_n) in $w'(i \rightarrow i)$ compared with $w(i \rightarrow i)$. We analyse the pdf of the number of links changed of original shortest paths in chapter 4.3.1 and that of new shortest paths in chapter 4.3.2.

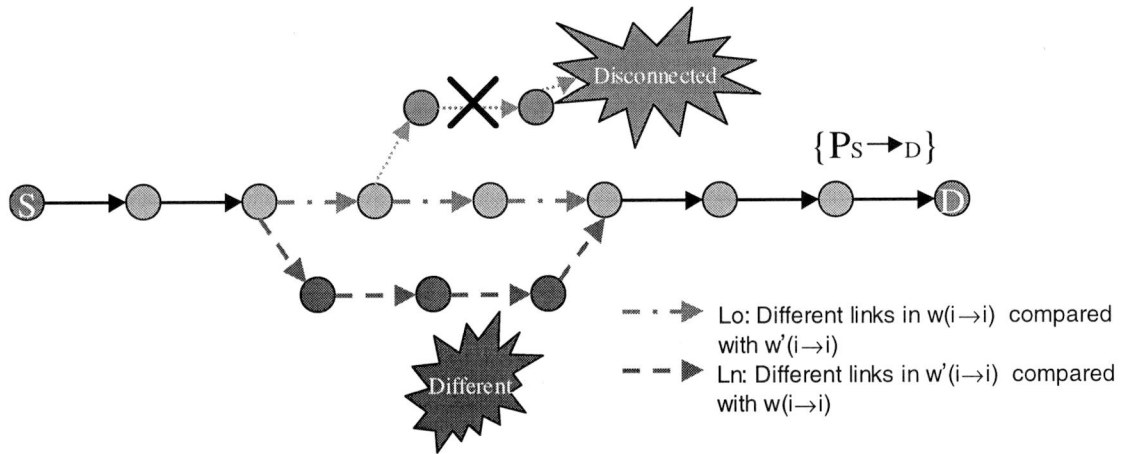


Figure 11. The original links L_o and the new links L_n of paths

Illustrated as figure 11, to a different shortest path, we call those different links in the path compared to the original one new links, and use L_n to represent the number of new links. On the other hand, we use old links L_o to represent the number of links in the original path compared to the different path. To better understand the problem, figure 12 shows an example.

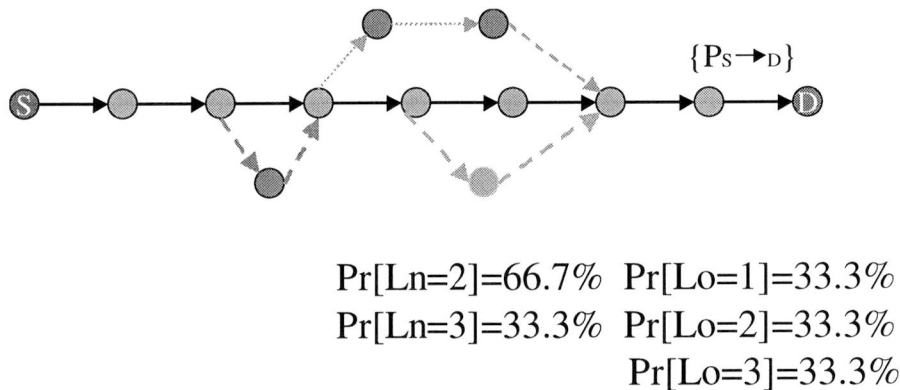


Figure 12. An example of the probability of the L_n and L_o

If the histogram has three different paths in its record, the histogram would calculate that there are 2 different paths having 2 different new links L_n , while 1 different path having 3 different new links. So it would give these output: $\Pr[L_n=2]=66.7\%$ and $\Pr[L_n=3]=33.3\%$. In the same way, the histogram would also output the probability of the old links L_o in the records.

3.2.1.1 The probability density function of the number of changed links of the original shortest paths

Firstly, we investigated the mean and variance of the number of original links L_o in $[M]$ after the topology is changed.

Given the different paths of each $[M]$, the value of mean $E[Lo]$ and the value of variance $var[Lo]$ are shown in the Table 3, for a same value of $p=0.08, m=10$, as a function of N and removed percentage r .

Topologies after links removed				Topologies after nodes removed			
N=50	E[Lo]	Var[Lo]	Var[Lo]/E[Lo]	N=50	E[Lo]	Var[Lo]	Var[Lo]/E[Lo]
r=1%	3.231729	2.224502	0.688332	r=1%	3.654474	1.877619	0.513786
r=2%	3.246482	2.249766	0.692986	r=2%	3.664325	1.892789	0.516545
r=5%	3.224700	2.223522	0.689528	r=5%	3.636006	1.871643	0.514752
r=10%	3.172533	2.213772	0.697793	r=10%	3.609377	1.853359	0.513481
r=20%	3.083533	2.181802	0.790649	r=20%	3.548064	1.8261610	0.514692
N=100	E[Lo]	Var[Lo]	Var[Lo]/E[Lo]	N=100	E[Lo]	Var[Lo]	Var[Lo]/E[Lo]
r=1%	3.806977	2.946805	0.774054	r=1%	4.179169	2.567754	0.614417
r=2%	3.805368	2.935874	0.771509	r=2%	4.157753	2.570507	0.618244
r=5%	3.767782	2.885520	0.760182	r=5%	4.140938	2.547334	0.615159
r=10%	3.728397	2.903207	0.778674	r=10%	4.112021	2.527102	0.614564
r=20%	3.664943	2.902171	0.791873	r=20%	4.063634	2.526724	0.621789

Table 3. Mean and Variance of the number of 'original' links changed after the topology changed

In Table 3, it seems that the number of the different original links (Lo) is rather stable and independent with the p . The figures 13-16 also show this result.

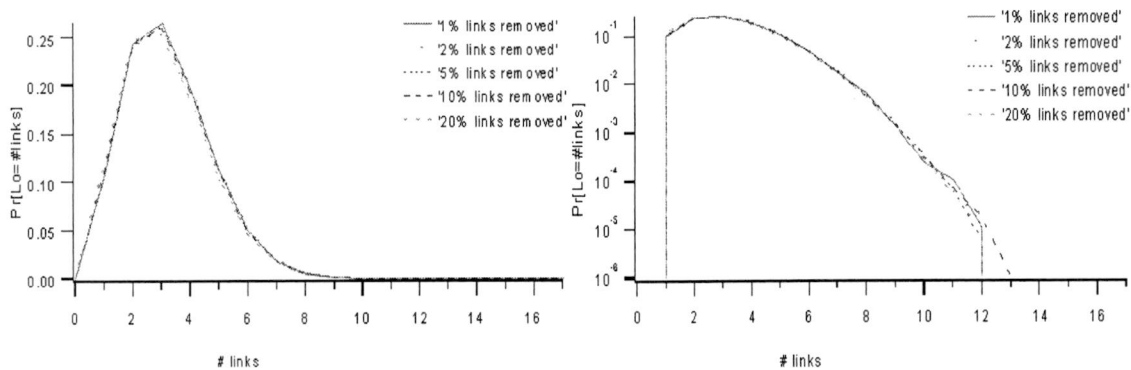


Figure 13. $Pr[L_n=\#links]$ for $N=50, m=10$ and $p=0.08$

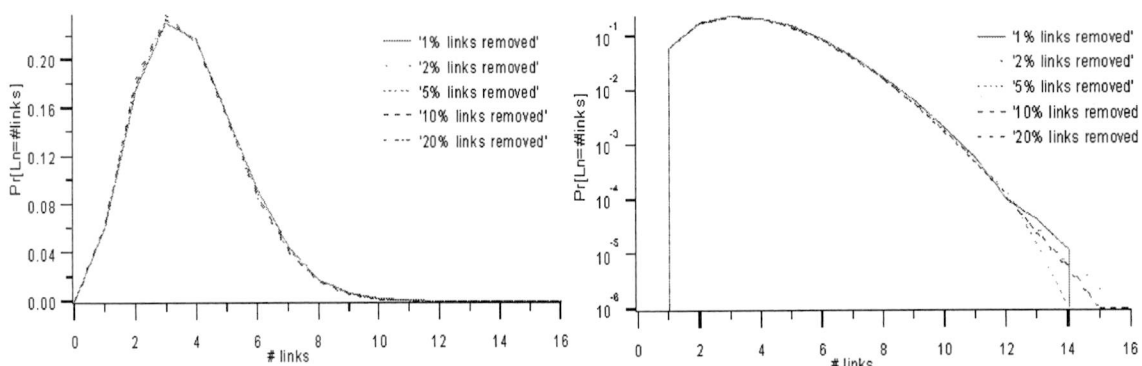


Figure 14. $Pr[L_n=\#links]$ for $N=100, m=10$ and $p=0.08$

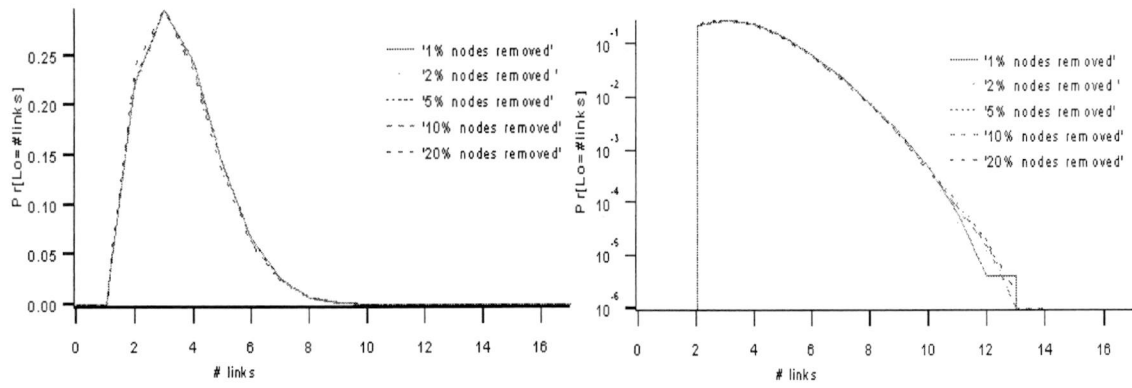


Figure 15. $\text{Pr}[L_n=\#\text{links}]$ for $N=50, m=10$ and $p=0.08$

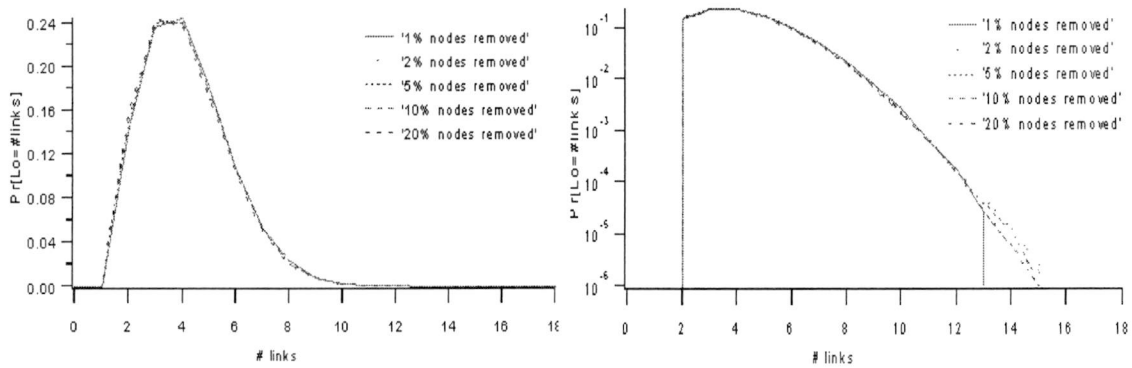


Figure 16. $\text{Pr}[L_n=\#\text{links}]$ for $N=100, m=10$ and $p=0.08$

3.2.1.2 The pdf of the number of links changed in new shortest paths of sub-graph

Table 5 investigates the information about the values of mean ($E[L_n]$) and the variance ($\text{var}[L_n]$) of the number of different links in the $[M']$ and $[M']$.

Topologies after links removed				Topologies after nodes removed			
N=50	$E[L_n]$	$\text{Var}[L_n]$	$\text{Var}[L_n]/E[L_n]$	N=50	$E[L_n]$	$\text{Var}[L_n]$	$\text{Var}[L_n]/E[L_n]$
r=1%	3.481061	2.260359	0.649330	r=1%	3.653310	2.408399	0.659237
r=2%	3.515175	2.316201	0.658915	r=2%	3.657537	2.420689	0.661836
r=5%	3.532165	2.322478	0.677522	r=5%	3.639836	2.398810	0.659043
r=10%	3.555197	2.351019	0.661291	r=10%	3.640135	2.417576	0.664145
r=20%	3.629028	2.476168	0.682323	r=20%	3.656177	2.478971	0.678023
N=100	$E[L_n]$	$\text{Var}[L_n]$	$\text{Var}[L_n]/E[L_n]$	N=100	$E[L_n]$	$\text{Var}[L_n]$	$\text{Var}[L_n]/E[L_n]$
r=1%	3.821951	2.912612	0.762075	r=1%	3.893414	2.988525	0.767585
r=2%	3.814055	2.910263	0.763036	r=2%	3.890913	2.960826	0.760959
r=5%	3.795829	2.885520	0.760182	r=5%	3.842955	2.918252	0.759377
r=10%	3.774323	2.856145	0.756730	r=10%	3.789117	2.849350	0.751983
r=20%	3.750670	2.830508	0.754667	r=20%	3.692460	2.718481	0.736225

Table 4: Mean and variance of the number of 'new' links in the shortest path information matrix

Surprisingly, Table 4 also shows that the values of mean and the variance of the number of different links in new links are stable, either.

The Figures 17-20 show the probability density function of the number of 'new' links L_n in the different topologies.

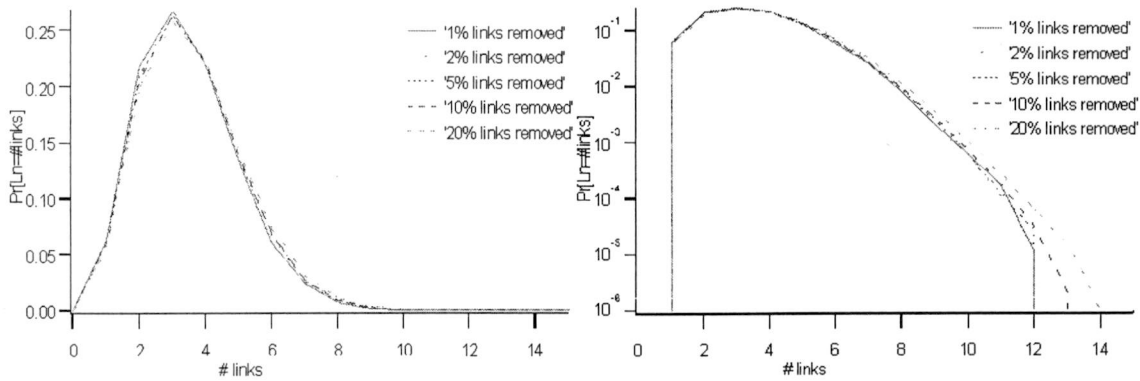


Figure 17. $\Pr[L_n=\#\text{links}]$ for $N=50, m=10$ and $p=0.08$

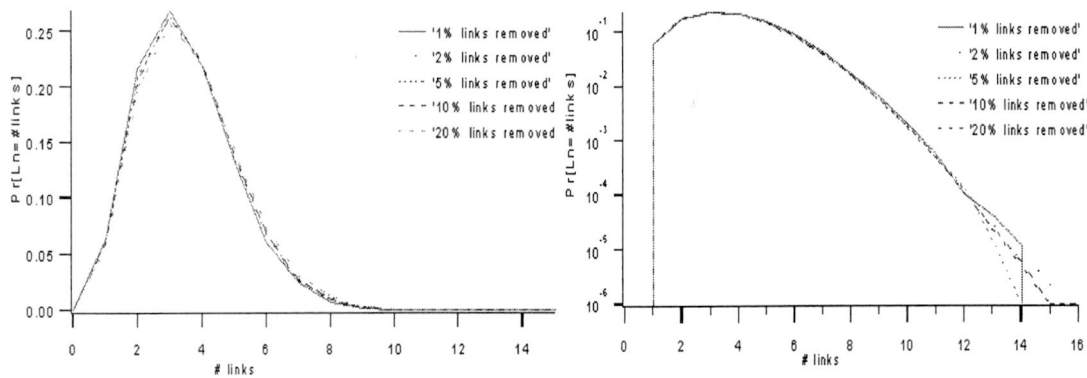


Figure 18. $\Pr[L_n=\#\text{links}]$ for $N=100, m=10$ and $p=0.08$

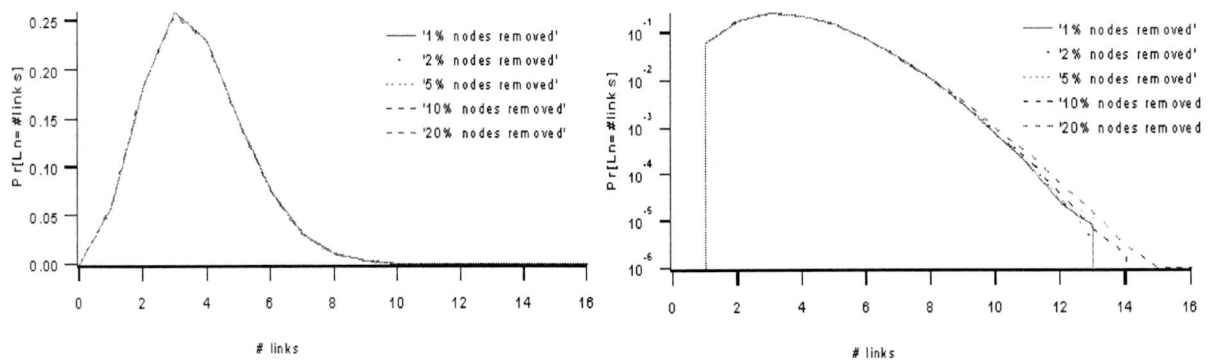


Figure 19. $\Pr[L_n=\#\text{links}]$ for $N=50, m=10$ and $p=0.08$

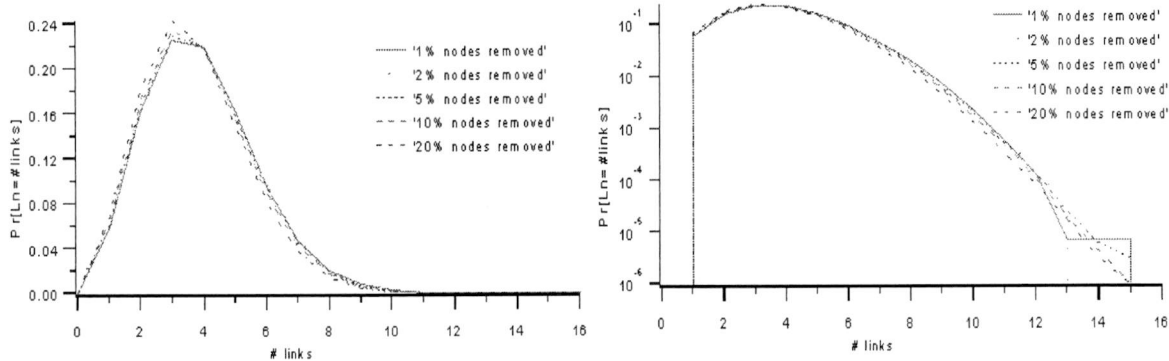


Figure 20. $\Pr[L_n=\#\text{links}]$ for $N=100, m=10$ and $p=0.08$

Compared to above Figures 13-20, we can observe that the probability distribution functions of different topologies are quite close to each other.

Compared the values in the table 4 with those in the table 3, we can observe that the corresponding values are roughly similar. It indicates the $E[L_n] \cong E[L_o]$. This result leads to the number of hopcount is rather stable under the similar condition.

Compared the probability of the number of new links or old links to the probability of the hopcount, the similar values indicate that if the topologies changed in the measurements, the different paths from a source to the destination are almost total different from the original shortest paths.

Another interest is that the pdf of the number of changed links in both L_o and L_n in the random graphs show a Gaussian or triangle like shape.

3.3 The probability density function of a node ID being visited by the paths

This aim of this part is to show the observation of a node being visited by the paths. In the uniformly distributed link metrics w , each node has the same probability being seen k times by the paths in the shortest path information matrix. We assumed that probability distribution function for every node should be same with each other. The results do conform it. The pdf of a node visited k times by the paths ($\Pr[k=\#\text{times}]$) are plotted in the Figures 21-30, for a same value of $p=0.08$, as a function of N and removed percentage r , with different m .

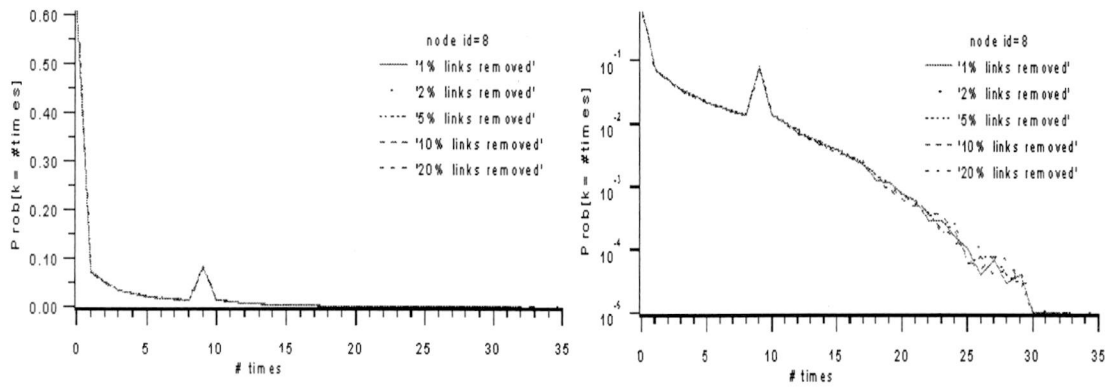


Figure 21. $\Pr[k=\#times]$ for $N=100$, $m=10$ and $p=0.08$

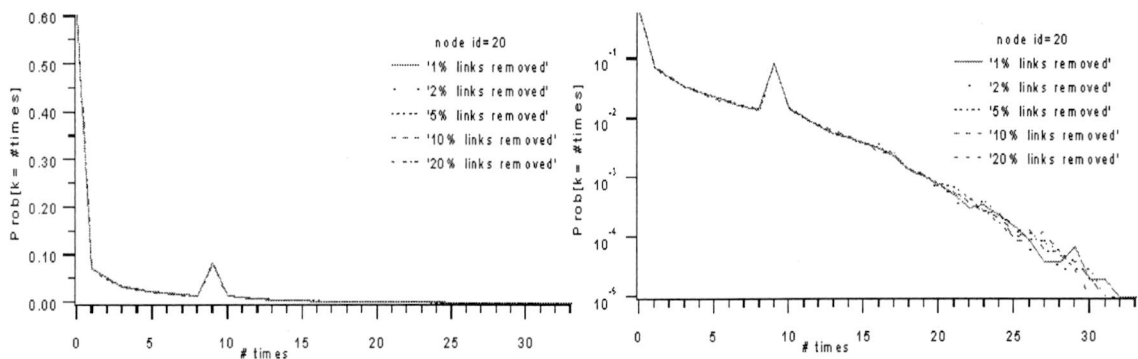


Figure 22. $\Pr[k=\#times]$ for $N=100$, $m=10$ and $p=0.08$

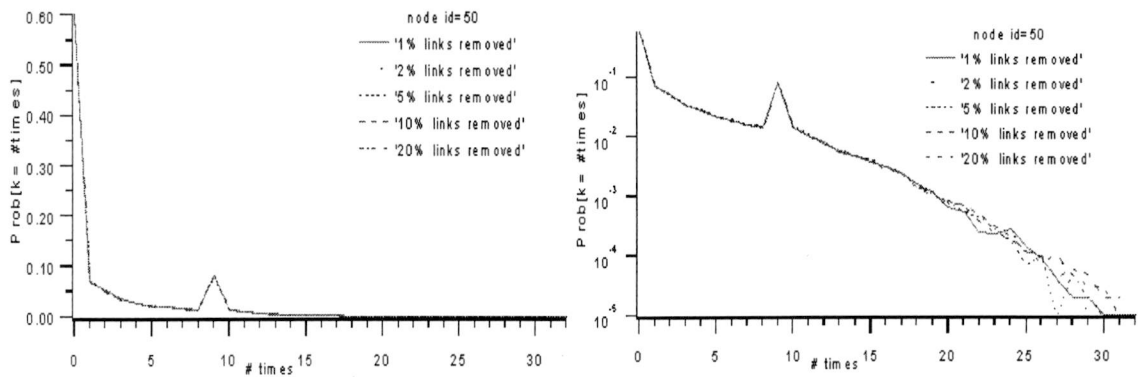


Figure 23. $\Pr[k=\#times]$ for $N=100$, $m=10$ and $p=0.08$

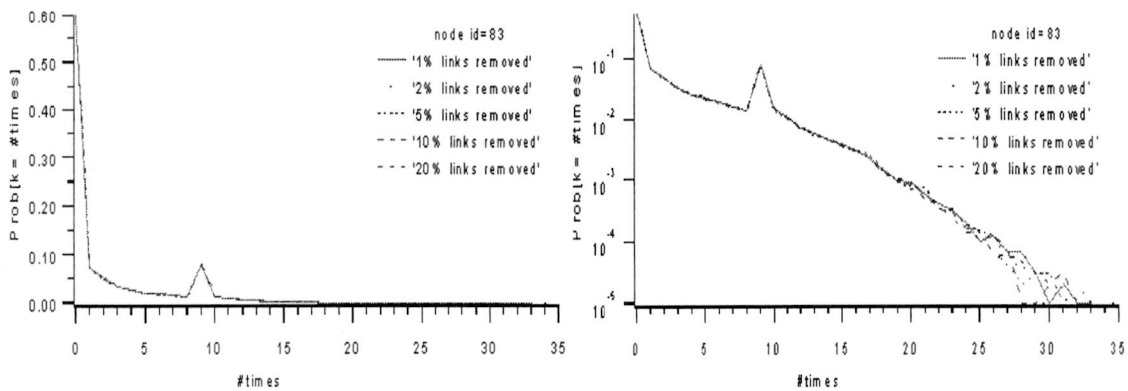


Figure 24. $\Pr[k=\#times]$ for $N=100$, $m=10$ and $p=0.08$

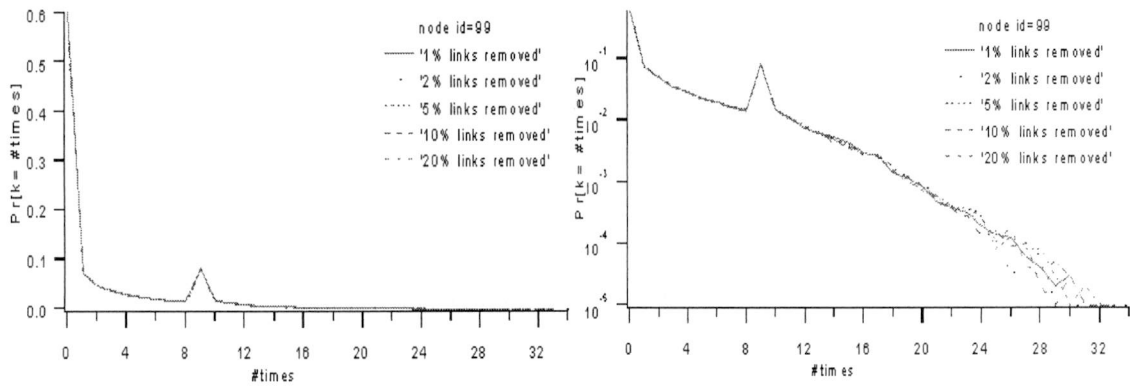


Figure 25. $\Pr[k=\#times]$ for $N=100$, $m=10$ and $p=0.08$

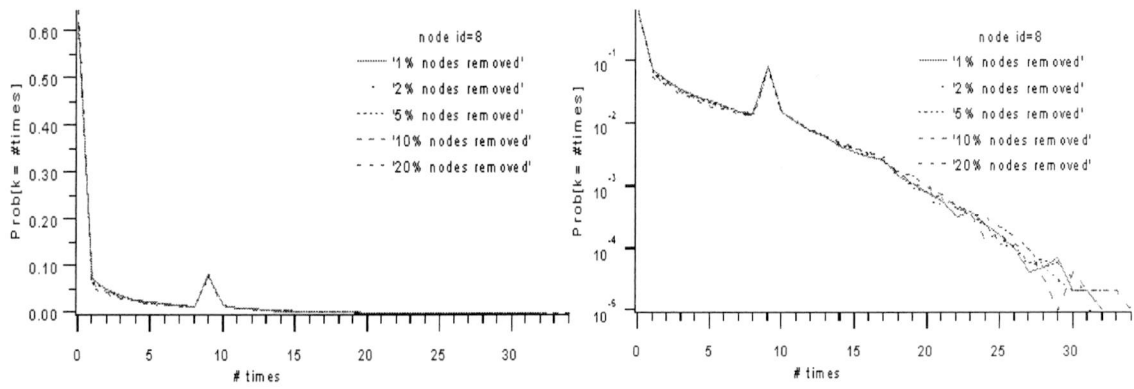


Figure 26. $\Pr[k=\#times]$ for $N=100$, $m=10$ and $p=0.08$

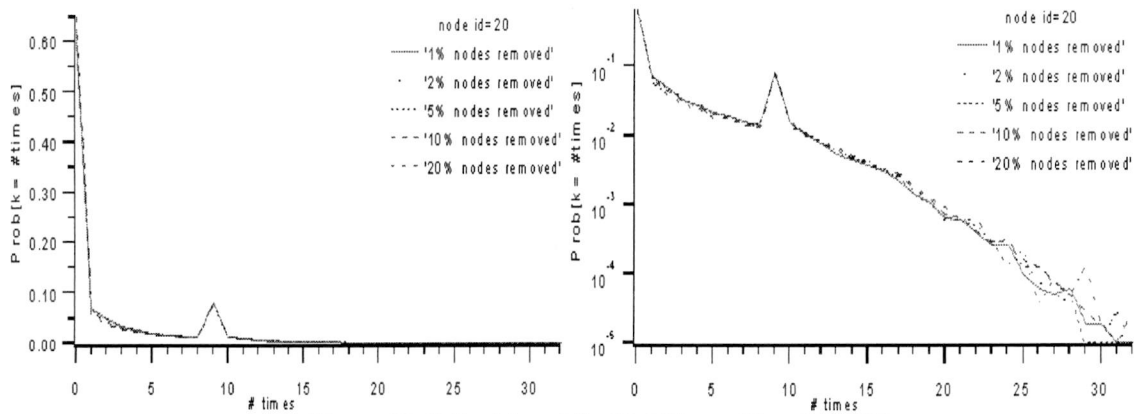


Figure 27. $\Pr[k=\#times]$ for $N=100$, $m=10$ and $p=0.08$

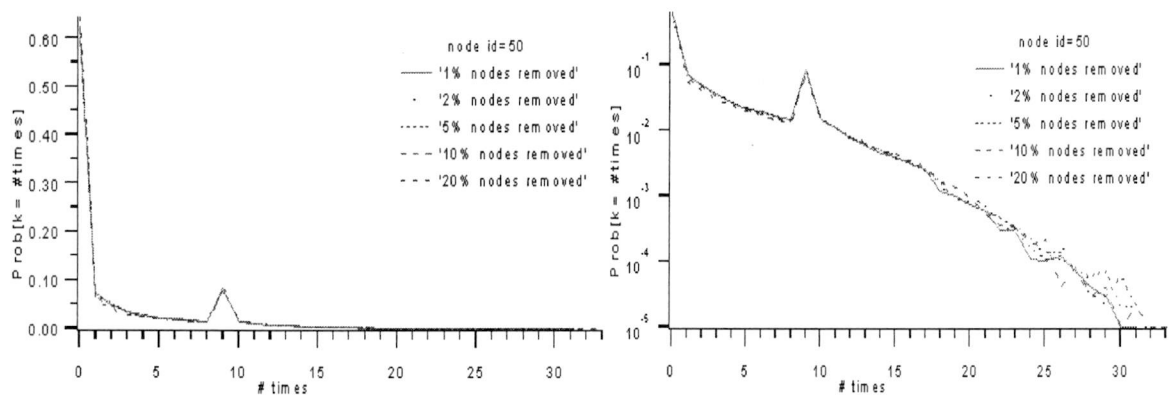


Figure 28. $\Pr[k=\#times]$ for $N=100$, $m=10$ and $p=0.08$

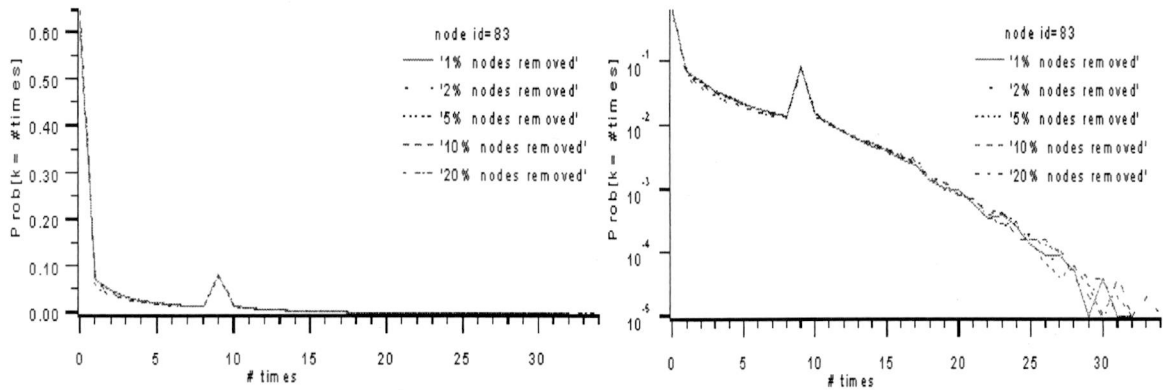


Figure 29. $\text{Pr}[k=\#\text{times}]$ for $N=100$, $m=10$ and $p=0.08$

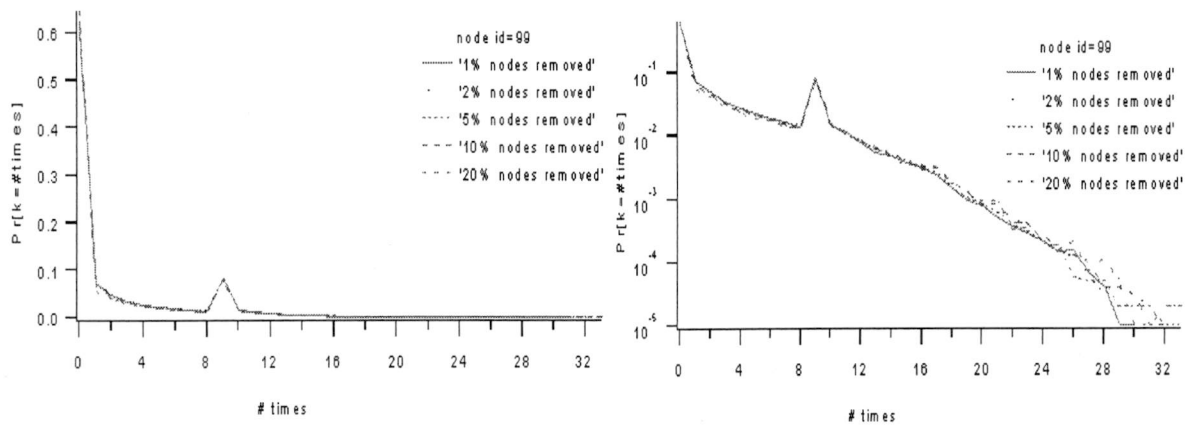


Figure 30. $\text{Pr}[k=\#\text{times}]$ for $N=100$, $m=10$ and $p=0.08$

It's surprise that there is always a peak near the value of $m-1$ in x axis, the reason is that in the shortest paths information matrix $[M]$, $[M']$ or $[M'']$, each source or destination could be seen by paths $m-1$ times. If N is large enough, the peak will disappear. The figures in chapter 10 do conform the assumption.

Since the topology is uniform link distribution, so the pdf's of a node visited k times by the paths equally likely.

3.4 Measurements of the Hopcount

The aim of this part is to list the hopcount H_n of Source-Destination pairs pathways between any two end points.

3.4.1 The Mean and variance of the Hopcount

In order to investigate the behaviour of the transfer of packets, we observe the average hopcount H_n in the different topologies. The second point of interest was to investigate the dynamics of the change of the hopcount H_n for those different topologies. The values of the mean and the variance of the hopcount H_n were given by the table 5.

Topologies after links removed				Topologies after nodes removed			
N=50	E[Hn]	Var[Hn]	Var[Hn]/E[Hn]	N=50	E[Hn]	Var[Hn]	Var[Hn]/E[Hn]
Original	3.784698	2.829465	0.747607	Original	3.785432	2.826676	0.746725
r=1%	3.789207	2.834827	0.748132	r=1%	3.781739	2.827681	0.747720
r=2%	3.797540	2.848153	0.750000	r=2%	3.780665	2.823631	0.746861
r=5%	3.824474	2.883029	0.753837	r=5%	3.774430	2.836380	0.751473
r=10%	3.877708	2.954803	0.761997	r=10%	3.769989	2.852519	0.756639
r=20%	4.011704	3,171849	0.790649	r=20%	3.774149	2.951901	0.782137
N=100	E[Hn]	Var[Hn]	Var[Hn]/E[Hn]	N=100	E[Hn]	Var[Hn]	Var[Hn]/E[Hn]
Original	4.211650	3.373707	0.801042	Original	4.210078	3.368230	0.800040
r=1%	4.212124	3.372609	0.800691	r=1%	4.200622	3.357036	0.799176
r=2%	4.213557	3.370354	0.799883	r=2%	4.193248	3.347799	0.798376
r=5%	4.214807	3.365768	0.7743405	r=5%	4.163553	3.312686	0.795639
r=10%	4.223218	3.367962	0.797487	r=10%	4.118312	3.257638	0.791013
r=20%	4.242261	3.369131	0.794183	r=20%	4.022627	3.133782	0.779039

Table 5. Mean and Variance of the hopcount

To check our results about the hopcount, we use the expression for the expectation of the hopcount from Piet Van Mieghem (see e.g. [1]) as $E(H_n) \approx \ln N + \gamma - 1$, $\text{Var}(H_n) \approx \ln N + \gamma - (\pi^2)/6$, where $\gamma \approx 0.5772$, is Euler's constant). We got almost the same results.

As verified from above table, for the topologies with same N , the percentages of removed links or nodes affect the values of means or variances of hopcount slightly. It indicates that the hopcount of new path of different topologies is almost the same as its previous.

3.4.2 The probability density function of the hopcount H_n in the different paths

In the network, the amount of traversed vertices from the source to the destination is denoted as the hopcount of the specific path. The distributions of the hopcount H_n for those useful shortest paths of different topologies are illustrated in Figure 31-34. In the Figures, $\text{Prob}[H_n = \# \text{hops}]$ represents the probability of the source-destination pairs whose hopcount H_n is equal to a number of hops .

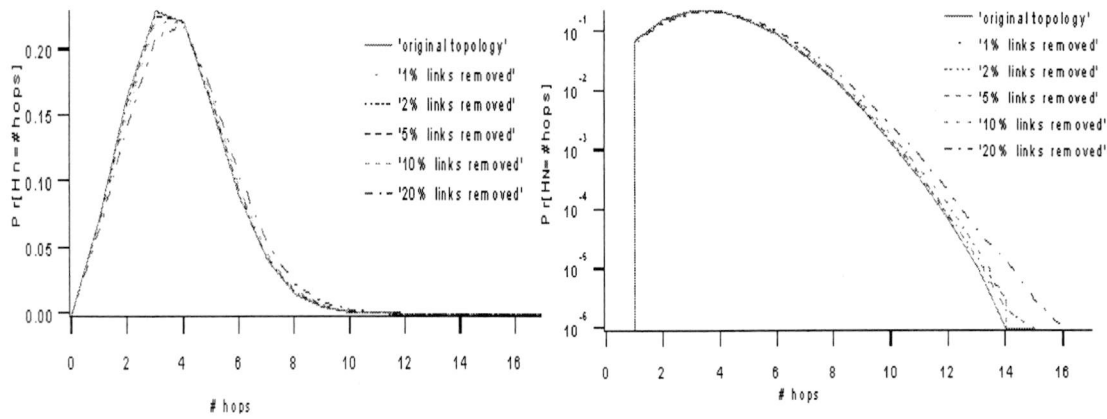


Figure 31. $\Pr[H_n=\#hops]$ for $N=50, m=10$ and $p=0.08$

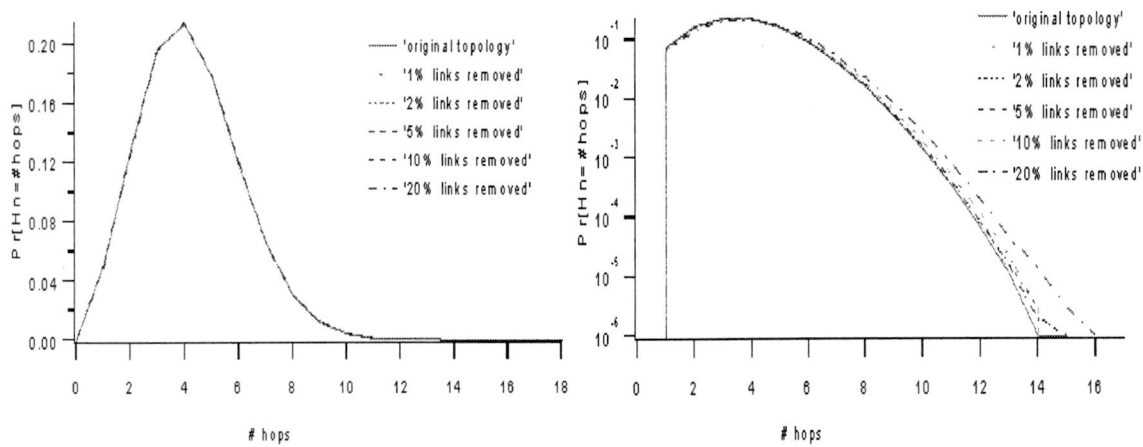


Figure 32. $\Pr[H_n=\#hops]$ for $N=100, m=10$ and $p=0.08$

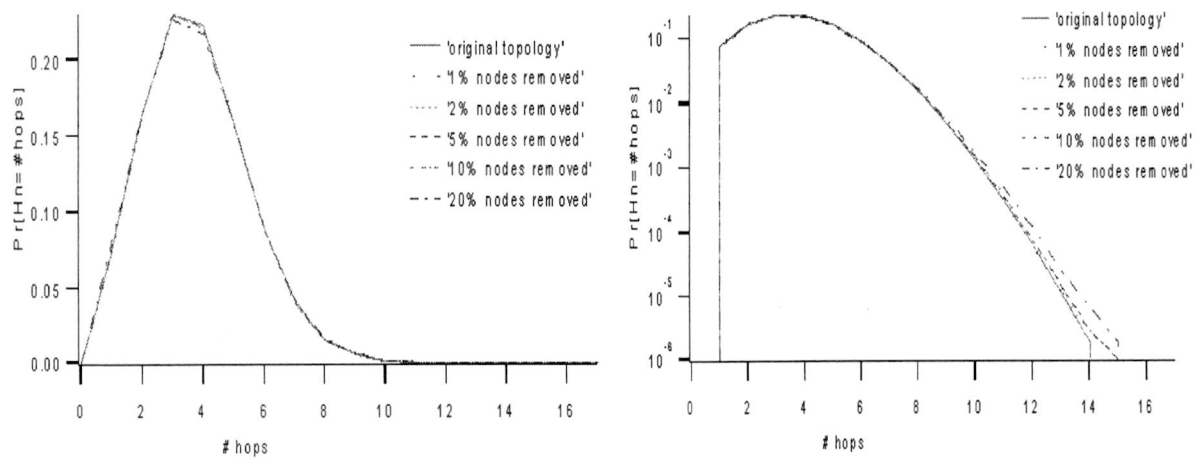


Figure 33. $\Pr[H_n=\#hops]$ for $N=50, m=10$ and $p=0.08$

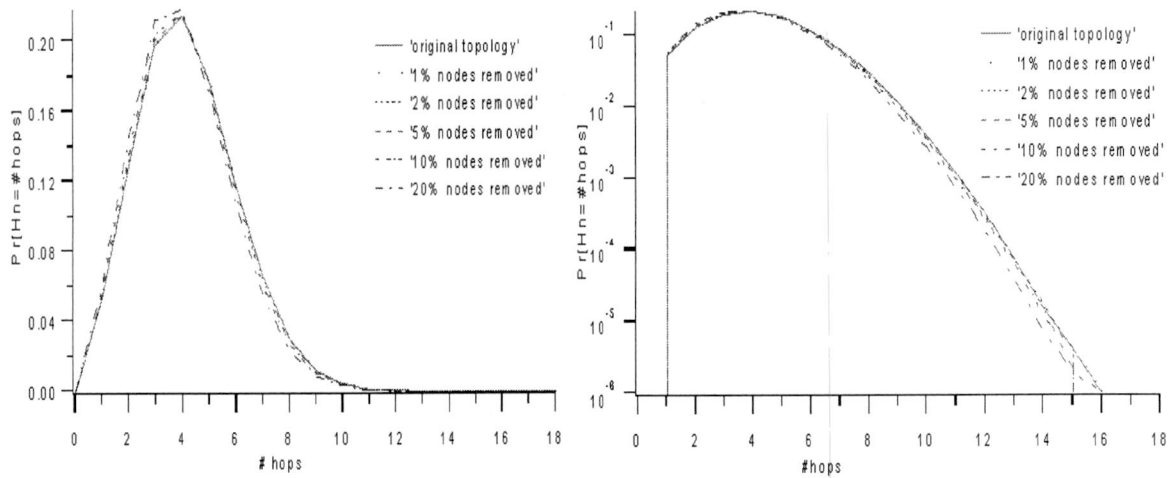


Figure 34. $\text{Pr}[H_n=\#\text{hops}]$ for $N=100, m=10$ and $p=0.08$

It's interesting that both the pdf of hopcount of two kinds of sub-graphs are similar with their original. All of the figures show approximate central limit shape. We follow the idea that the hopcount in the random graph $G_p(N)$ still has the similar distribution as the hopcount of complete graph K_N as long as $\frac{Np}{(\log N)^3} \rightarrow \infty$, we can deduce that sub-graphs also have the similar distribution as the hopcount of complete graph.

When we compared all the pdf results of hopcounts of different topologies we discovered that the results of the hopcounts did not change significantly after some links or nodes are removed.

Chapter 4. Conclusion of part A

This article focuses on the study investigates the sensitivity of shortest path in the random topology. Given a number of shortest paths in the classes $G_p(N)$, the special interest in this part lies in studying how those paths change if the topology is changed from $G_p(N)$ to $G_p'(N)$ or $G_p(N')$. The study found that the number of different paths between the different topologies is sensitive to some parameters of the topology; such as the total nodes number N in the topology and the number of the removed links/nodes. In those different paths, we analysed how the links change. The study found that the figure of the probability density function of the number of changed links in the different random graphs shows an approximate Gaussian or triangle like shape.

The dynamic change of the shortest path is further studied in the part B based on the measurement of the Internet.

Part B: Dynamic of the Internet

Chapter 5. Introduction

With the Internet growing larger every year and continuously changing overtime, the measurement of large-scale dynamic behaviours of Internet routing become much harder. While routing protocols have been a subject of a lot of study in the last years, considerably less work has been done on investigating properties of Internet path. To understand the properties of Internet path, it is very important to understand how current routing algorithms affect the behaviour of Internet path.

Most of the papers dealing with this subject mainly focus on routing dynamics [9][10][11]. Literature also contains a significant number of papers discussing path characteristics such as packet loss, round-trip time and bandwidth [11].

The errors occurred in Internet routing are poor studied, the exception being Paxson's [4] analysis of the dynamic behaviour of Internet routing in 1995. At that time, he analysed 40,000 end-to-end path measurements, made by repeating *traceroute* utility [14] among 37 Internet sites. In that study, some routing pathologies behaviours had been analysed in details. His data also showed that around half of the paths were asymmetric.

At any time there are many potential paths through the Internet connecting any two hosts. Recently, H. Tangmunarunkit *et al* [12] investigated how do both routing protocols and routing policies affect the paths on Internet, and concluded that about 20 % of paths are enlarged for more than five hops.

Another work has been carried out by S. Savage *et al* [13]. They showed that in 30-80 % of cases, an alternate path with better quality—higher bandwidth, lower propagation delay and less congestion-- could be found.

In this project, we were triggered to conduct the measurement-based analysis, aiming at giving answers to these two questions:

1. Which types of errors do we observe in the current Internet routing?
2. Whether paths that packets follow are shortest with respect to a link weight structure?

In order to compare actual paths to the shortest paths, accurate Internet measurement data are needed. The most direct method to obtain information about paths on Internet is the

traceroute utility. However, as shown in this paper, the Traceroute concept is highly sensitive to changes in topology during the measurement.

To answer the motivated questions, some steps are necessary to be performed. First of all, an authoritative project environment is needed. The project environment is described in chapter 6. Moreover, the routing pathologies should be omitted. Those routing pathologies are classified and compared to Paxson's data in chapter 7. We found that the likelihood of encountering a major routing pathology in recent years more than that of 1995. Third, the most representative set of paths between each source-destination pair must be performed. Armed with a set of paths, the graph representing these paths and properties (hopcount and degree) are described in Chapter 8. To each link of that graph consisting of the union of paths, polynomially distributed link weights were assigned. The difference of shortest paths and corresponding traceroutes is described in Chapter 9. In Chapter 10, a rough estimate of the number of nodes in the real underlying graph deduced from traceroutes is addressed. Finally, conclusions and recommendations are given in Chapter 11.

Chapter 6. Methodology

This Chapter shows the methodology used in our study: the project environment, how to get the measurement data, and which data of our database are plausibly representative of Internet traffic and which not.

6.1 Introduction of RIPE & TTM Project

For the accurate measurement results of the Internet, this project used the routing records got from the Test Traffic Measurements (TTM) Project, which is held by RIPE Network Coordination Centre (RIPE NCC) since 2000. RIPE (Réseaux IP Européens) is a collaborative organisation open to all parties operating wide area IP networks in Europe. The objective of RIPE is to ensure the administrative and technical coordination necessary to enable the operation of a pan-European IP network. The RIPE NCC is one of 3 Regional Internet Registries (RIR) which exist in the world today, providing allocation and registration services which support the operation of the Internet globally. Due to its unique position, the RIPE NCC can play an important role in facilitating new projects and services for its members as well as for the RIPE community. Test Traffic Measurements (TTM) is such a project that has been under development since 1997 and RIPE NCC announced it on October 20, 2000. Totally, there are 2 ways to measure the networking, the first way is the passive measurement by monitoring the amount of traffic that passes a certain point, and another way is the active measurement by generating test traffic and measuring how much time it takes to ship the test traffic over the network. The goal of TTM project is to do independent Internet active measurements of connectivity parameters, such as delays and routing-vectors (traceroutes), using test traffic generated by test-boxes.

6.2 Participating sites

In the TTM project, About 40 test boxes are installed over Europe (and a few in the US and New Zealand, see Figure 35) in March 2001, measuring accurately (within 10 μ s) the one-

way delay between each pair of boxes and the traceroutes. And more test boxes will be installed in the coming future. Table 6 list the information of those sites participated in our study, such as their abbreviation, their geographical coordinates, and their hosting sites and locations.

TTbox	Geographical coordinates	Hosting site & Location
<u>tt01</u>	<u>52.3728:4.8878</u>	RIPE NCC,Singel 258, 1016AB,NL
<u>tt02</u>	<u>52.3726:4.8880</u>	RIPE NCC,Singel 258,NL
<u>tt03</u>	<u>52.3728:4.8878</u>	RIPE NCC,Singel 258,NL
<u>tt04</u>	<u>52.3728:4.8878</u>	RIPE NCC,Singel 258,NL
<u>tt07</u>	<u>59.3176:18.2310</u>	Stupi,Stockholm,SE
<u>tt08</u>	<u>59.3491:18.6910</u>	NORDUnet,Stockholm,SE
<u>tt09</u>	<u>59.3306:17.9630</u>	Telia Network,Stockholm,SE
<u>tt12</u>	<u>48.1851:11.6015</u>	Spacenet,Munich,DE
<u>tt13</u>	<u>52.3561:4.9531</u>	Surfnet,Amsterdam,NL
<u>tt14</u>	<u>47.3900:8.5151</u>	Swisscom,Ittingen,CH
<u>tt15</u>	<u>40.4036:-3.6953</u>	Telefonica Data,Madrid,ES
<u>tt16</u>	<u>56.1081:10.1405</u>	Tele Denmark Datanet,Viby,DK
<u>tt17</u>	<u>44.4861:11.2601</u>	CINECA,Bologna,IT
<u>tt19</u>	<u>32.6306:35.6750</u>	Golan Consulting,Haifa,IS
<u>tt20</u>	<u>50.1015:14.3916</u>	CESNET,Prague,CZ
<u>tt21</u>	<u>49.1260:8.4236</u>	Xlink,Karlsruhe,DE
<u>tt22</u>	<u>48.1515:17.1131</u>	SANET,Bratislava,SK
<u>tt23</u>	<u>41.1160:-73.7096</u>	Advanced,Armonk,US
<u>tt25</u>	<u>53.3343:-6.2573</u>	Ireland Online,Dublin,IE
<u>tt26</u>	<u>51.4968:-0.1880</u>	LINX,London,UK
<u>tt27</u>	<u>30.3195:-97.7006</u>	Matrix.Net/MIDS,1160 Clayton Lane, Suite 501W, Austin TX78723,US
<u>tt30</u>	<u>49.6936:6.3288</u>	Astra.Net,Luxembourg,LU
<u>tt31</u>	<u>46.2326:6.4630</u>	CERN,Geneva,CH
<u>tt32</u>	<u>45.4000:7.6500</u>	CSP,Torino,IT
<u>tt34</u>	<u>60.1838:24.8173</u>	FUNET,Espoo,FI
<u>tt35</u>	<u>53.3381:-6.2403</u>	HEAnet,Dublin,IE

<u>tt36</u>	<u>45.1936:5.7700</u>	IMAG,Grenoble,FR
<u>tt38</u>	<u>45.7280:7.6820</u>	ITGate Network,Torino,IT
<u>tt39</u>	<u>51.3541:8.2510</u>	MEGLA Gmbh,Meschede,DE
<u>tt40</u>	<u>42.6558:23.3708</u>	Mobikom,Sofia,BU
<u>tt41</u>	<u>50.3230:8.7051</u>	Nacamar,Dreieich,DE
<u>tt42</u>	<u>37.9856:23.7335</u>	NTUA,Athens,GR
<u>tt43</u>	<u>48.1896:11.6505</u>	Prosieben Info Serv,Munich,DE
<u>tt44</u>	<u>39.6825:-104.9691</u>	Qwest,Denver,US
<u>tt45</u>	<u>59.9243:10.8106</u>	Tele2,,NO
<u>tt46</u>	<u>39.5713:-104.8808</u>	Verio,,US

Table 6: Sites participating in TTM

Figure 35 locates those sites of the test boxes that participated in our study.

Worldwide TT Testboxes

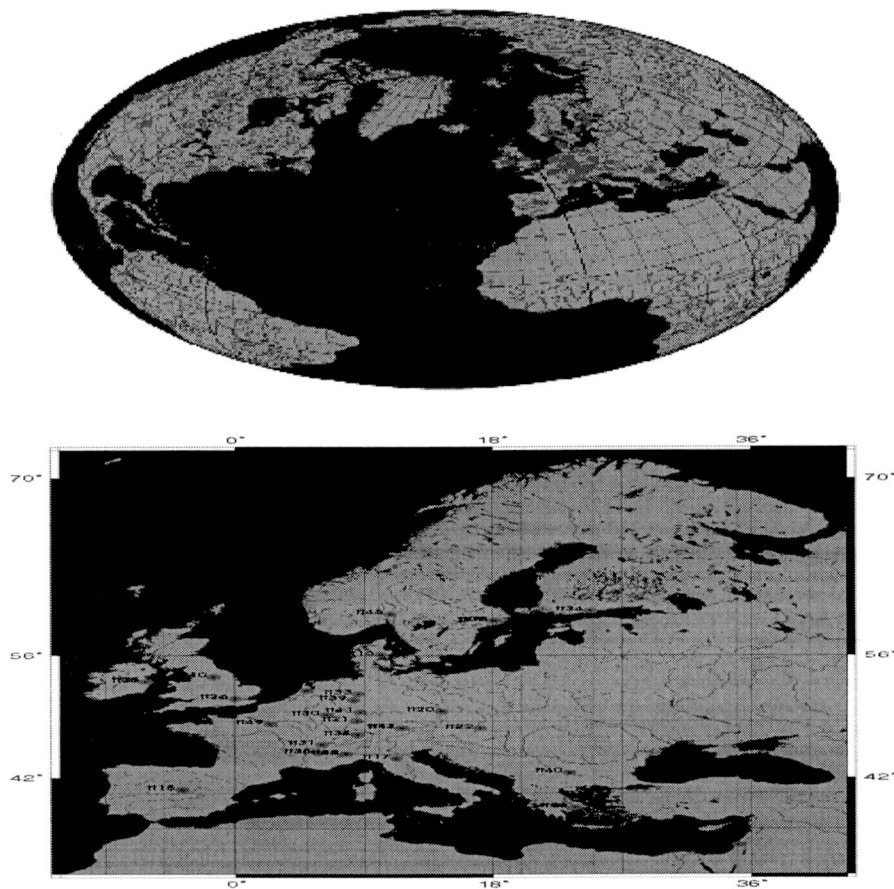


Figure 35. The location of the test boxes

6.3 The measurement configuration

The measurement configuration is described in Figure 36, more details can be checked from [2][3]. For measuring large-scale behavior of routing in the Internet accurately, all the test boxes are close to BGP-router to exclude the effect of internal networks.

To determine the routing path information, TTM uses around the well-known traceroute program. The traceroute program is written by Van Jacobson to return the path, specified by a sequence of IP-address of routers along the path, from source to destination. In TTM, a traceroute between each source-destination is done approximately 10 times an hour. In the Internet, there is no guarantee that IP packets will follow a same way from a source to a destination. Some changes, e.g. link-failures, policy-updates or load balancing, will lead to the change of traceroute. For those 40 test boxes (both can be sources and destinations), 1,329,019 different routes have been obtained (1329019 different *routeIDs*) with in total 24,181,803 routes (the sum of the rows in *count* column for all source-destination pairs). After removing some test boxes whose paths often meet error, 31 out of 40 test boxes are chosen in this study. There are 31 test boxes, corresponding to $\binom{31}{2} = 465$ most dominant paths. In order to collect the information from both senders and receivers, and to be accessed easily from a same place for the data files, there is a central point in RIPE CCN to collect all the traceroutes from each source-destination pairs.

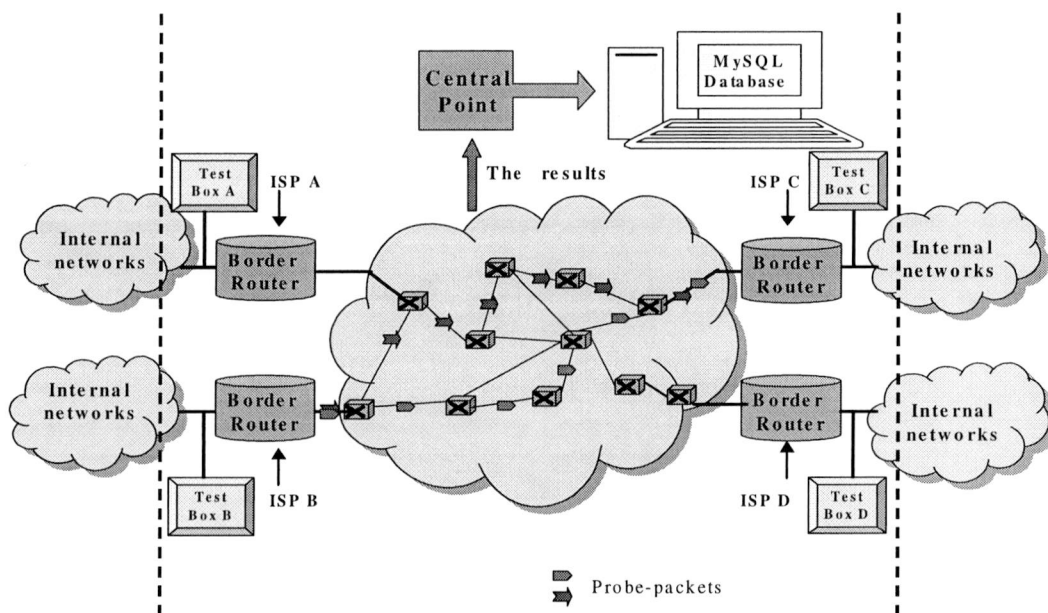


Figure 36. The measurement configuration

Then, shown in Figure 37, the traceroutes are inserted into 2 tables (see table 7 and table 8) in a MySQL database [see www.mysql.com] in the local computer in Delft University of Technology, the Netherlands. MySQL database is chosen for easier performance reason. The first table, one example is shown in table 2, contains routing vectors—which are for each unique combination of IP-addresses seen between the source test box and the destination test-box-- and the count of the routing vector recorded by the database. The second table, examples are shown in table 3, contains all IP-addresses of each router that appeared in the routing vector, and the length of the traceroute. The traceroutes between the boxes can be queried through the MySQL database. Here, table 2 shows all the traceroute records output between tt1.ripe.net to tt18.ripe.net, route ID 5 presents one special series IP addresses shown as table 3.

```

mysql> SELECT routeid,COUNT(*)
AS count FROM Records WHERE
src=1 AND dst=18 GROUP BY
routeid ORDER BY count DESC;
+-----+-----+
| routeid | count |
+-----+-----+
| 5 | 1255 |
| 25 | 1250 |
| 63712 | 671 |
| 63679 | 670 |
| 7980 | 541 |
| 19503 | 540 |
| 1290 | 40 |
| 16017 | 10 |
| 62260 | 8 |
| 62262 | 7 |
| 1281 | 1 |
| 140632 | 1 |
| 1298 | 1 |
| 1304 | 1 |
| 1348 | 1 |
| 16015 | 1 |
| 16550 | 1 |
| 32920 | 1 |
| 131678 | 1 |
+-----+-----+
19 rows in set (0.11 sec)

```

Table 7

```

mysql> SELECT len,route FROM Routes WHERE ID= 5;
+-----+-----+
| len | route |
+-----+-----+
| 5 | 3238002702 3238002738 3238002932 3247705900 3285074646 |
+-----+-----+
1 row in set (0.04 sec)

mysql> SELECT len,route FROM Routes WHERE ID= 25;
+-----+-----+
| len | route |
+-----+-----+
| 5 | 3238002702 3238002742 3238002932 3247705900 3285074646 |
+-----+-----+
1 row in set (0.00 sec)

mysql> SELECT len,route FROM Routes WHERE ID= 63712;
+-----+-----+
| len | route |
+-----+-----+
| 10 | 3238002702 3238002738 3238002932 3247705890 2435385229 |
| 2435383377 3556884657 3556884994 3285074666 3285074646 |
+-----+-----+
1 row in set (0.00 sec)

```

Table 8

Figure 37: Tables in the MySQL database

Moreover, in the RIPE CNN, users can query the routings between any two random test boxes using the routing vectors. Table 9 is an example of the output of the script, which is given by RIPE CNN. A user asked for the routes between tt20 and tt17 from February 14, midnight, to February 16, midnight. The script returned a page starting with this table.

Dates	Route-ID	Records	Element	IP Address	Hostname
From Sat Feb 13 22:44:38 1999 To Mon Feb 15 23:40:42 1999	11821	706	1	195.178.64.1	r1-prg-le.ten.cz
			2	194.108.60.1	rab.ctt.cz
			3	192.121.157.65	czpra301-ta-s0-0-1.ebone.net
			4	192.121.158.185	<i>Unknown address</i>
			5	192.121.158.169	<i>Unknown address</i>
			6	195.158.226.137	<i>Unknown address</i>
			7	195.158.226.134	<i>Unknown address</i>
			8	195.158.226.142	demun704-ta-p5-0-0.ebone.net
			9	192.121.157.137	itmil201-ta-s1-0-1.ebone.net
			10	192.121.156.137	<i>Unknown address</i>
			11	192.121.156.142	s0-1-1-gw0.nettuno.it
			12	193.43.2.18	ntp.nettuno.it

Table 9. The traceroute output between tt20.ripe.net to tt17.ripe.net.

The traceroute can enhance our view to the structure of Internet. The changes of traceroute (say, caused by load balance) can explain how the way that IP packets were transferred between two points is suddenly changed. Moreover, it also can tell in which way the Internet communication change accurately.

6.4 Are the observations representative of Internet traffic?

Measurements of the *traceroutes* have been accessed from a local MySQL database provided by Test Traffic Measurements (TTM) Project of RIPE NCC. Shown as appendix A, only 31 test boxes have been selected as the sources and destinations for this project.

31 test boxes is only a small part of the estimated 6.6 millions Internet hosts as of July 1995 [13]. However, the authoritative TTM project got thousands of different routers in the records of the Internet routing, we argue that the large and long-term communication measurements (traceroutes) can give us a very rich cross-chapter of Internet, and so it can reflect a significant character of the Internet behavior (part of the Internet behavior). The appendix B gives some hierarchical structures that got from RIPE traceroute measurement. However, how to describe a reasonable graph of the Internet with a hierarchical model is still a hot research topic.

Chapter 7. Routing Pathologies

We begin our study from the errors in traceroutes of the Internet. In order to investigate the diagnostics of routing paths in the current Internet, in this chapter, we ask such questions: which types of errors do we observe in the Internet, what is the cause of these errors. Pathologies perceived in the behavior of routing paths have been categorized following nomenclature proposed by Paxson [4], and compared to his results. First, we analyze the most frequently occurring traceroutes records of each source-destination pairs in details, and then we go down until the 8th frequently occurring traceroutes records.

7.1 Unresponsive routers

There are a certain number of routers that do not reply with the required messages in response to *traceroute* probes. That results in no record in the MySQL databases for the particular pair of routers, referenced by “Empty set” in the database. Here is an example of output of an unresponsive case between tt3 and tt10.

```
Mysql> SELECT routeid COUNT(*) AS count FROM Records WHERE src=3 AND DST=10 GROUP BY routeid ORDER BY count DESC;
Empty set (0.13 sec)
```

Totally, when checking the most frequently occurring paths, 4 *traceroutes* expressed unresponsive routers, forming 0.86% of all the records. Table 10 represents these sources and destinations.

Sources	Destinations
tt3	tt25,tt27,tt42
tt26	tt27

Table 10. unresponsive routers in MySQL databases

7.2 Routing Loops

Suppose there is one or more IP appear in the traceroute more than once, we call this routing loop.

In this part, we analyze our measurements for the prevalence of routing loops. These loops are classified as two types, “persistent routing loops” if traceroutes show loops that were not resolved by the end of the traceroutes (i.e. after probing 30 hops) and “temporary routing loops” if traceroutes resolve loops within the routes. Below we will look at these two types.

7.2.1 Persistent routing loops

A persistent routing loop is easy to detect in its traceroute. Table 11 is an example of a persistent routing loop between tt1 (*RIPE NCC, Singel 258, 1016AB, NL*) and tt49 (*Groupe des Ecoles de Telecommunications / Institut National des Telecommunications, 9 rue Charles Fourier 91011 EVRY CEDEX, FR*).

Element	IP Address	Hostname
1	193.0.0.14	e01.overtoom.ripe.net
2	193.0.0.54	s10.pampus.ripe.net
3	193.0.0.244	fe20.marken.ripe.net
4	193.148.15.34	Unknown address
5	145.41.7.141	BR7.Amsterdam.surf.net
6	212.1.193.146	ge.nl40.ten-155.net
7	212.1.197.58	nl-uk-1.uk40.ten-155.net
8	212.1.197.45	fr-uk-1.fr40.ten-155.net
9	212.1.193.137	ge.fr1.ten-155.net
10	212.1.196.42	ten155-gw.renater.fr
11	193.51.206.146	rerif-nio-n1.cssi.renater.fr
12	195.220.180.42	stamand2.rerif.ft.net
13	193.48.53.13	Unknown address
14	255.255.255.255	Unknown address
15	255.255.255.255	Unknown address
16	255.255.255.255	Unknown address
17	255.255.255.255	Unknown address
18	255.255.255.255	Unknown address
19	255.255.255.255	Unknown address
20	255.255.255.255	Unknown address
21	255.255.255.255	Unknown address
22	255.255.255.255	Unknown address
23	255.255.255.255	Unknown address

24	255.255.255.255	Unknown address
25	255.255.255.255	Unknown address
26	255.255.255.255	Unknown address
27	255.255.255.255	Unknown address
28	255.255.255.255	Unknown address
29	255.255.255.255	Unknown address
30	255.255.255.255	Unknown address

Table 11. persistent routing loops in MySQL databases

The first sign of trouble is at hop 13, where, after having made it to an unknown address. After hop 13, the traceroute was lost till to the end. It indicates the connectivity deteriorating before a routing change, which led to an inconsistent state.

Of the 465 frequently occurring traceroutes, 1 path exhibited persistent routing loops happened between tt19 to tt26, 0.2% of all the records.

7.2.2 Temporary routing loops

To those temporary routing loops, the traceroute probe traveled beyond the loop and attain to the destination. Here is an example of a temporary routing loop between tt10 (*Energis Squared, Leeds, UK*) and tt31 (*CERN, Geneva, CH*).

1	195.92.70.193	Unknown address
2	195.92.201.98	Unknown address
3	195.92.201.128	Marrow.AS5388.NET
4	195.92.201.128	Marrow.AS5388.NET
5	195.92.71.194	Unknown address
6	192.121.154.201	Unknown address
7	195.158.226.233	gblon307-tb-p0-1.ebone.net
8	195.158.225.29	gblon303-tc-p8-0.ebone.net
9	195.158.228.149	Unknown address
10	195.158.228.21	Unknown address
11	195.158.228.30	Unknown address
12	192.65.185.39	tt31.ripe.net

At hop 3 and hop 4, the traceroute detects some IP-address 195.92.201.128. It suggests that either the propagation of a single fault's effects through the network sometimes leads to widespread, temporary instability, or that a mechanism separate from the exchange of routing information is producing widespread faults.

Of the 465 most frequently occurring traceroutes, 35 exhibited persistent routing loops, 7.53% of all the records.

Compared with that got by Paxson (see table 7), the probability of temporary routing got from RIPE TTM increases largely. The difference is mainly caused by the definition about the unknown IP address (255.255.255.255) in RIPE TTM, “if a router does not return it’s IP-address, then it will appear as 255.255.255.255 in the list”. This rule makes lots of different unknown IP-address to the same 255.255.255.255, which leads to temporary routing and increases the probability of temporary. Of all this pathology, there are about 77% temporary routing paths caused by unknown IP address (255.255.255.255).

Here is another example of a temporary routing loop, which is caused by the unknown IP-address, between tt8 (*NORDUnet,Stockholm,SE*) and tt10 (*Energis Squared,Leeds,UK*).

1	193.0.0.14	<i>e01.overtoom.ripe.net</i>
2	134.222.249.81	<i>r12-Se1-7.asd-SNG.NL.kpnqwest.net</i>
3	134.222.186.5	<i>r5-Fe0-0-0.asd-SNG.NL.kpnqwest.net</i>
4	134.222.228.162	<i>r16-PO0-3.asd-KQ1.NL.kpnqwest.net</i>
5	134.222.228.82	<i>r4-PO3-0.ledn-KQ1.NL.kpnqwest.net</i>
6	134.222.228.22	<i>r3-PO3-0.nyk-KQ1.US.kpnqwest.net</i>
7	134.222.228.41	<i>r4-PO5-0-0.prs-KQ1.FR.kpnqwest.net</i>
8	134.222.228.146	<i>Unknown address</i>
9	192.157.69.12	<i>sprint-nap.es.net</i>
10	134.55.24.13	<i>slac1-atms.es.net</i>
11	192.68.191.17	<i>Unknown address</i>
12	255.255.255.255	<i>Unknown address</i>
13	255.255.255.255	<i>Unknown address</i>
14	134.79.196.38	<i>RIPE-IDM.SLAC.Stanford.EDU</i>

7.3 Infrastructure failure

This failure reflects a problem inside the Internet infrastructure: the terminating router in the traceroute was in the middle of the network, not at the source of destination. Here is an example of infrastructure failure between tt4 (*RIPE NCC,Singel 258,NL*) and tt23 (*Advanced,Armonk,US*).

1	193.0.0.14	<i>e01.overtoom.ripe.net</i>
2	134.222.249.81	<i>r12-Se1-7.asd-SNG.NL.kpnqwest.net</i>
3	134.222.186.5	<i>r5-Fe0-0-0.asd-SNG.NL.kpnqwest.net</i>
4	134.222.228.162	<i>r16-PO0-3.asd-KQ1.NL.kpnqwest.net</i>
5	134.222.228.194	<i>r4-PO1-3.ledn-KQ1.NL.kpnqwest.net</i>
6	134.222.228.70	<i>r3-PO2-0.nyk-KQ1.US.kpnqwest.net</i>
7	134.222.228.41	<i>r4-PO5-0-0.prs-KQ1.FR.kpnqwest.net</i>
8	134.222.228.146	<i>Unknown address</i>
9	192.157.69.60	<i>Unknown address</i>
10	137.39.100.2	<i>Hssi0-1-0.hr1.NYCI.ALTER.NET</i>
11	137.39.33.225	<i>Fddi0-0.GW1.NYCI.ALTER.NET</i>
12	157.130.219.246	<i>adv-3-gw.customer.alter.net</i>
13	207.24.7.8	<i>Unknown address</i>

At hop 13, the traceroute stops, though hop 13 isn't the destination.

Because most test boxes are installed in Europe, we supposed there would be small probability of this failure. However, we are surprised about this fact that of the 465 frequently occurring traceroutes, 37 exhibited this failure, 7.96% of all the records.

These failures could be due to infrastructure problems of Internet. Another reason is perhaps that some network sites have "firewalls" in place to filter incoming network traffic for security purposes. The firewalls drop the packet without returning an ICMP Time Exceeded message. Thus, The packets are lost and traceroute never receives a reply for a given hop.

7.4 Circuitous routing

These routes do not represent pathologies but rather triumphs of robust routing. Here is an example for a traceroute from test box A in Bratislava to test box B in Munich, on a specific day (March 5, 2001)

The hostnames of the routers contain abbreviations of cities that can be recognized. For example in router `debln302-tc-p2-0.Ynet` the abbreviation `de` stands for Deutschland and `bln` stands for Berlin. In this traceroute a few other locations can be recognized. The locations of the other unknown nodes are ignored and we assume these nodes will not affect the path-length considerably. Figure 38 displays the geographical traceroute from test box A (*Bratislava, SK*) to test box B (*Munich, DE*). We observe that the distance is 5 times larger than the Line of Sight distance.

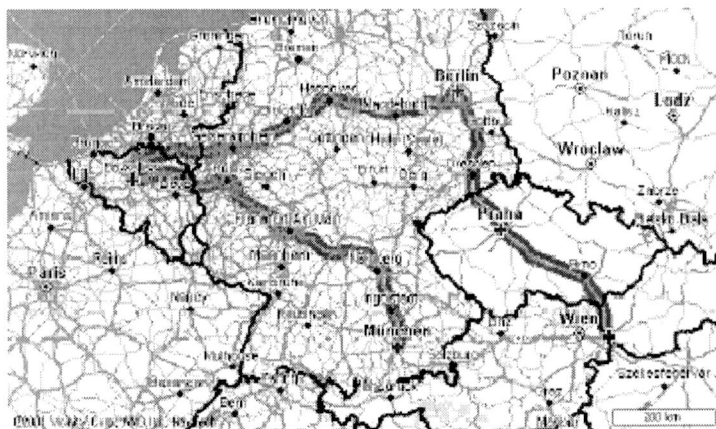


Figure 38. Traceroute (line) from Bratislava (SK) to Munich (DE)

The reason is perhaps due to different Internet Service Providers there and different available capacity networks in that place. For a packet, it would like to choose higher available capacity network.

Finding this type of pathology is a really hard job, since it's necessary to check the exactly geographic location of each router appeared in the traceroute. Moreover, this pathology seems that affected the quality of the traceroute measurement slightly. For the time being of this project, not much attention was paid to this research. However, this topic is an interest for the further study.

7.5 Summary

In Table 12 the analyzed routing pathology are summarized (more details can be got from appendix A) and compared to results obtained by Paxson in 1995.

	<i>Unresponsive routers</i>	<i>Persistent routing loops</i>	<i>Temporary routing loops/percentage led by unknown IP address</i>		<i>Infrastructure failure</i>	<i>Maximum Probability Of errors</i>	<i>Total paths records</i>
<i>Paxson[3]</i>	0.00-0.53%	0.13-0.16%	0.055-0.078%	/	0.16%±0.44%	1.21%	40000
<i>RIPE TTM 1st frequently occurring routing</i>	0.86%	0.2%	7.53%	60%	7.96%	16.55%	461703
2 nd	0.86%	0.65%	5.38%	56%	7.31%	14.2%	422295
3 rd	0.86%	1.29%	6.45%	66.7%	6.67%	15.27%	294699
4 th	0.86%	1.72%	5.81%	48.15%	5.81%	14.2%	261942
5 th	1.08%	1.29%	6.24%	68.97%	7.96%	16.57%	204858
6 th	1.51%	3.01%	7.53%	72.22%	7.53%	19.58%	185218
7 th	1.94%	2.37%	8.82%	65.85%	7.96%	20.99%	162320
8 th	2.15%	2.15%	8.82%	68.29%	7.74%	20.86%	151346

Table 12. Comparing results obtained by Paxson and RIPE TTM

Among these first 10 most frequently occurring paths, the maximum probability of user-visible pathologies in RIPE TTM is 21%, which indicates that the quality of traceroute measurements seems to have decreased over time of that the part of the Internet over time.

Chapter 8. Graph representation of a part of Internet

In this Chapter, the method of graph construction based on Internet measurement data has been presented, as well as the results of comparison of routes obtained through measurements with shortest paths determined in simulations. Data obtained in Internet (node degree, route length, etc) could be also used for calibration of tree and graph generators that are used for simulating network protocols. Comparing real data to our topology model and polynomial link weight distribution with different coefficient α might deepen our understanding of the current structure of Internet.

8.1 Graph representation of a part of Internet

The analysis we present in this Chapter and the method of the graph construction can be better understood with the help of Figure 39.

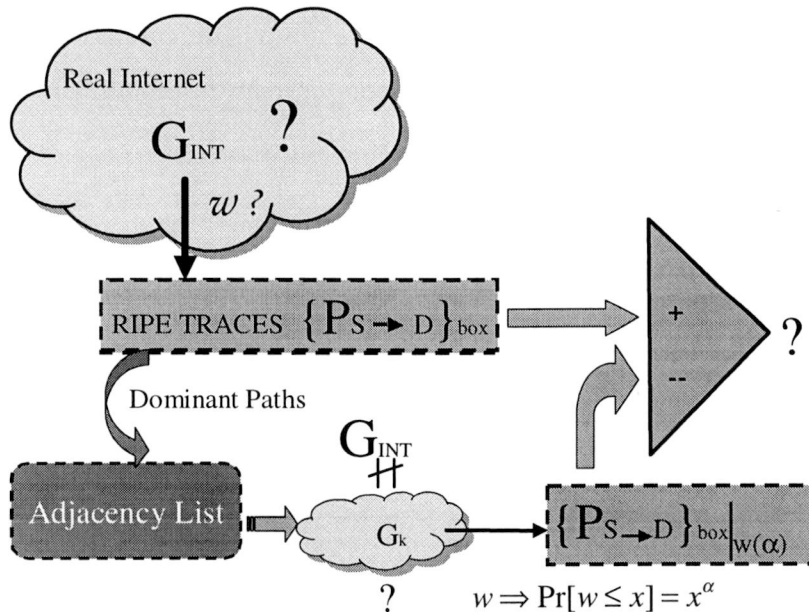


Figure 39. The analysis description

The Internet is continuously changing over time. It is difficult to determine its topology and link weights structure. Based on *traceroute* data of a part of Internet we have constructed a topology. First, we constructed the graph G_1 by only the most frequently occurring non-erroneous paths. After that, we assigned polynomially-distributed values to link weights, obtaining in this way a graph different than that of Internet. Of course, the graph G_1 of the paths between the 386 source-destination pairs is not the same as the real Internet G_{INT} , however, as mentioned in Chapter 6.4, it seems a reasonable approximation to a part of G_{INT} . Through comparing paths in this graph to paths obtained from measurement, we hope to understand the current structure and behavior of Internet better.

8.2 Collecting routes

The data recorded in the MySQL database has been analyzed. For each source-destination pair (t_i, t_j) the number of paths with different *routeIDs* is very large, in some cases reaching 9032, for examples, the records between tt_1 - tt_{44} . In order to determine the critical number of different paths that we had to take into consideration in our analysis, on the left side of Figures 40-47, for 8 randomly chosen source-destination pairs, we have plotted the probability density function that a particular correct path is the k^{th} frequently occurring path. NR represents the total number of records in the *count* column while NP represents the total number of different paths. The right hand side plots on these Figures represent probability distribution of the correct paths. The value of $\text{Pr}[0]$ represents the probability that there is no path in right plot, or there is a probability of errors on path in the left plot. However, the right hand side plots do not include the point at $k=0$ and $\text{Pr}[P \leq 0]=0$.

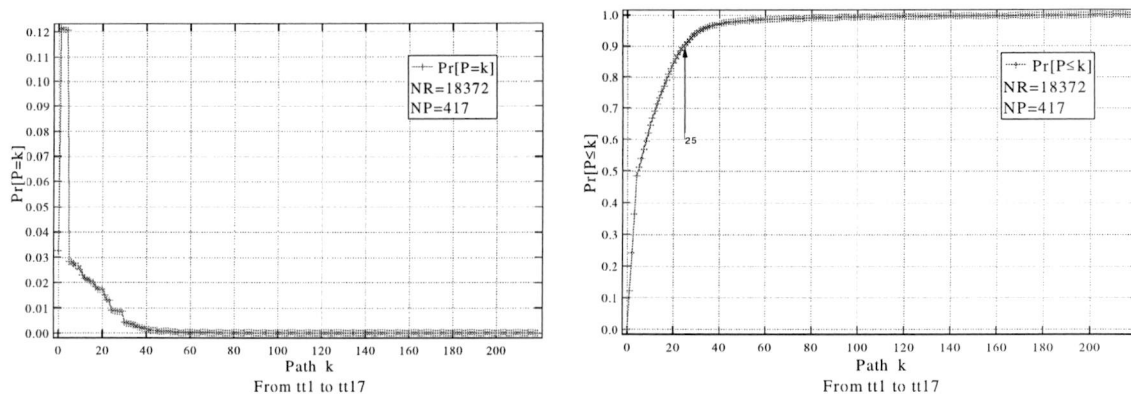


Figure 40. The probability density function and probability distribution of the correct path dominance (tt_1, tt_{17})

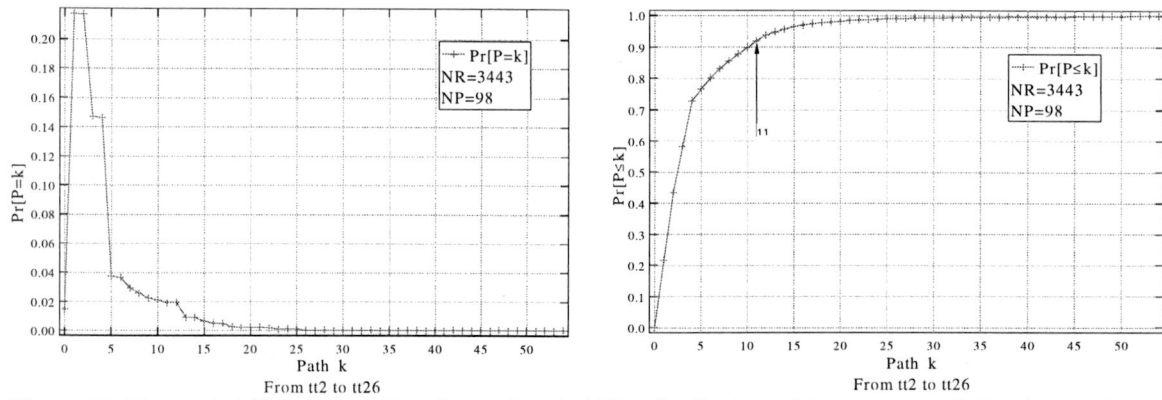


Figure 41. The probability density function and probability distribution of the correct path dominance (tt_2, tt_{26})

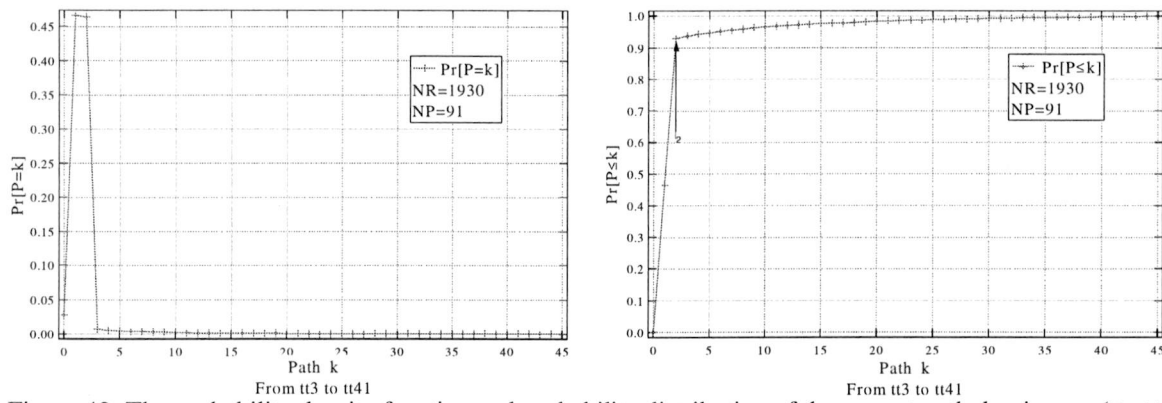


Figure 42. The probability density function and probability distribution of the correct path dominance (tt_3, tt_{41})

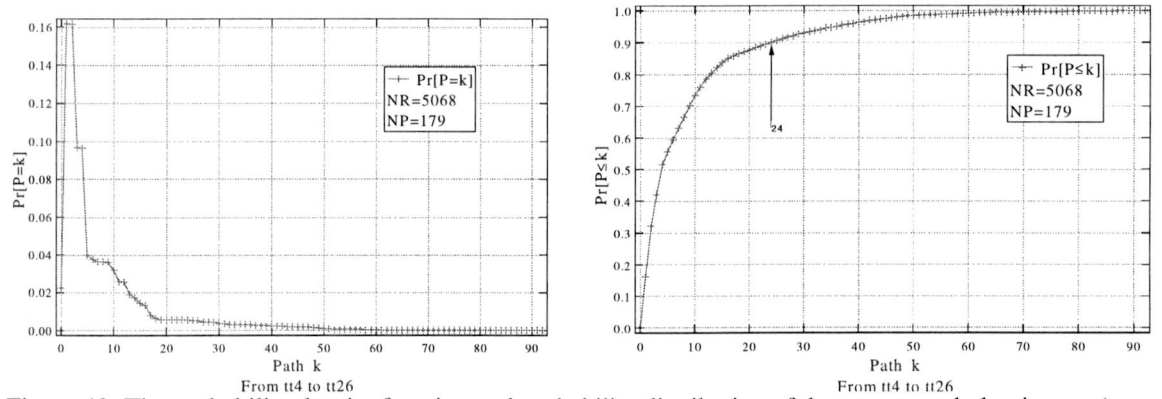


Figure 43. The probability density function and probability distribution of the correct path dominance (tt_4, tt_{26})

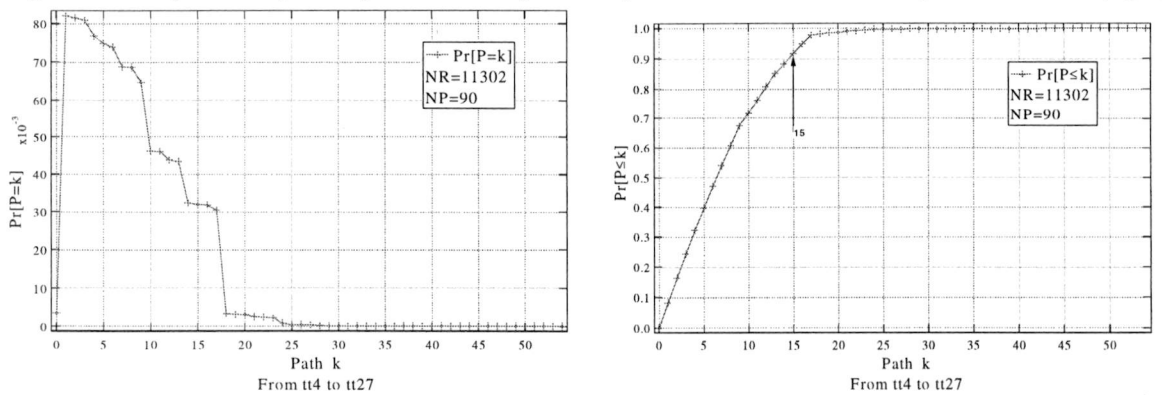


Figure 44. The probability density function and probability distribution of the correct path dominance (tt_4, tt_{27})

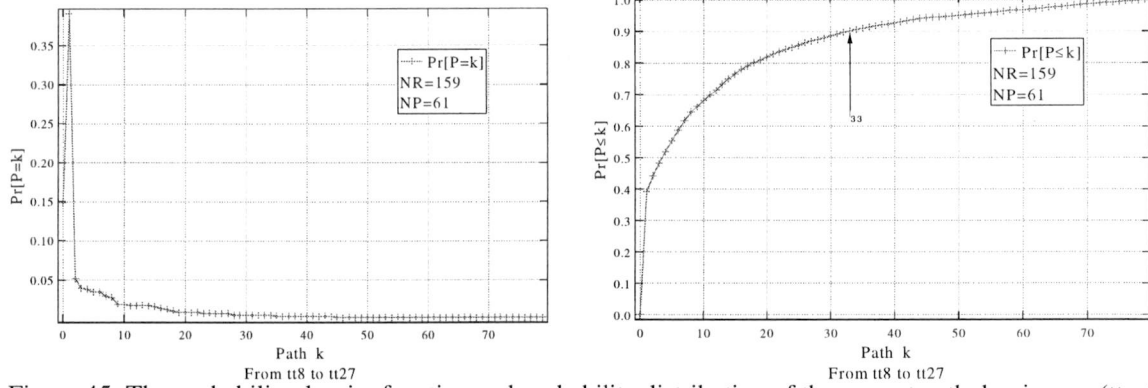


Figure 45. The probability density function and probability distribution of the correct path dominance (tt_8, tt_{27})

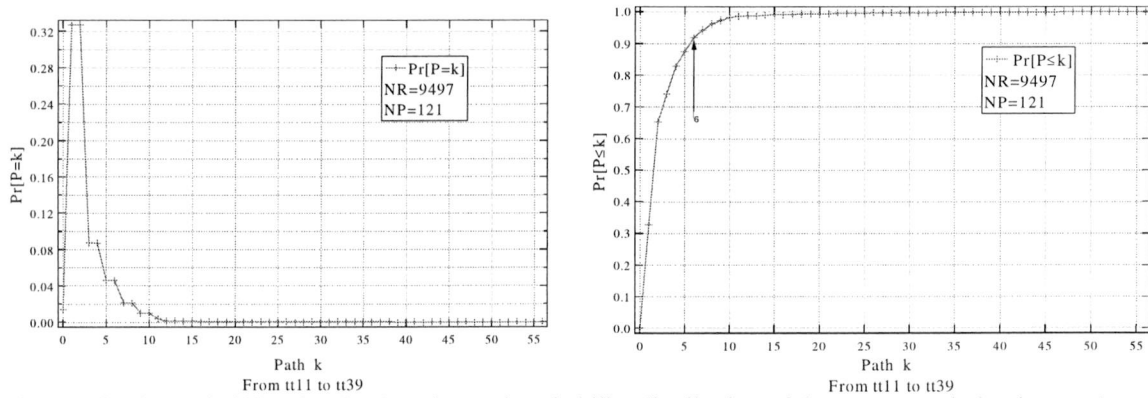


Figure 46. The probability density function and probability distribution of the correct path dominance (tt_{11}, tt_{39})

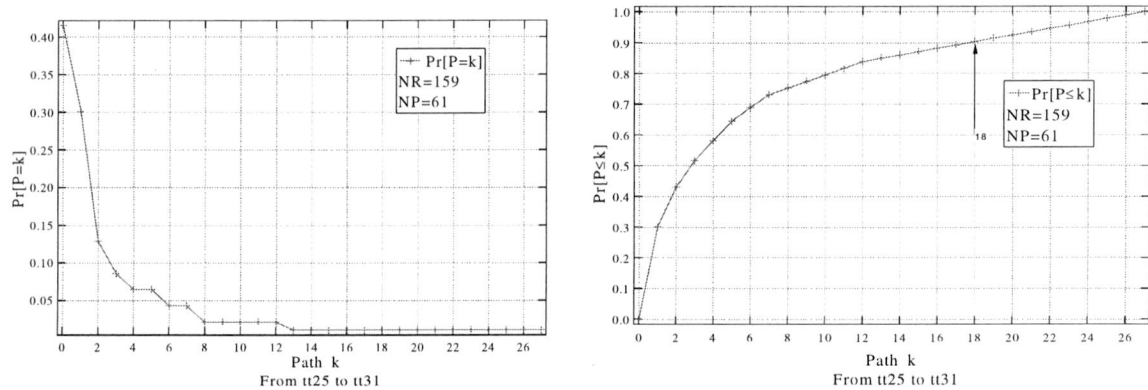


Figure 47. The probability density function and probability distribution of the correct path dominance (tt_{25}, tt_{39})

We observe that for some source-destination (tt_i, tt_j) pairs, the probability that a path is the 1st frequently occurring path and the probability that it is the 2nd frequently occurring path (even the 3rd one) do not differ significantly, which indicates that IP packets often follow different paths (probably due to the load balancing). Figure 48 shows that it's difficult to tell some things about the distribution of the number of path to attain $Pr[P \leq k] = 90\%$, but we do notice that the number of frequently occurring paths necessary to satisfy the condition $Pr[P \leq k] = 90\%$ varies largely.

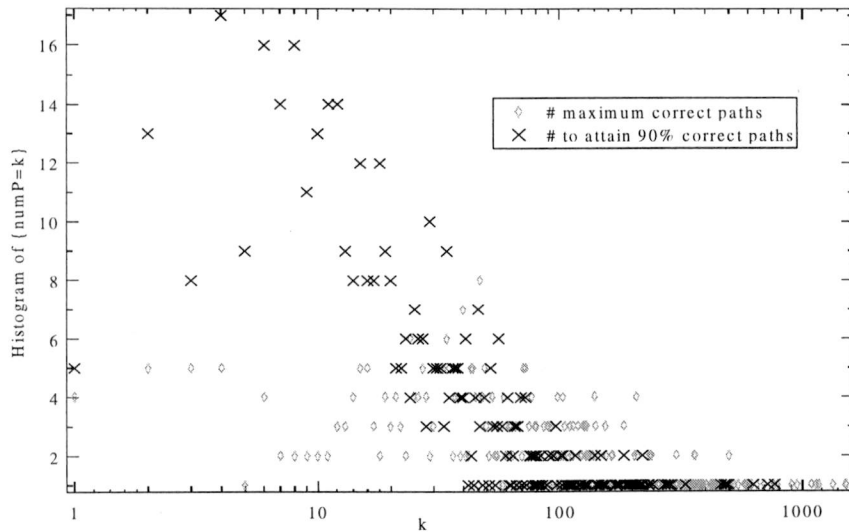


Figure 48: The histogram of the number of the correct path.

8.3 Building graph from routes

Based on our collection of routes, we constructed the graph by adding every link that belongs to the most frequently occurring, non-erroneous path for each pair (tt_i, tt_j) . The idea is shown in Figure 49. In this way, a graph comprising 1888 nodes and 2628 edges was created. We observe that if the graph has been constructed based on routes obtained for (any) 18 sources to all destinations, nearly 85% of the total number of nodes would already be included in the graph. Furthermore, when adding nodes obtained from all most frequently occurring routes for a single source, it appears that only 1.5% ($\pm 1\%$) new nodes are being added to the topology.

It is interesting to mention that in 99% of cases the most frequently occurring non-erroneous paths connecting tt_i to tt_j and tt_j to tt_i are traversing different nodes, in other words routes are in 99% of cases asymmetric.

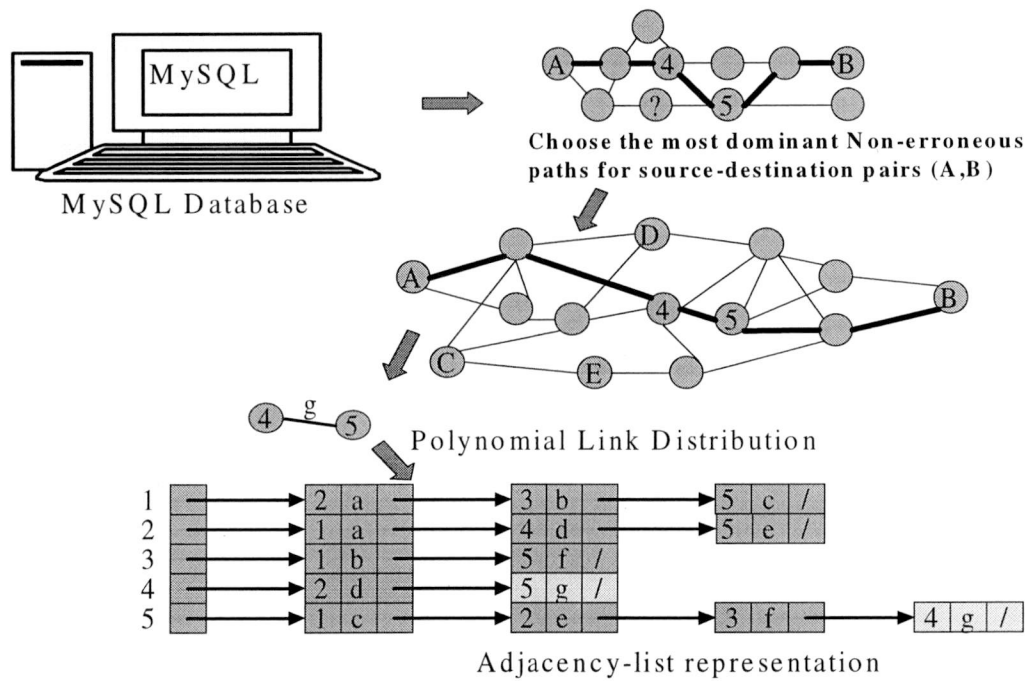


Figure 49. The schematic representation of the graph construction

The information about hopcount (the number of traversed routers in the traceroute) is very important to understand the current topology and dimensioning of the Internet. This understanding could allow us improvements of the network infrastructure.

In Figures 50 and 51 we have plotted the probability density function of the hopcount and node degree (the number of neighbors of a node), respectively. Since this Figures and the table indicate characteristics similar to the characteristics of random graphs, we were triggered to compare the hopcount data obtained from RIPE traces, with the mathematically derived formula for probability that hopcount of shortest path in random graph (when the number of nodes $N \rightarrow \infty$) consists of precisely k hops [1]:

$$\Pr[h_N = k] = \frac{(1 + o(1))}{N} \sum_{m=1}^{N-1} c_{m+1} \frac{\ln^{k-m} N}{(k-m)!} \quad (8.3.1)$$

where c_k are the Taylor coefficients of $\frac{1}{\Gamma(x)}$ listed in [15], and N is numbers of nodes in the graph.

Remarkably, Figure 50 illustrates that fit with (8.3.1) is reasonable.

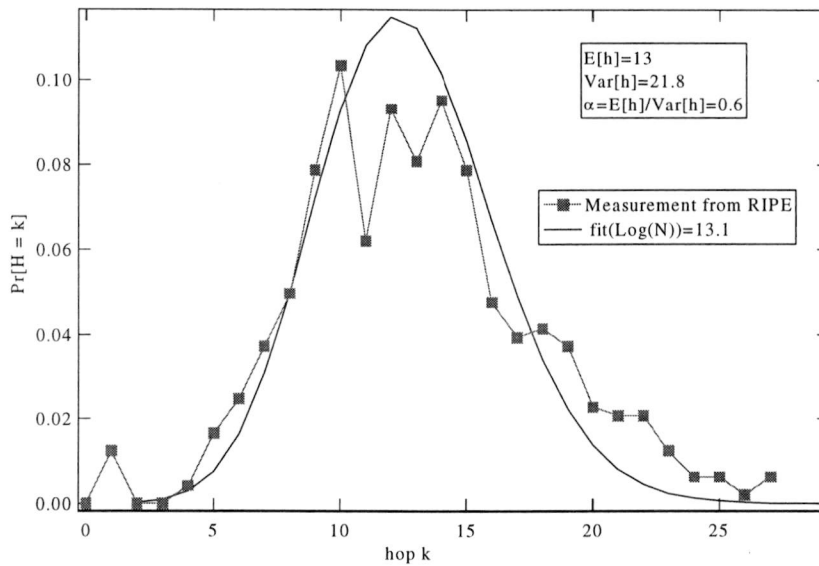


Figure 50. Fitting the pdf of hopcount with mathematical formula

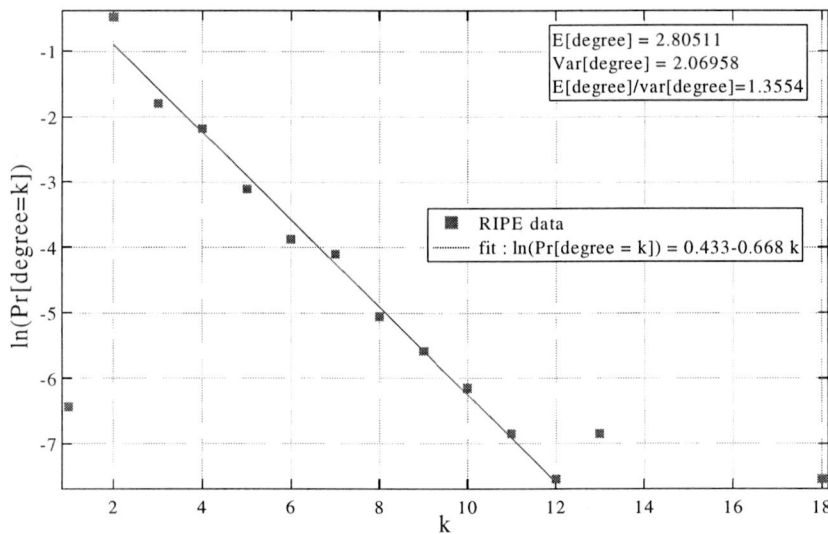


Figure 51. The pdf of the node degree (RIPE data)

Earlier, Faloutsos *et al.* [5] have reported a power law for the degrees in the graph of the Internet. This discrepancy points to the fact that G_1 is not representing the graph of the Internet well. Or, put differently, the graph deduced from the routing paths seems to possess a quite different structure.

The output results of the hopcount and that of node degree could also be used for calibration of tree and graph generators that are used for simulating network protocols.

In today's networks, the number of nodes grows very fast. In the large networks hierarchical structure enhances our understanding the internality of the Internet. Figure 52 shows an

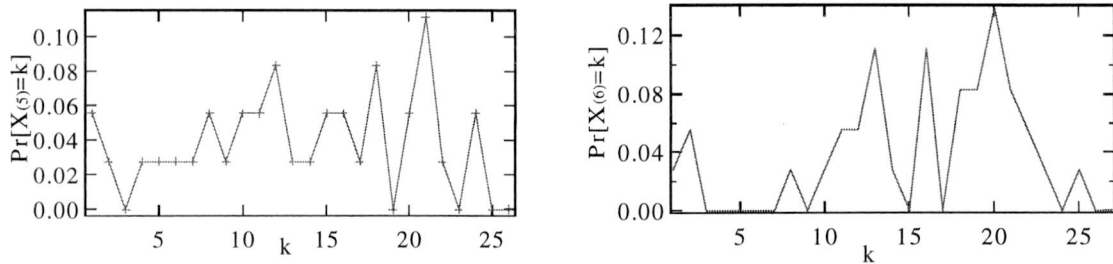


Figure 53: the node degree of the first 6 tops level in the RIPE hierarchy structure

8.4 Constructing the graph G_{10} based on the 10 most frequently occurring paths

In the previous Chapter 8.3, the graph G_1 only contains the most frequently occurring non-erroneous paths. But the Figure 48 shows that the G_1 does not cover the majority of the paths between the source-destination pair. Before going further, we analyzed all the correct source-destination pairs records in the database.

Totally, among those 436 paths in the database, we defined all of them in 5 different classifications based on the following definitions:

Class A: It attains its 90% correct paths before the first 10 frequently occurring correct paths, and without a heavy tail in its Figure. Its separation is illustrated in Figure 54 where shows the records from tt10 to tt41 and from tt11 to tt21.

Class B: It attains its 90% correct paths before the first 10 frequently occurring correct paths, and with a heavy tail in its Figure. Its separation is illustrated in Figure 55 where shows the records from tt1 to tt31 and from tt12 to tt17.

Class C: It attains its 90% correct paths before the first 25 frequently occurring correct paths. Its separation is illustrated in Figure 56 where shows the records from tt4 to tt25 and from tt12 to tt19.

Class D: It attains its 90% correct paths after the first 25 frequently occurring correct paths, and the total number of different paths is less than 300. Its separation is illustrated in Figure 57 where shows the records from tt1 to tt21 and from tt15 to tt44.

Class E: Those paths whose total number of different paths is larger than 300. Its separation is illustrated in Figure 58 where shows the records from tt19 to tt21.

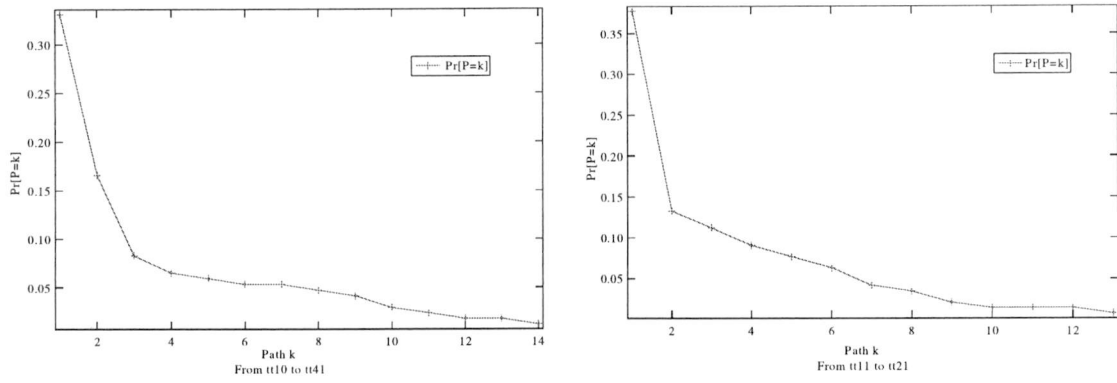


Figure 54. A Class A distribution

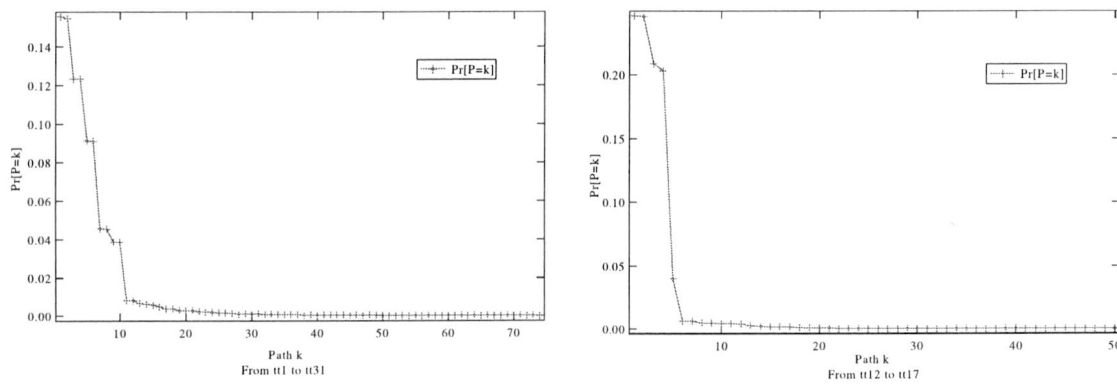


Figure 55. A Class B distribution

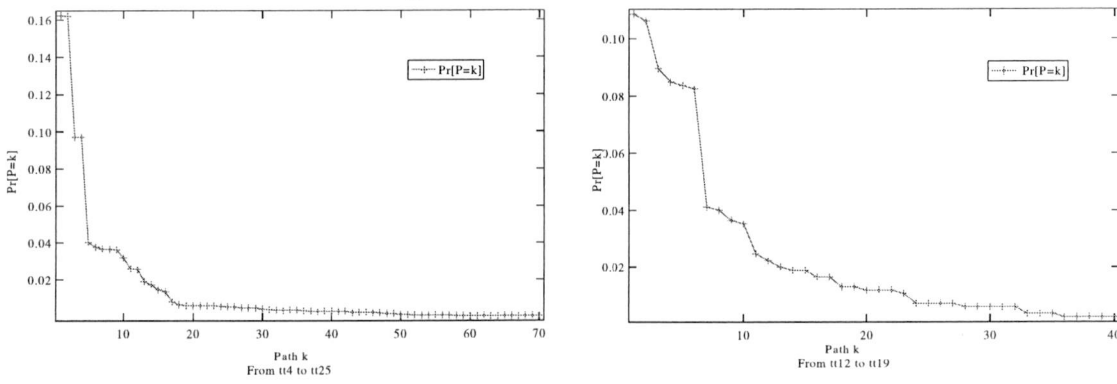


Figure 56. A Class C distribution

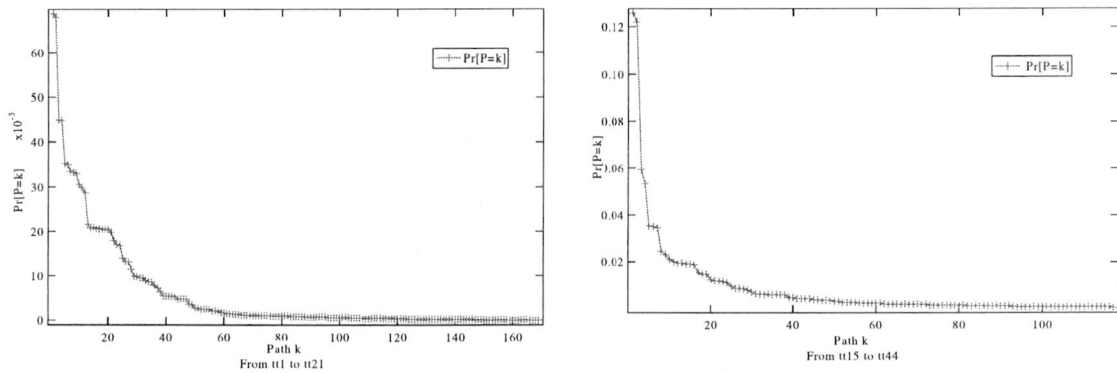


Figure 57. A Class D distribution

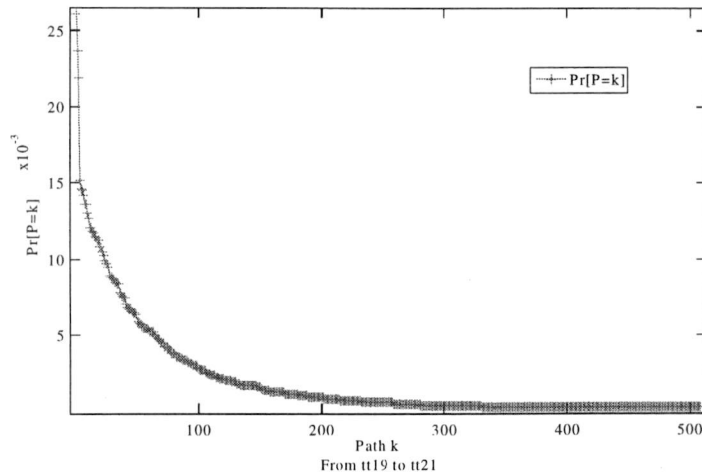


Figure 58. A Class E distribution

In classifying those non-erroneous paths, sometimes we cannot tell one class from another class easily. However, at least, the different classes can give us some feelings about the information of all the non-erroneous records. Table 13 shows the probability of each class in the database.

Class	$\#[P \in \text{Class}]$	$\text{Pr}[P \in \text{Class}]$
1	97	22.25%
2	35	8.03%
3	99	22.71%
4	143	47%
5	62	14.22%

Table 13: The probability of each class in the database

The main observation is that about 78% of these distributions own a heavy tail. Here for analyzing the main character of the routing, to all the non-erroneous records, we chose the 90% of non-erroneous paths to represent the path from source tt_i to destination tt_j in the classes A and B, while chose the first 10 most frequently occurring non-erroneous paths to represent the path from source tt_i to destination tt_j in classes C, D and E. Figures 59 and 60 show the probability density function of the hopcount and node degree, respectively.

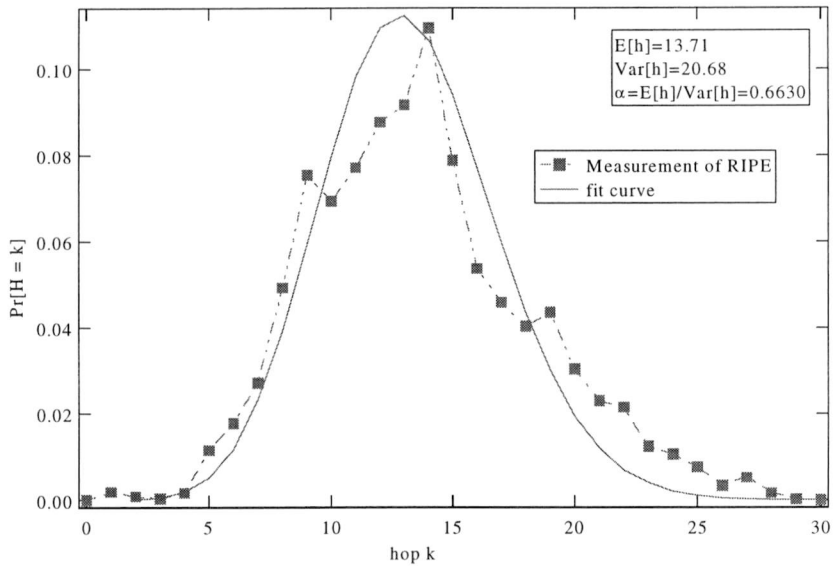


Figure 59. Fitting the pdf of hopcount with mathematical formula

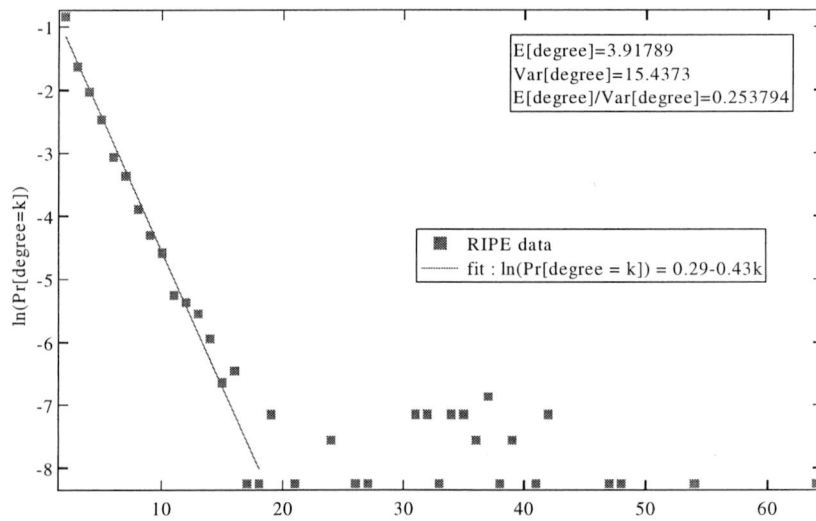


Figure 60. The pdf of the node degree (RIPE data)

For those Internet simulators, it's also interesting to know how many real routers have been visited during the number of frequently occurring paths G_k increasing. Figure 61 shows this information. We observe that the number of nodes increases slowly.

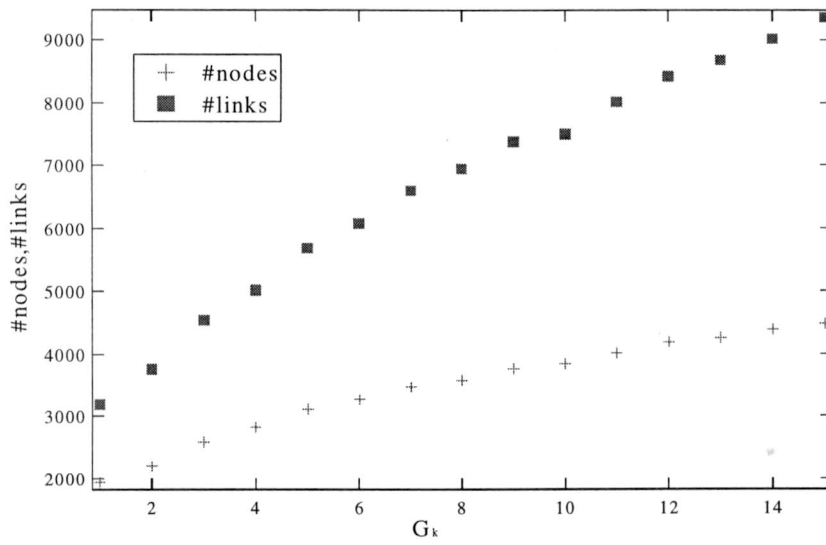


Figure 61. The distribution of the links and nodes (RIPE data)

Chapter 9. The link weight structure

In order to determine whether Internet traces satisfy a certain link weight structure, we have assigned polynomially-distributed link weights to each edges in G_1 . The simulation process can be described as follows (shown as Figure 49): the topology has been constructed based on G_1 of RIPE TTM data, and has been represented in the form of adjacency list. Further, different link weights have been assigned. Polynomial link weight distribution obeys

$$P[w \leq x] = x^\alpha 1_{0 \leq x \leq 1} + 1_{x \geq 1};$$

where a variety of values for exponent $\alpha = 0.05; 0.2; 0.5; 1; 2; 5; \infty$. has been chosen.

9.1 Simulation results

For each value of exponent α , the process of assigning link weight values in G_1 has been repeated 300 times. For each source-destination (t_i, t_j) pair and for each topology, the shortest path was computed using Dijkstra algorithm. Since it is possible to have several shortest paths for a (t_i, t_j) pair, a criterion for comparison of paths was the number of hops of paths. Each path determined via simulations has been compared to paths in the MySQL database, and the difference in the number of hops in those paths ($\Delta = h_{RIPE} - h_{SIM}$), as well as the total number of different links forming those paths are stored in a histogram. An example is given in the Figure 62, which shows a path returned by the RIPE traceroute and another one returned by shortest path. The difference in the number of hops in two paths is 0, because they have the same value of hopcount. However, as shown in the hop 8, because the IP packets of two paths pass different router, there are 4 different links in these two paths, totally.

#Hop	RIPE Traceroute	Shortest Path
0	2	2
1	51	51
2	52	52
3	53	53
4	54	54
5	55	55
6	56	56
7	57	57
8	70	58
9	59	59
10	60	60
11	61	61
12	7	7

Figure 62: the difference between RIPE traces and simulated shortest paths of tt2-tt7 pair

The corresponding probability density functions have been plotted on Figures 63 and 67, respectively. The mean and the standard deviation of the difference in hops in paths obtained from RIPE NCC and shortest paths determined via simulations $E[\Delta h]$ and $var[\Delta h]$ have been plotted on Figure 68. Figure 69 represents the mean and the standard deviation of the total number of different links in paths obtained from RIPE NCC and shortest paths determined via simulations. Figure 70 represents the alpha values of difference in hops ($E[\Delta h] / var[\Delta h]$) and that of different links ($E[\#different\ links] / var[\#different\ links]$).

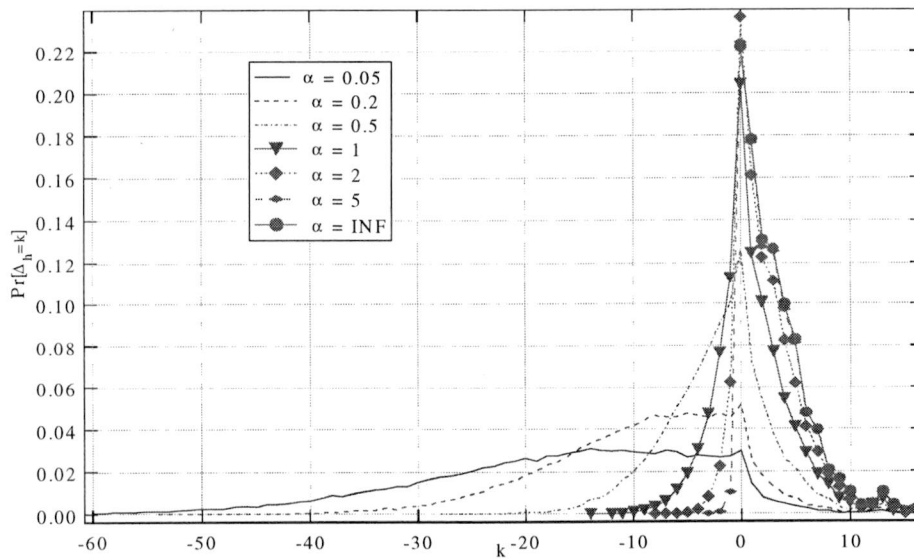


Figure 63. The probability density function of the different number of hops in RIPE traces and simulated shortest paths ($\Delta = h_{RIPE} - h_{SIM}$)

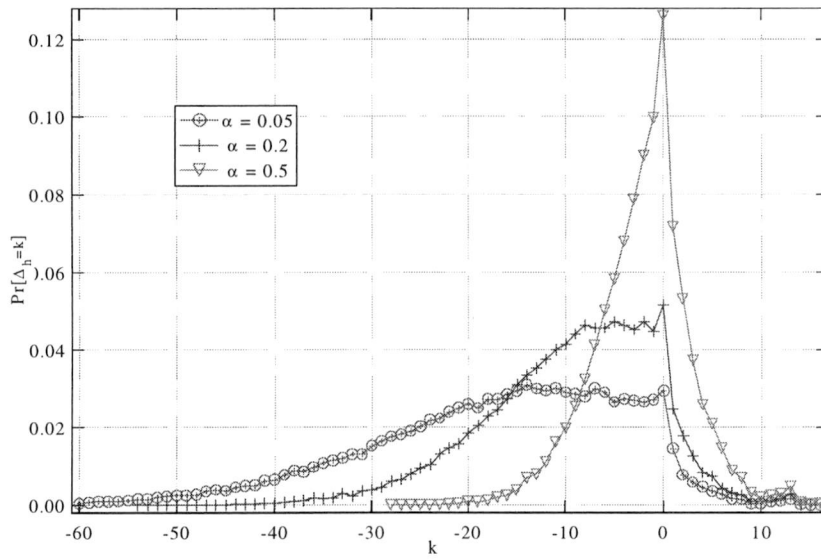


Figure 64. The probability density function of the different number of hops in RIPE traces and simulated shortest paths ($\Delta=h_{RIPE}-h_{SIM}$), ($\alpha=0.05,0.2, 0.5$)

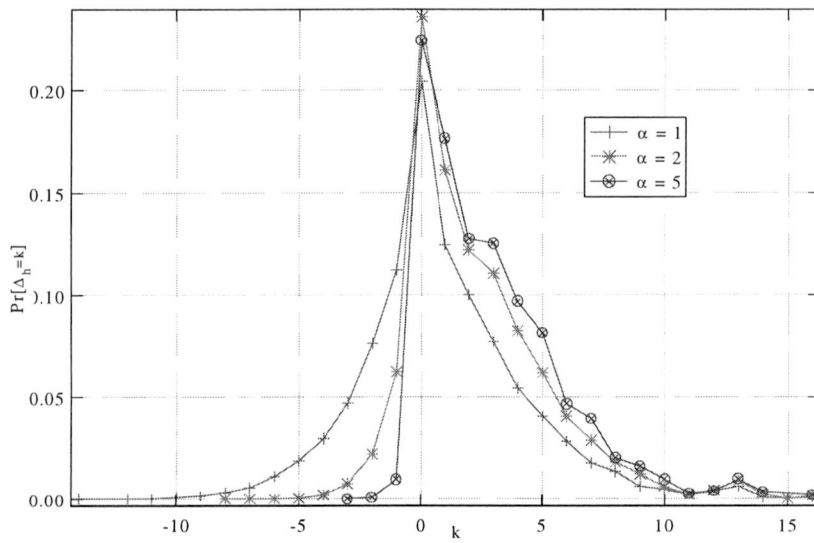


Figure 65. The probability density function of the different number of hops in RIPE traces and simulated shortest paths ($\Delta=h_{RIPE}-h_{SIM}$), ($\alpha=1,2,5$)

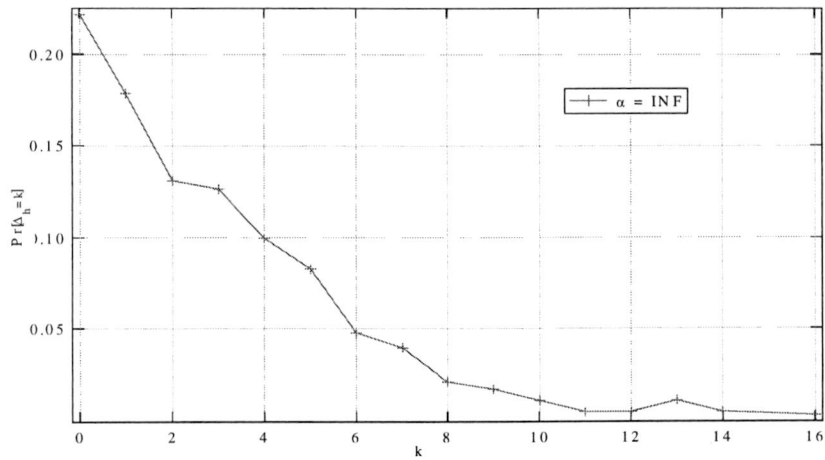


Figure 66 The probability density function of the different number of hops in RIPE traces and simulated shortest paths ($\Delta = h_{RIPE} - h_{SIM}$) ($\alpha = \infty$)

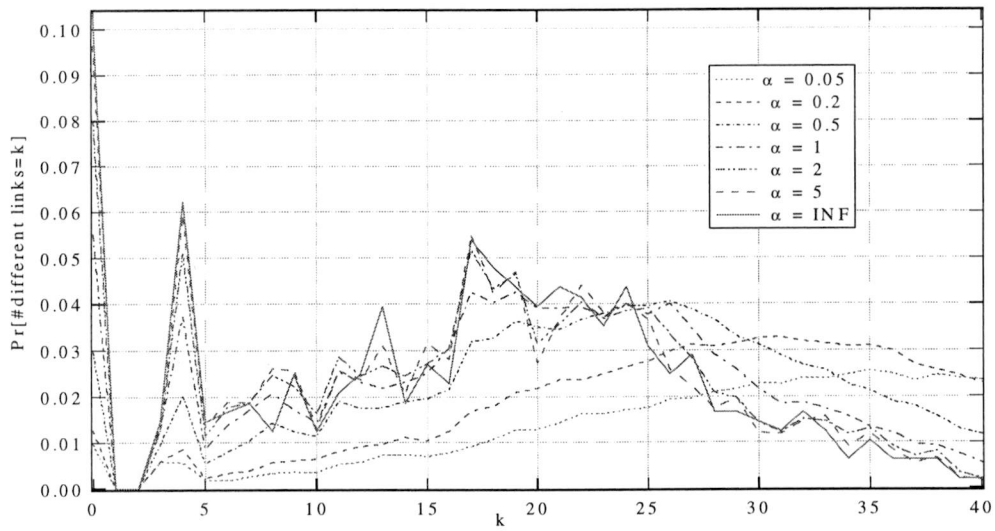


Figure 67. The probability density function of the total number of links in RIPE traces and simulated shortest paths

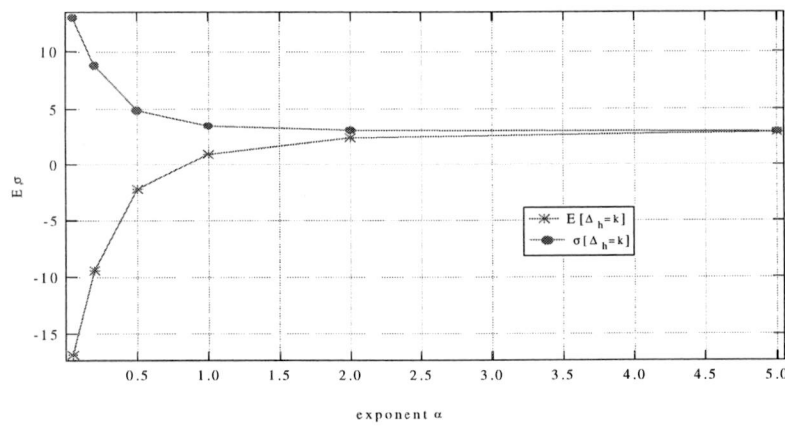


Figure 68. The mean and the standard deviation of the different number of hops

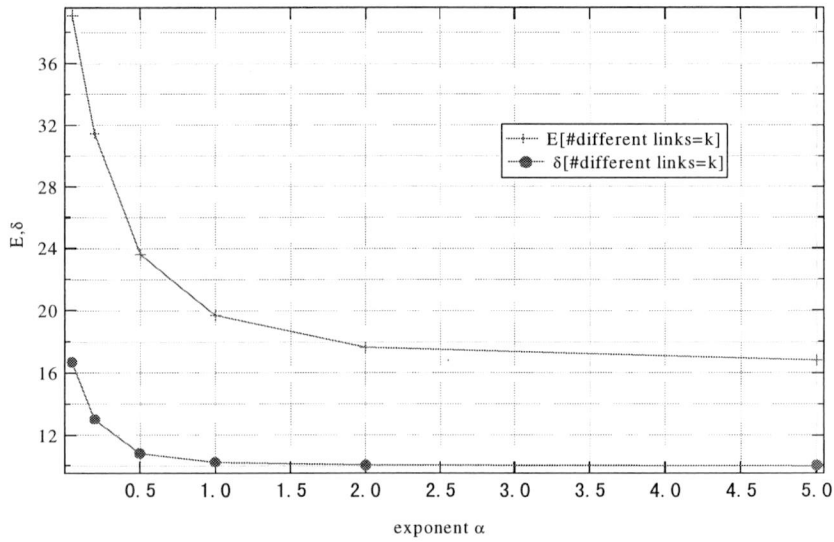


Figure 69. The mean and the standard deviation of the total number of different links in real and shortest path. δ

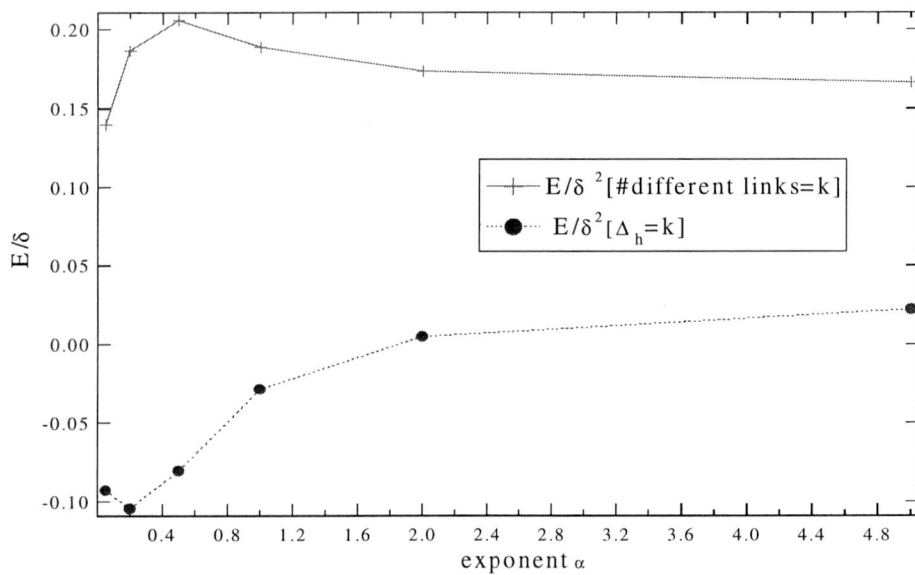


Figure 68 The alpha (mean/variance) of two above Figures

We observe from Figures 64-66 that the majority of paths obtained via simulations are different from those determined from RIPE TTM. The explanation lies in the fact that there can be several shortest paths for a (t_i, t_j) pair, and it is probable that router selects the different path than the one returned by Dijkstra algorithm.

Since Tangmunarunkit et al. investigated how both routing protocols and routing policies affect the paths on Internet [6], on Figure 37,38,39 we compared the results we obtained for

path inflation difference (different number of hops in RIPE traces and computed shortest paths) with results they published. We observe that these two functions are almost identical. The following Figure 71,72,73 shows the ratio $\alpha [\Delta h]$ between the traceroutes hopcount and that of the shortest path where link weights are equal to 1.

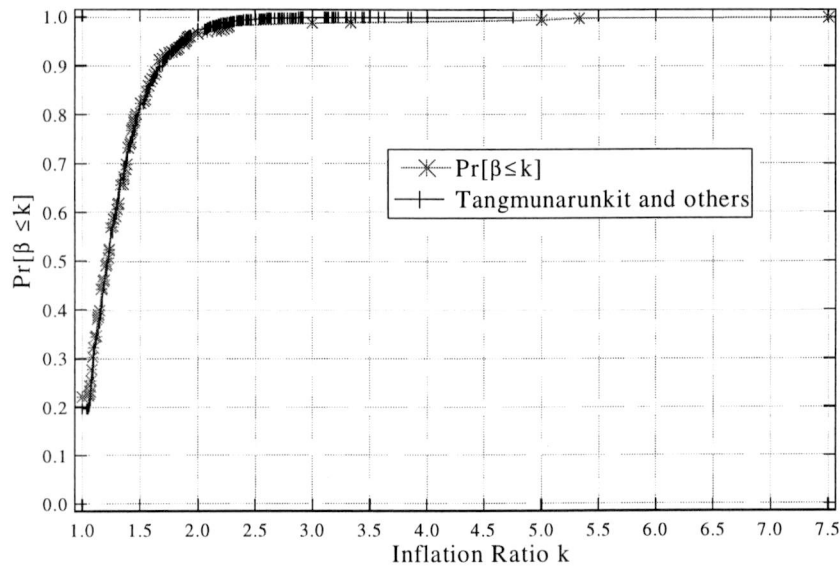


Figure 71: The comparison of cumulative probability functions of path inflation for RIPE traces and results of Tangmunarunkit et al.

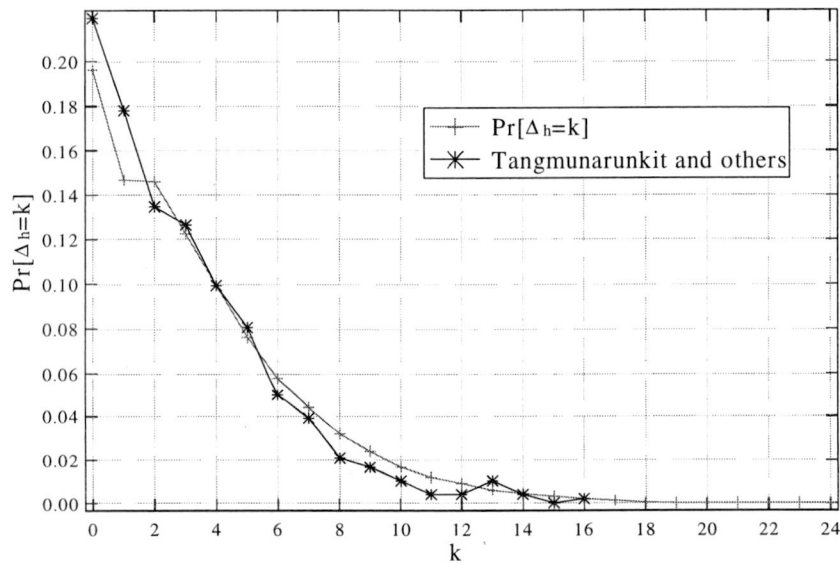


Figure 72. The comparison of probability density functions of path inflation for RIPE traces and results of Tangmunarunkit et al.

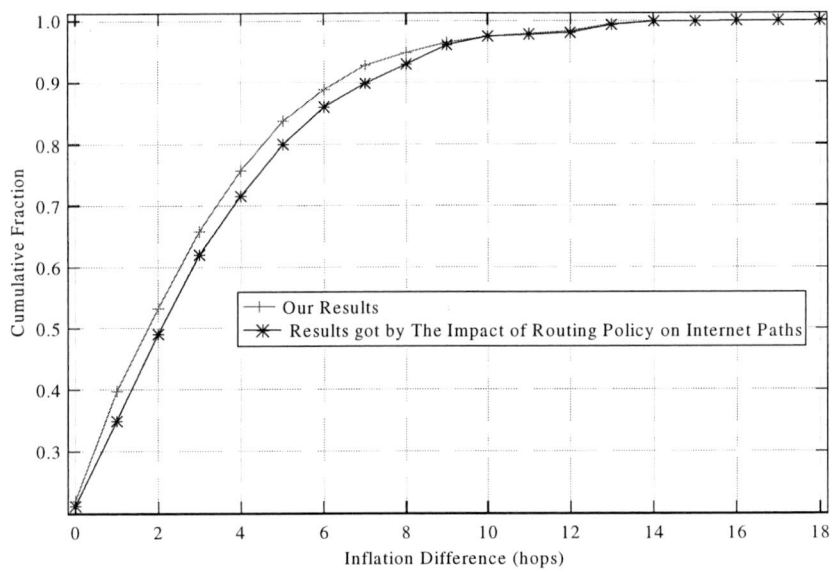


Figure 73. Cumulative distribution of inflation difference

No clear conclusions about the link weight structure can be deduced. But in the best case, where link weights are equal to 1, only 22% of the traceroutes correspond to shortest paths. Surprisingly, our result seems fit the results by Tangmunarunkit very well.

Chapter 10. Correlation

In this Chapter, we present results of short theoretical analysis on the number of times arbitrary node appears in a path on Internet, and we compare theoretical results with those obtained from measurement. We will show that they match each other remarkably reasonable, but remain argument.

10.1 Theory

Van Mieghem *et al* [1] have shown that the hopcount in topology models with constant and equal link weights doesn't fit data obtained from Internet satisfyingly, suggesting that the link weights on Internet vary significantly. It has also been shown that structured or regular graphs do not match the measurements as well. However, one model, random graphs of the class $G_p(N)$ [7] with N nodes, link density p and with exponentially or, with uniformly distributed link weights is demonstrated to describe the Internet hopcount properties well.

Same authors have proven in [1,8] that for the random graphs of the class $G_p(N)$, polynomially distributed link weights and when the number of nodes $N \rightarrow \infty$, the probability that the hopcount of the shortest path between two arbitrary nodes consists precisely of k hops is given with:

$$\Pr[h_N = k] \sim \frac{1}{N} \frac{(\ln \alpha N)^{\alpha k}}{\Gamma(\alpha k + 1)} \quad (10.1.1)$$

where k is the number of hops, and α is the coefficient in polynomial distribution function. In the case of $\alpha=1$, which is the special case of polynomial distribution analogous to the uniform distribution, the right-hand side of (10.1.1) equals the probability that a Poisson variable with parameter $(\ln N)$ equals k :

$$\Pr[h_N = k] \sim e^{-\ln N} (\ln N)^k / K! \quad (10.1.2)$$

This result will be used in the following Subchapter.

10.2 Derivation of mathematical expression

Let us assume that the source and destination are randomly chosen out of N nodes, and that all links in a route are independent of each other. If with $P_r[IPnode \in P]$ we denote the probability that a certain node with address $IPnode$ belongs to a path P , then for a large N , this probability can be expressed by the law of total probability:

$$\Pr[IPnode \in P] = \sum_{k=1}^{N-1} \Pr[IPnode \in P \mid h_N[P] = k] \Pr[h_N[P] = k] \quad (10.2.1)$$

Substituting (10.1.2) in (10.2.1), we obtain

$$\Pr[IPnode \in P] = \sum_{k=1}^{N-1} \frac{k+1}{N} \frac{(\ln N)^k}{k!N} \quad (10.2.2)$$

$$\Pr[IPnode \in P] \sim \frac{\ln N}{N} \quad (10.2.3)$$

Since there are totally r paths, with r given with

$$r = \binom{N}{2} = \frac{N(N-1)}{2}$$

the probability that a node denoted with $IPnode$ appeared in k paths becomes:

$$\Pr[IPnode = k] = \binom{\binom{N}{2}}{k} \Pr\left(\frac{\ln N}{N}\right)^k \left(1 - \frac{\ln N}{N}\right)^{r-k} \quad (10.2.4)$$

10.3 RIPE NCC data

The same probability $\Pr[IPnode = k]$ can also be computed from RIPE NCC data. The number of times each node in the graph constructed as described in Figure 73 appeared in most frequently occurring non-erroneous records for each pair (tt_i, tt_j) has been calculated, with the assumption that the routes are symmetrical (route for (tt_i, tt_j) pair the same as for (tt_j, tt_i)), but also for the case of asymmetrical routes. These values have been saved in a

histogram, from which the probability function could be deduced. Since the next step was to determine how good our mathematical expression fits the real data, for N ranging from 2000 to 5500 the difference in mathematical expression and RIPE data has been computed, and after several iteration, the minimum difference for $N \approx 3000$ has been determined (Figure 74)

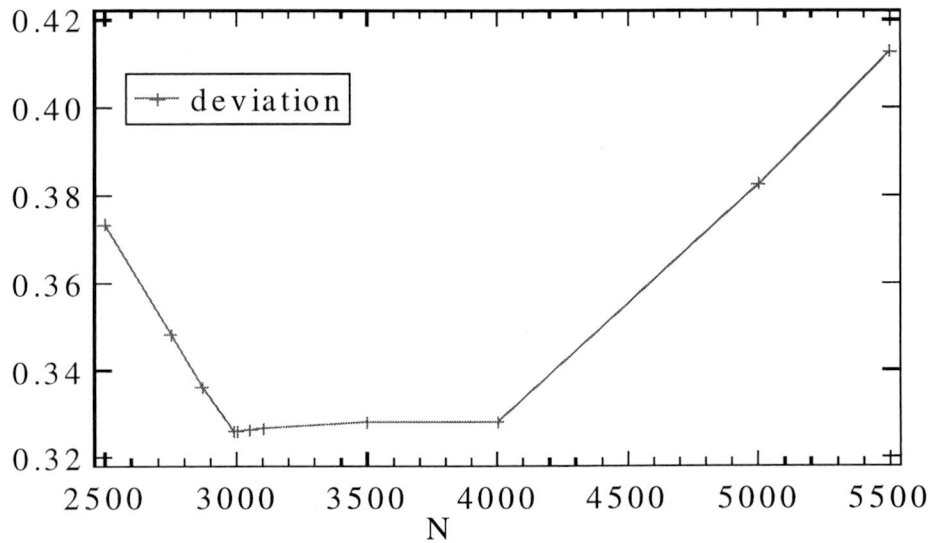


Figure 74. Fitting N for the minimum difference between real data and mathematic

Both functions obtained from measurements, together with the mathematically obtained expression, have been plotted on Figure 75.

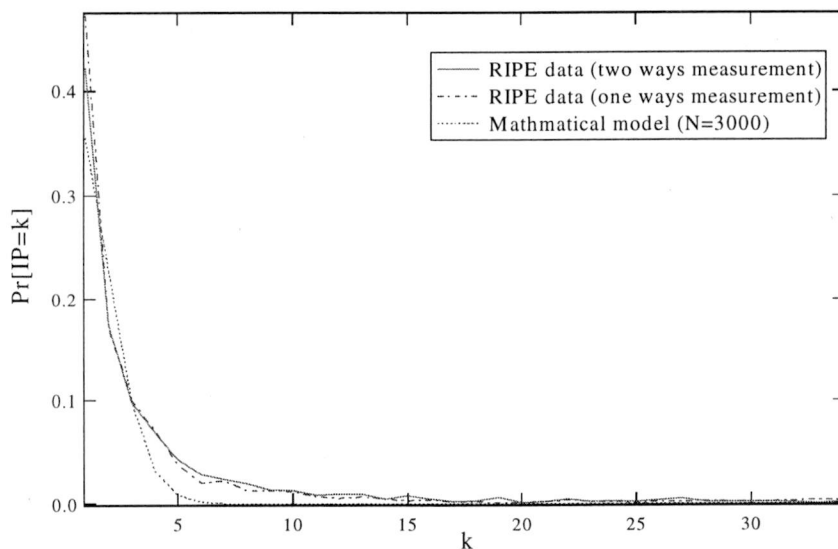


Figure 75: The probability density function of the number of appearances of an IP address in a Internet paths in linear scale

We notice that there exists large enough N ($N=3000$) for which the curve determined through mathematical computation approaches the curve obtained from the Internet.

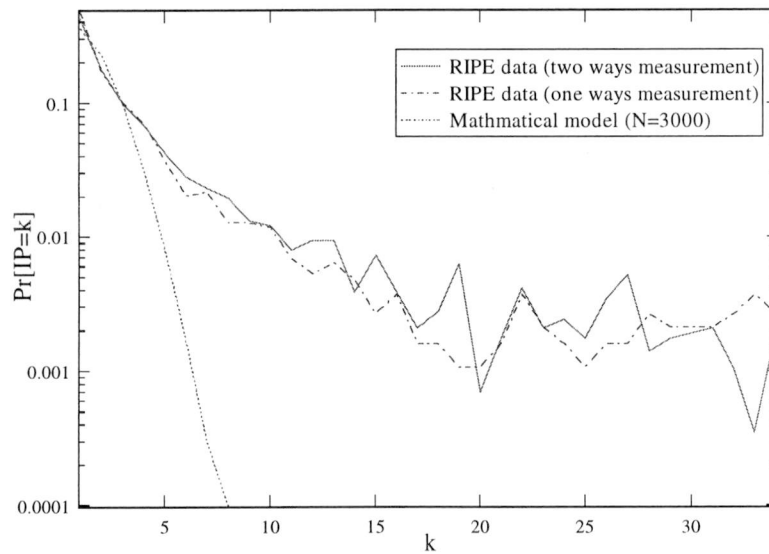


Figure 76. The probability density function of the number of appearances of an IP address in a Internet paths in logarithmic scale

However, the Figure 76 shows that the curve got from mathematical expression doesn't fit the curve got from RIPE data if k is large than 5. The detail behaviour clearly demonstrates that the assumption of independence does not apply.

Chapter 11. Conclusion and recommendation

In this project, the traceroutes from RIPE NCC measured between 31 test-boxes on March 2001 are analyzed in depth. We examined characteristics of real networking, mainly focused on the study of understanding which types of errors users can observe in the current Internet routing, and understanding the how current routing algorithms affect the behavior of Internet paths. Several of our results are worth emphasizing:

First, the analysis of the pathologies in path routing has shown that compared with results obtained by Paxson in 1995, the value of errors increased. And we may conclude that the quality of traceroute measurements seems to have decreased over time.

Second, the analysis of the different number of paths between a same source-destination pair has shown that (a) there are many paths existed and no path dominant others and (b) in those most frequently occurring non-erroneous paths, 99% of the paths are asymmetric.

Third, based on these non-erroneous paths, the class of graphs G_k consisting of the union of the k most frequently occurring paths per source-destination pair has been constructed. To each link of that graph, polynomially distributed link weights were assigned, and then compared to the corresponding traceroutes. No clear conclusions about the link weight structure can be deduced. But in the best case, where link weights are equal to 1, only 22% of the traceroutes correspond to shortest paths. Our result seems fit the results by Tangmunarunkit very well.

For the further research of this field, we make following recommendations.

If an authoritative hierarchy of Internet is known, the better picture of the routes packets take could be got. However, many questions should be analyzed, for examples, is the Internet growth exponential in time, and how can this be measured? What kind of graph that is a reasonable model for the Internet graph should be studied.

One of the topics this report did not cover was the connection between the hopcount and the delay. Intuitively, the more hops traversed, the higher the degradation in QoS qualifiers

(such as delay, jitter and packet loss). So it is a reach topic that is there any relation between the hopcount and the end-to-end delays.

Understanding traffic dynamics is helpful to build networks that can deliver high performance. In the study, load balancing should be further analyzed to determine which instabilities are due to load balancing versus true instabilities (say, a router is broken).

References:

- [1] P. Van Mieghem, G. Hooghiemstra and R. W. van der Hofstad, "*Scaling Law for the Hopcount*", Delft University of Technology, report2000125, 2000.
- [2] F. Georgatos, F. Gruber, D. Karrenberg, M. Santcroos, A. Susanj, H. Uijterwaal and R. Wilhem, "*Providing Active Measurements as a Regular Service for ISP's*", Proceedings of Passive and Active Measurements (PAM2001), Amsterdam, The Netherlands, April 23-24, pp.45-56,2001.
- [3] RIPE Test Traffic Measurements, <http://www.ripe.net/ripenc/mem-services/ttm/>
- [4] V.Paxson. "*End-to-end Routing Behavior in the Internet*", IEEE/ACM Transactions on Networking, 5(5): 601-615, October 1997
- [5] C. Faloutsos, P. Faloutsos, and M. Faloutsos. *What does the Internet Look Like? Empirical Laws of Internet Topology*. In *Proceeding of the ACM SIGCOMM*, September 1999.
- [6] H. Tangmunarunkit, R. Govindan, S. Shenker, and D. Estrin, "*The impact of routing policy on internet paths*", In Proceedings of IEEE INFOCOM'01, 2001.
- [7] B. Bollobas, "*Random Graphs*", Cambridge University Press, second edition, 2001.
- [8] R. Van der Hofstad, G. Hooghiemstra and P. Van Mieghem, "*First Passage Percolation on the Random Graph*", Probability in the Engineering and Informational Sciences (PEIS), vol. 15, pp. 225-237, 2001.
- [9] B. Chinoy, "*Dynamics of Internet Routing Information*", In Proceedings of the ACM SIGCOMM '94, San Francisco, 1993.
- [10] C. Labowitz, G. R. Malan and F. Jahanian, "*Internet Routing Stability*", In Proceedings of the ACM SIGCOMM '97, Cannes, 1997.
- [11] V. Paxson, "*End-to-end Internet Packet Dynamics*", In Proceedings of the ACM SIGCOMM '97
- [12] S. Savage, A. Collins, E. Hoffman, J. Snell and T. Anderson, "*The End-to-End Effects of Internet path Selection*", in Proceedings of ACM SIGCOMM '99, Boston, September 1999.
- [13] M.Lottor. (Oct. 1989). Available FTP: <ftp://nic.merit.edu/nsfnet/statistics>

- [14] W.Richard Stevens. *TCP/IP Illustrated*, volume 1, The Protocols. Addison-Wesley, Reading, Massachusetts, 1994.
- [15] M. Abramovitz and I.A. Stegun, "*Handbook on Mathematical Functions*" Dover Publications, Inc., N.Y.,1968
- [16] Piet Van Mieghem, "*Advances in Networking*", Delft University of Technology Publications, Inc., Delft, 2000.
- [17] Begtasevic, F. and P. Van Mieghem, 2001, "*Measurements of the Hopcount in Internet*", Proceedings of Passive and Active Measurement (PAM2001), Amsterdam, The Netherlands, April 23-24, pp. 183-190

Appendix A Pathologies in the Internet

Table A.1 summarizes the routing pathologies we analyzed in this report, and moreover, we would like to compare the results with those got by Paxson in 1995. The difference shows the quality change of the Internet in recent years.

	<i>Unresponsive routers</i>	<i>Persistent routing loops</i>	<i>Temporary routing loops/percentage led by unknown IP address</i>		<i>Infrastructure failure</i>	<i>Maximum Probability Of errors</i>	<i>Total paths records</i>
<i>Paxson[3]</i>	<i>0.00-0.53%</i>	<i>0.13-0.16%</i>	<i>0.055-0.078%</i>	<i>/</i>	<i>0.16%±0.44%</i>	<i>1.21%</i>	<i>40000</i>
<i>RIPE TTM Ist dominant routing</i>	<i>0.86%</i>	<i>0.2%</i>	<i>7.53%</i>	<i>60%</i>	<i>7.96%</i>	<i>16.55%</i>	<i>461703</i>
<i>2nd</i>	<i>0.86%</i>	<i>0.65%</i>	<i>5.38%</i>	<i>56%</i>	<i>7.31%</i>	<i>14.2%</i>	<i>422295</i>
<i>3rd</i>	<i>0.86%</i>	<i>1.29%</i>	<i>6.45%</i>	<i>66.7%</i>	<i>6.67%</i>	<i>15.27%</i>	<i>294699</i>
<i>4th</i>	<i>0.86%</i>	<i>1.72%</i>	<i>5.81%</i>	<i>48.15%</i>	<i>5.81%</i>	<i>14.2%</i>	<i>261942</i>
<i>5th</i>	<i>1.08%</i>	<i>1.29%</i>	<i>6.24%</i>	<i>68.97%</i>	<i>7.96%</i>	<i>16.57%</i>	<i>204858</i>
<i>6th</i>	<i>1.51%</i>	<i>3.01%</i>	<i>7.53%</i>	<i>72.22%</i>	<i>7.53%</i>	<i>19.58%</i>	<i>185218</i>
<i>7th</i>	<i>1.94%</i>	<i>2.37%</i>	<i>8.82%</i>	<i>65.85%</i>	<i>7.96%</i>	<i>20.99%</i>	<i>162320</i>
<i>8th</i>	<i>2.15%</i>	<i>2.15%</i>	<i>8.82%</i>	<i>68.29%</i>	<i>7.74%</i>	<i>20.86%</i>	<i>151346</i>

Table A.1. Comparison the probabilities of some pathologies got by Paxson and RIPE TTM

The maximum probability of user-visible pathologies in RIPE TTM is 21%, which indicates the poor quality of current Internet.

In chapter A.1, introduction of all acceptable test boxes is given. In chapter A.2, the methodology of selecting sample nodes is shown. Finally, in chapter A.3, proof of table A.1 is described in details.

A.1 Introduction

The total number of acceptable test boxes analysed in our study are 31. The acceptable test boxes are listed as:

tt—1,2,3,4,7,8,12,13,14,15,16,17,19,20,21,22,23,25,26,27,31,32,34,35,

36,39,40,41,42,44,46

Each decimal number has its corresponding IP address, more details could be checked in the [3].

A.2 Sample nodes

In the project, the routing paths between some special nodes met pathologies frequently. After removing those boxes from our records, 31 tests boxes were chosen for the analysis. In the following, selecting mythology is given in details.

a. Some test boxes have no record in RIPE TTM databases. The boxes numbers are 5,6,9,18,24,29,30,33,37,38,43,45,48,50

b. Some test boxes are removed for special reasons:

Removed test box: tt10 reason: the Traceroutes always meet these errors:
Persistent loops

Removed test box: tt11 reason: The traceroutes always meet these errors:
Destination is an Unknown address

Removed test box: tt28 reason: The traceroutes always meet these errors:
Temporary Loops

Removed test box: tt47, tt49 reason: The traceroutes always meet these errors:
Persistent loops, Temporary Loops, Destination is an Unknown address

c. So there are only 31 test boxes for the project

d. For each Source-Destination Pairs, there is no guarantee that IP packets will follow a same way. So in the MySQL database, two tables (Figure A.1) record all the routing of S-D pairs. Table 1 gives some routing vectors (routeid in table 1) for each unique combination of IP-addresses seen between the source test box and the destination test box and the count of the each routing vector recorded by the database. The table 2 contains IP-address of each router that appeared in the routing vector and the length of the Traceroute.

```

mysql> SELECT routeid,COUNT(*)
AS count FROM Records WHERE
src=1 AND dst=18 GROUP BY
routeid ORDER BY count DESC;
+-----+-----+
| routeid | count |
+-----+-----+
| 5 | 1255 |
| 25 | 1250 |
| 63712 | 671 |
| 63679 | 670 |
| 7980 | 541 |
| 19503 | 540 |
| 1290 | 40 |
| 16017 | 10 |
| 62260 | 8 |
| 62262 | 7 |
| 1281 | 1 |
| 140632 | 1 |
| 1298 | 1 |
| 1304 | 1 |
| 1348 | 1 |
| 16015 | 1 |
| 16550 | 1 |
| 32920 | 1 |
| 131678 | 1 |
+-----+-----+
19 rows in set (0.11 sec)

```

Table 1

```

mysql> SELECT len,route FROM Routes WHERE ID= 5;
+-----+-----+-----+-----+-----+-----+
| len | route
+-----+-----+-----+-----+-----+-----+
| 5 | 3238002702 3238002738 3238002932 3247705900 3285074646 |
+-----+-----+-----+-----+-----+-----+
1 row in set (0.04 sec)

```

Table 2

```

mysql> SELECT len,route FROM Routes WHERE ID= 25;
+-----+-----+-----+-----+-----+-----+
| len | route
+-----+-----+-----+-----+-----+-----+
| 5 | 3238002702 3238002742 3238002932 3247705900 3285074646 |
+-----+-----+-----+-----+-----+-----+
1 row in set (0.00 sec)

```

```

mysql> SELECT len,route FROM Routes WHERE ID= 63712;
+-----+-----+-----+-----+-----+-----+
| len | route
+-----+-----+-----+-----+-----+-----+
| 10 | 3238002702 3238002738 3238002932 3247705890 2435385229 |
2435383377 3556884657 3556884994 3285074666 3285074646 |
+-----+-----+-----+-----+-----+-----+
1 row in set (0.00 sec)

```

Figure A.1 Tables in the MySQL database

A.3 The errors in the first 10 most frequently occurring paths

1. The most frequently occurring paths

In those 31 test boxes, even to the most frequently occurring paths for each source-destination (S-D) pairs, there is no guarantee that all the Traceroutes records are “correct”-- each correct Traceroute does not meet these 3 types of errors: Unknown address, routing loops and the end node of the Traceroute is not the expected Destination.

P.S. Analysis the pathology in the most frequently occurring paths for each Source-destination pairs

- a. The value of total expected paths= $31 \times 30 / 2 = 465$
- b. The number of Unresponsive routers=5, and the probability of Unresponsive routers= $4 / 465 = 0.86\%$

Those unresponsive S-D pairs: tt3->25, 27,42; tt26->27

Here is an example that we queried the Traceroutes records from MySQL databases from tt3 to tt25

```

mysql> SELECT routeid,COUNT(*) AS count FROM Records WHERE src=3 AND dst=25
GROUP BY routeid ORDER BY count DESC;
Empty set (0.00 sec)

```

c. The Number of Infrusture Failure=37, and the probability of Infrusture Failure= $37/465=7.96\%$

d. The number of Routing Loops

d.1 there is 1 Persistent Loops-from tt19 to tt26, probability=0.2%

d.2 there are 35 Temporary Loops, and the probability of Temporary Loops= $35/465=7.53\%$. Among these 35 Temporary Loops, 21 are led by Unknown IP Address (defined as 255.255.255.255), and the probability is= $(21/35=60\%)$

1.1 Conclusion:

a. The total number of counts of the most frequently occurring paths=461703;

b. Out of all the frequently occurring paths, the total probability of correct paths = $1-0.86\%-7.96\%-0.2\%-7.53\%=83.45\%$

2. The 2nd frequently occurring paths for each source-destination (S-D) pairs.

P.S. Analysis the pathology in the most frequently occurring paths for each source-destination pairs

a. The value of total expected paths= $31*30/2=465$

b. The number of Unresponsive routers=4, and the probability of Unresponsive routers= $4/465=0.86\%$

Those unresponsive S-D pairs: tt3->25, 27,42; tt4->13; tt26->27

c. The Number of Infrusture Failure=34, and the probability of Infrusture Failure= $34/465=7.31\%$

d. The number of Routing Loops

d.1 there is 3 Persistent Loops-from 2—3; 19—26 and 19--32, probability=0.65%

d.2 there are 33 Temporary Loops, and the probability of Temporary Loops= $25/465=5.38\%$. Among these 25 Temporary Loops, 14 are led by Unknown IP Address (defined as 255.255.255.255), and the probability is= $(14/25=56\%)$

2.1 Conclusion:

a. The total number of counts of the most frequently occurring paths=422295;

b. Out of all the frequently occurring paths, the total probability of correct paths = $1 - 0.86\% - 7.31\% - 0.65\% - 5.38\% = 85.8\%$

3. The 3rd frequently occurring paths for each source-destination (S-D) pairs.

P.S. Analysis the pathology in the most frequently occurring paths for each Source-destination pairs

a. The value of total expected paths = $31 * 30 / 2 = 465$

b. The number of Unresponsive routers = 4, and the probability of Unresponsive routers = $4 / 465 = 0.86\%$

Those unresponsive S-D pairs: tt3->25, 27,42; tt26->27

c. The Number of Infrastructure Failure = 31, and the probability of Infrastructure failure = $31 / 465 = 6.67\%$

d. The number of Routing Loops

d.1 there is 6 Persistent Loops-from 1--3;1--4;19--22;19--26;19--40;26--35; probability = 1.29%

d.2 there are 30 Temporary Loops, and the probability of Temporary Loops = $30 / 465 = 6.45\%$. Among these 30 Temporary Loops, 20 are led by Unknown IP Address (defined as 255.255.255.255), and the probability is = $(20 / 30 = 66.7\%)$

3.1 Conclusion:

a. The total number of counts of the most frequently occurring paths = 294699;

b. Out of all the frequently occurring paths, the total probability of correct paths = $1 - 0.86\% - 6.67\% - 1.29\% - 6.45\% = 84.73\%$

4. The 4th frequently occurring paths for each source-destination (S-D) pairs.

P.S. Analysis the pathology in the most frequently occurring paths for each source-destination pairs

a. The value of total expected paths = $31 * 30 / 2 = 465$

b. The number of Unresponsive routers = 4, and the probability of Unresponsive routers = $4 / 465 = 0.86\%$

Those unresponsive S-D pairs: tt3->25, 27,42; tt26->27

c. The Number of Infrastructure Failure=27, and the probability of Infrastructure Failure= $27/465=5.81\%$

d. The number of Routing Loops

d.1 there is 8 Persistent Loops-from 3--4;3--13;19--22;19--26;19--40;26--39;39--46;41--46;probability= $8/465=1.72\%$

d.2 there are 27 Temporary Loops, and the probability of Temporary Loops= $27/465=5.81\%$. Among these 27 Temporary Loops, 13 are led by Unknown IP Address (defined as 255.255.255.255), and the probability is= $(13/27=48.15\%)$

4.1 Conclusion:

a. The total number of counts of the most frequently occurring paths=261942;

b. Out of all the frequently occurring paths, the total probability of correct paths = $1-0.86\%-5.81\%-1.72\%-5.81\%=85.8\%$

5. The 5th frequently occurring paths for each source-destination (S-D) pairs.

P.S. Analysis the pathology in the most frequently occurring paths for each source-destination pairs

a. The value of total expected paths= $31*30/2=465$

b. The number of Unresponsive routers=5, and the probability of Unresponsive routers= $5/465=1.08\%$

Those unresponsive S-D pairs: tt3->4,25, 27,42; tt26->27

c. The Number of Infrastructure Failure=37, and the probability of Infrastructure Failure= $27/465=7.96\%$

d. The number of Routing Loops

d.1 there is 6 Persistent Loops-from 2--4;13--42;19--23;21--46;26--35;39--46;probability= $6/465=1.29\%$

d.2 there are 29 Temporary Loops, and the probability of Temporary Loops= $29/465=6.24\%$. Among these 29 Temporary Loops, 20 are led by Unknown IP Address (defined as 255.255.255.255), and the probability is= $(20/29=68.97\%)$

5.1 Conclusion:

- a. The total number of counts of the most frequently occurring paths=204858;
- b. Out of all the frequently occurring paths, the total probability of correct paths =1-1.08%-7.96%-1.29%-6.24%=83.43%

6. The 6th frequently occurring paths for each source-destination (S-D) pairs.

P.S. Analysis the pathology in the most frequently occurring paths for each source-destination pairs

- a. The value of total expected paths= $31*30/2=465$
- b. The number of Unresponsive routers=7, and the probability of Unresponsive routers= $7/465=1.51\%$

Those unresponsive S-D pairs: tt2->3; tt3->4,25, 27,42; tt26->27,42;

- c. The Number of Infrusture Failure=35, and the probability of Infrusture Failure= $35/465=7.53\%$

d. The number of Routing Loops

d.1 there is 14 Persistent

Loops-7--12;7--46;8--46;13--42;16--46;19--21;19--23;19--41;19--44;21--46;26--46;35--46;39--46;41--46;probability= $14/465=3.01\%$

d.2 there are 36 Temporary Loops, and the probability of Temporary Loops= $35/465=7.53\%$. Among these 36 Temporary Loops, 26 are led by Unknown IP Address (defined as 255.255.255.255), and the probability is= $(26/36=72.22\%)$

6.1 Conclusion:

- a. The total number of counts of the most frequently occurring paths=185218;
- b. Out of all the frequently occurring paths, the total probability of correct paths =1-1.51%-7.53%-3.01%-7.53%=80.42%

7. The 7th frequently occurring paths for each source-destination (S-D) pairs.

P.S. Analysis the pathology in the most frequently occurring paths for each source-destination pairs

- a. The value of total expected paths= $31*30/2=465$

b. The number of Unresponsive routers=9, and the probability of Unresponsive routers= $9/465=1.94\%$

Those unresponsive S-D pairs: tt2->3; tt3->4,25, 27,42; tt7-25; tt25->26; tt26->27,42;

c. The Number of Infrusture Failure=37, and the probability of Infrusture Failure= $37/465=7.96\%$

d. The number of Routing Loops

d.1 there is 11 Persistent Loops; 3—35; 7—46; 8—46; 12—46; 16—46; 19—21; 19—22; 19—41; 19—44; 20—35; 35—46; probability= $11/465=2.37\%$

d.2 there are 41 Temporary Loops, and the probability of Temporary Loops= $41/465=8.82\%$. Among these 41 Temporary Loops, 27 are led by Unknown IP Address (defined as 255.255.255.255), and the probability is= $(27/41=65.85\%)$

7.1 Conclusion:

a. The total number of counts of the most frequently occurring paths=162320;

b. Out of all the frequently occurring paths, the total probability of correct paths = $1-1.84\%-7.96\%-2.37\%-8.82\%=79.01\%$

8. The 8th frequently occurring paths for each source-destination (S-D) pairs.

P.S. Analysis the pathology in the most frequently occurring paths for each source-destination pairs

a. The value of total expected paths= $31*30/2=465$

b. The number of Unresponsive routers=10, and the probability of Unresponsive routers= $10/465=2.15\%$

Those unresponsive S-D pairs:

c. The Number of Infrusture Failure=36, and the probability of Infrusture Failure= $36/465=7.74\%$

d. The number of Routing Loops

d.1 there is 10 Persistent Loops; 2—14; 7—35; 7—46; 8—35; 8—46; 12—46; 16—46; 26—46; 35—46; and 36—46; probability= $11/465=2.15\%$

d.2 there are 41 Temporary Loops, and the probability of Temporary Loops= $41/465=8.82\%$. Among these 41 Temporary Loops, 28 are led by Unknown IP Address (defined as 255.255.255.255), and the probability is= $(27/41=68.29\%)$

8.1 Conclusion:

a. The total number of counts of the most frequently occurring paths=151346;

b. Out of all the frequently occurring paths, the total probability of correct paths = $1 - 2.15\% - 7.74\% - 2.15\% - 8.82\% = 79.14\%$

Appendix B The hierarchy of RIPE traceroute

B.1 Introduction

The very name of Internet is perhaps come from the idea of interconnected networks. Internet is continuous changing overtime, and one of the greatest things about the Internet is that nobody really owns it. It is a global collection of networks, both big and small. So how to reasonably describe the Internet is a difficult thing. These networks connect together in many different ways to form the single entity that we know as the Internet.

Totally, there are 2 ways to measure the networking, the first way is the passive measurement by monitoring the amount of traffic that passes a certain point, and another way is the active measurement by generating test traffic and measuring how much time it takes to ship the test traffic over the network. The traceroute utility [14] is popular in the active measurements because it is the most direct method to obtain information about the paths on Internet. The goal of TTM project is to do independent Internet active measurements of connectivity parameters, such as delays and routing-vectors, using test traffic generated by test-boxes.

B.2 Simulation results of the hierarchy of RIPE traceroute

In the study of constructing the graph G_1 by only the most frequently occurring non-erroneous paths, the hierarchy returned by RIPE traceroute are analysed and 5 examples of hierarchies are shown.

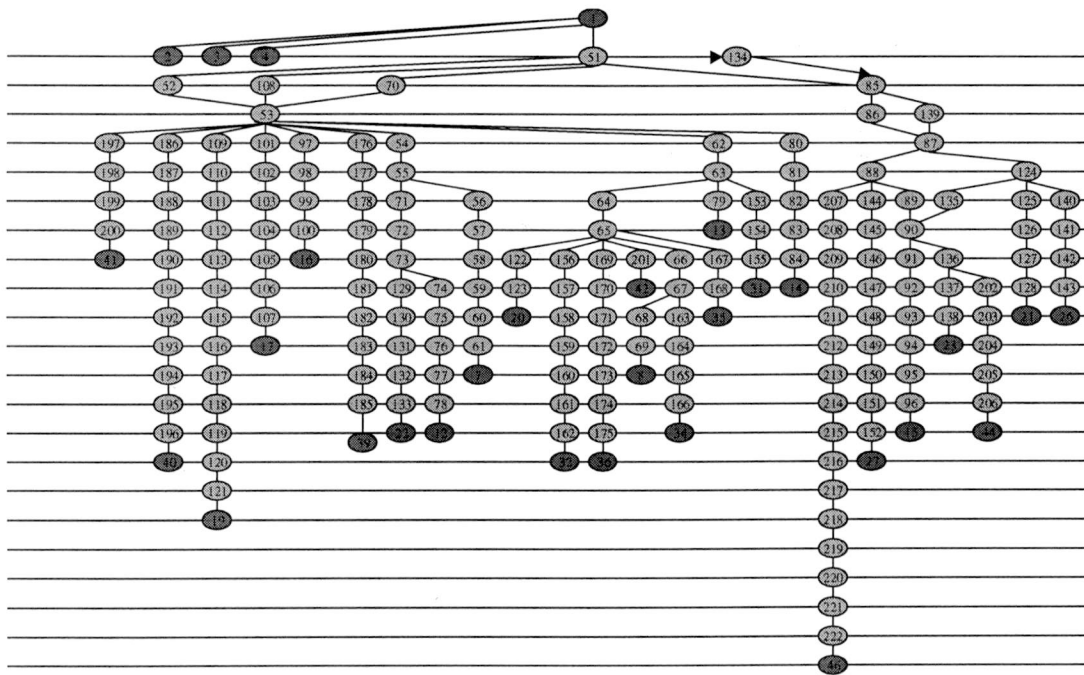


Figure B.1 a part of the hierarchy of RIPE traceroute (1)

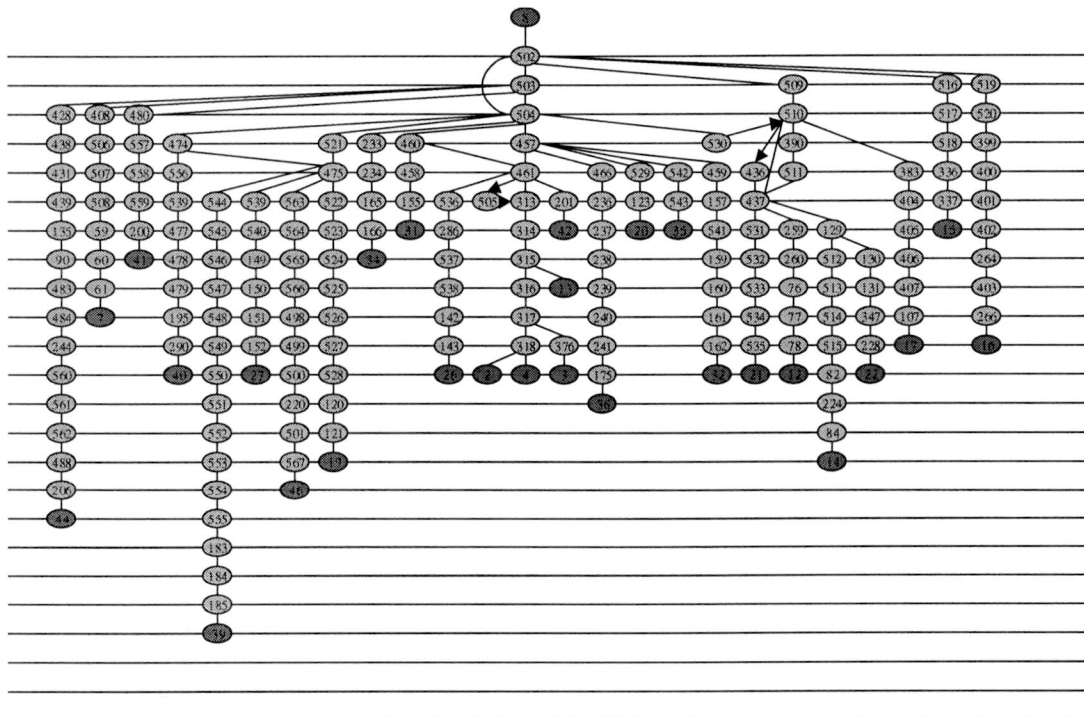


Figure B.2 a part of the hierarchy of RIPE traceroute (2)

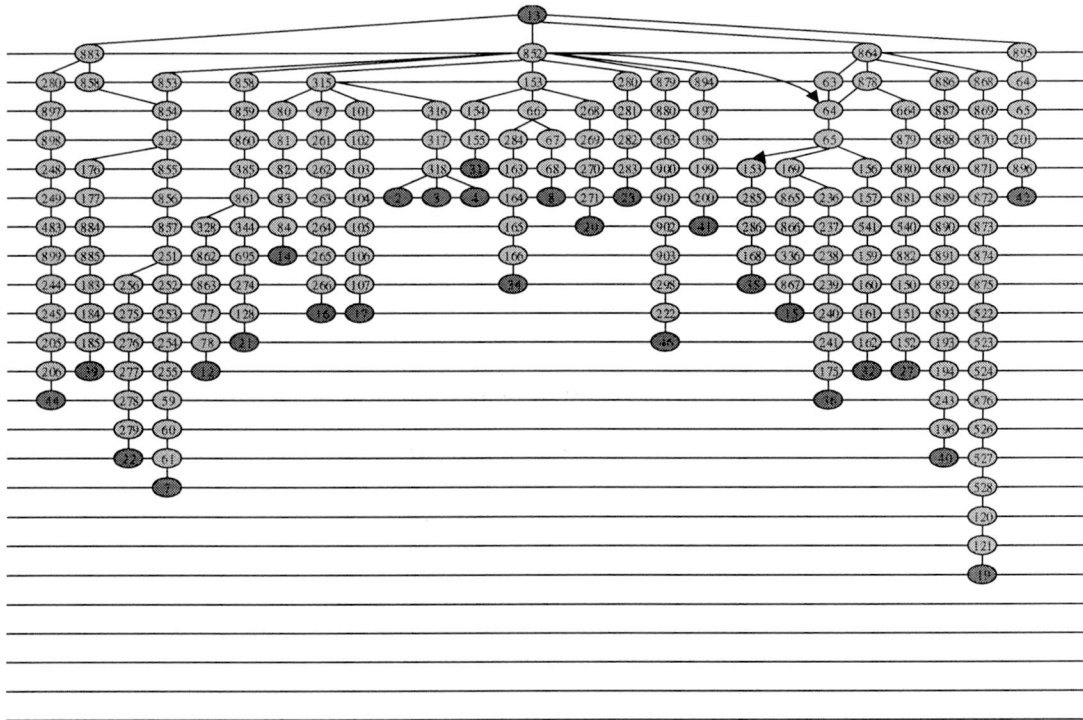


Figure B.3 a part of the hierarchy of RIPE traceroute (3)

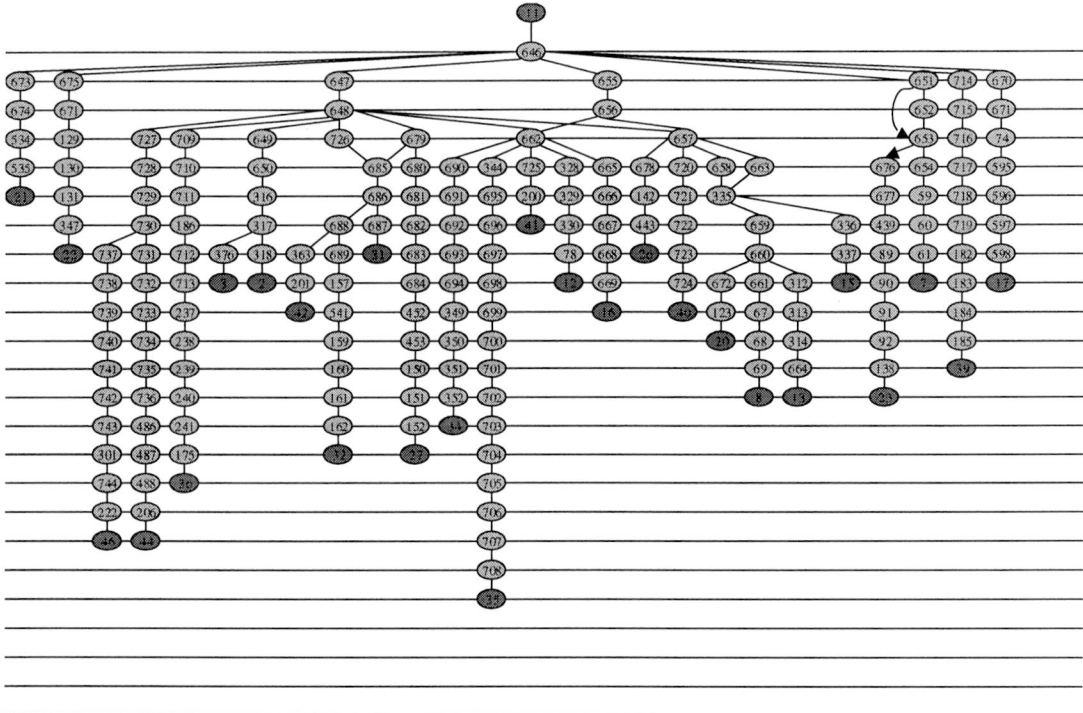


Figure B.4 a part of the hierarchy of RIPE traceroute (4)

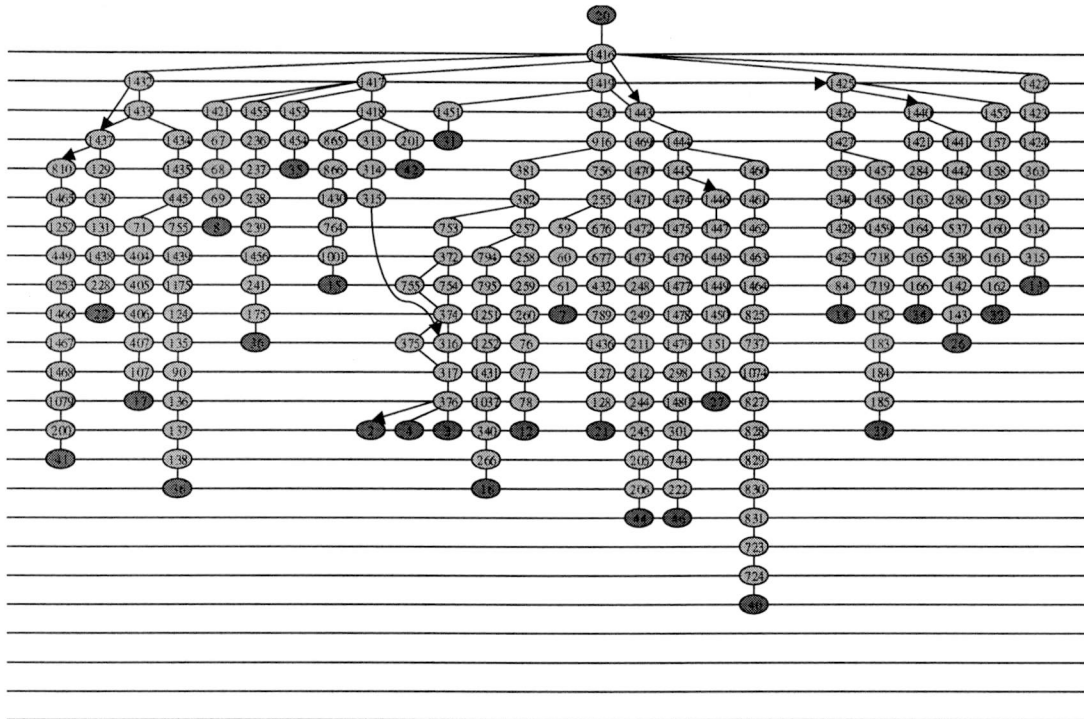


Figure B.5 a part of the hierarchy of RIPE traceroute (5)

However, to completely understand the hierarchy of Internet is a hard job. If an authoritative hierarchy of Internet is known, the better picture of the routes packets take could be got.

However, many questions are necessary to be analyzed, for examples, is the Internet growth exponential in time, and how can this be measured? What kind of graph that is a reasonable model for the Internet graph should be studied.

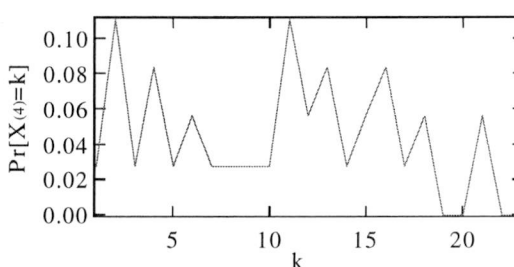
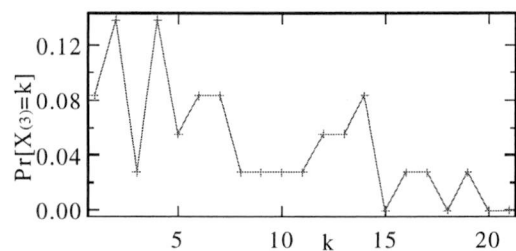
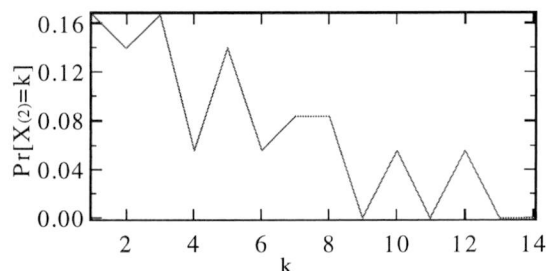
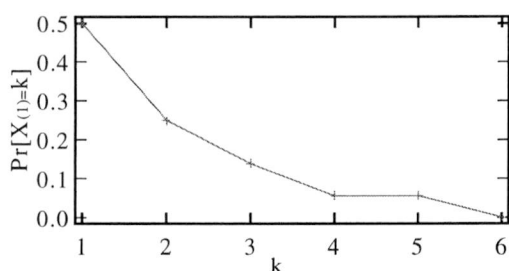
Appendix C The output degree of hierarchy level from RIPE TTM

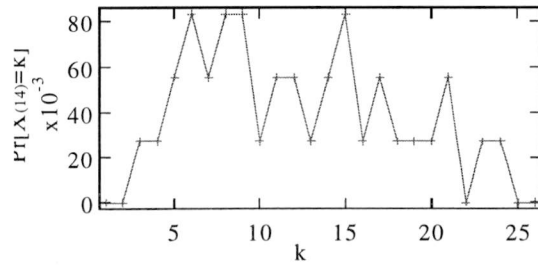
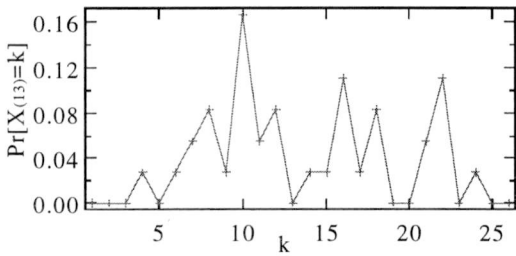
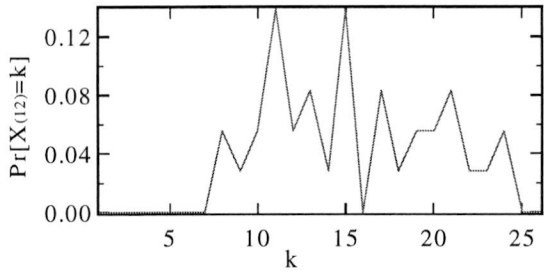
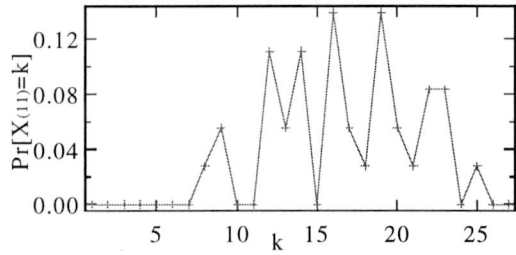
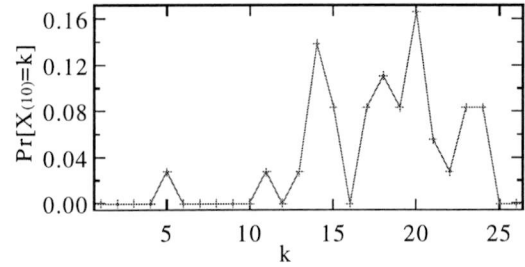
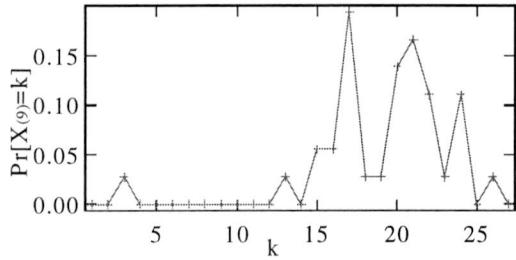
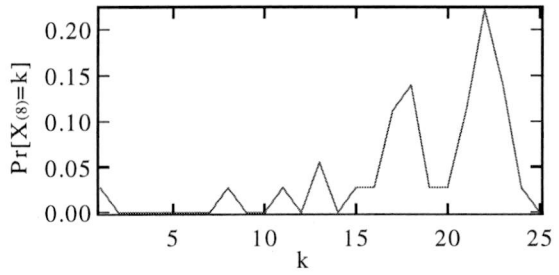
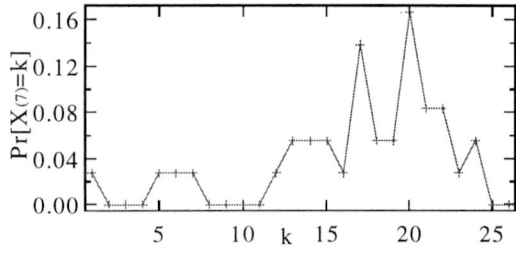
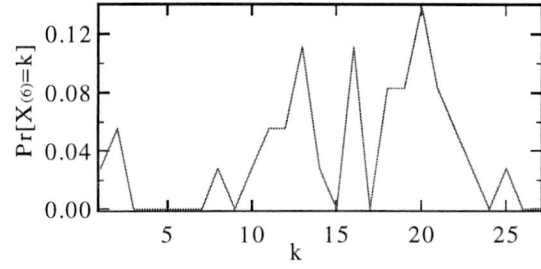
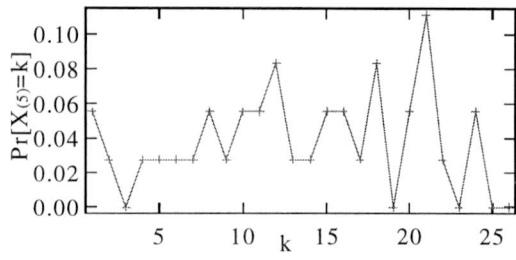
C.1 Introduction

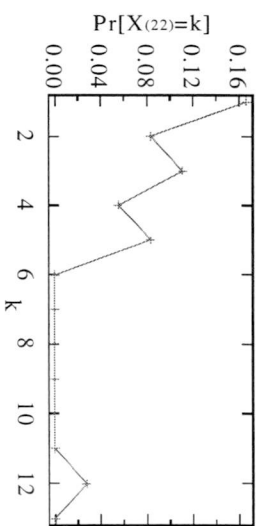
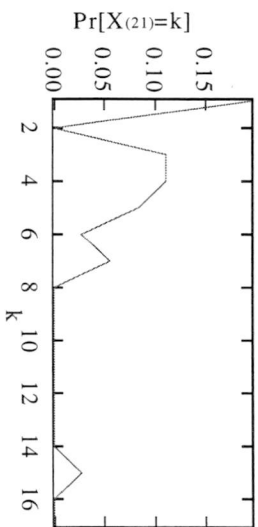
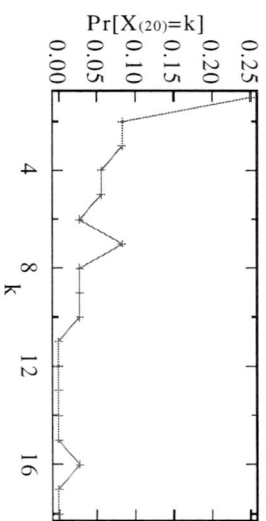
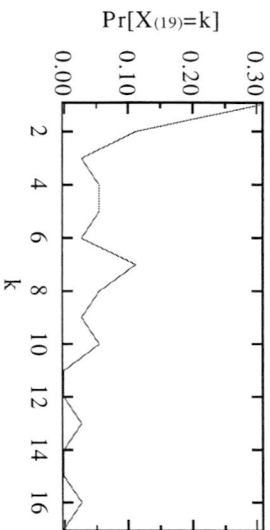
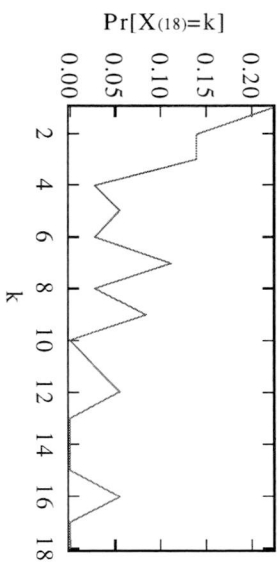
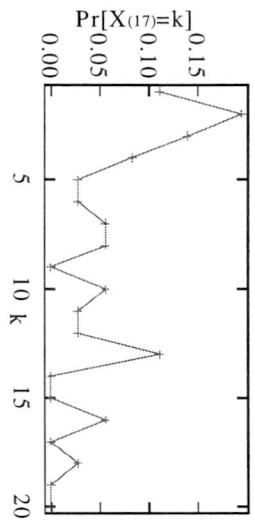
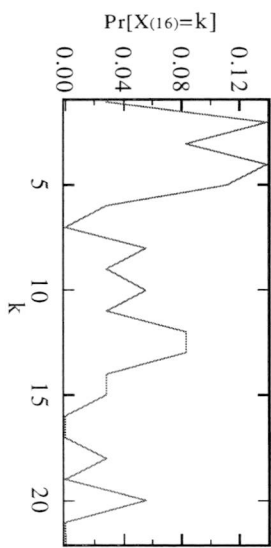
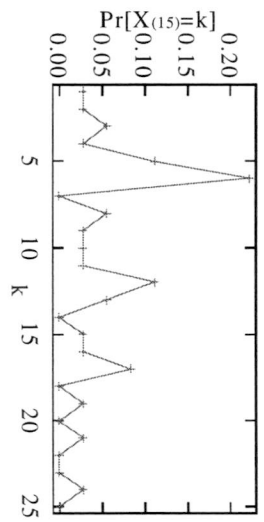
In the past years, many researches were carried out to characterize various aspects of Internet topology. Some arguments are that for some real topologies, the size of node neighborhoods grows exponentially with distance. And others argued that these real topologies could be described using power-laws [20]. This arguments encourage us to analyze the output of degree of each hierarchy level from RIPE TTM.

C.2 Simulation results

In the study of constructing the graph G_1 by only the most frequently occurring non-erroneous paths, the degree output of each hierarchy level returned by RIPE traceroute is analyzed and all the results are shown in the following Figures.







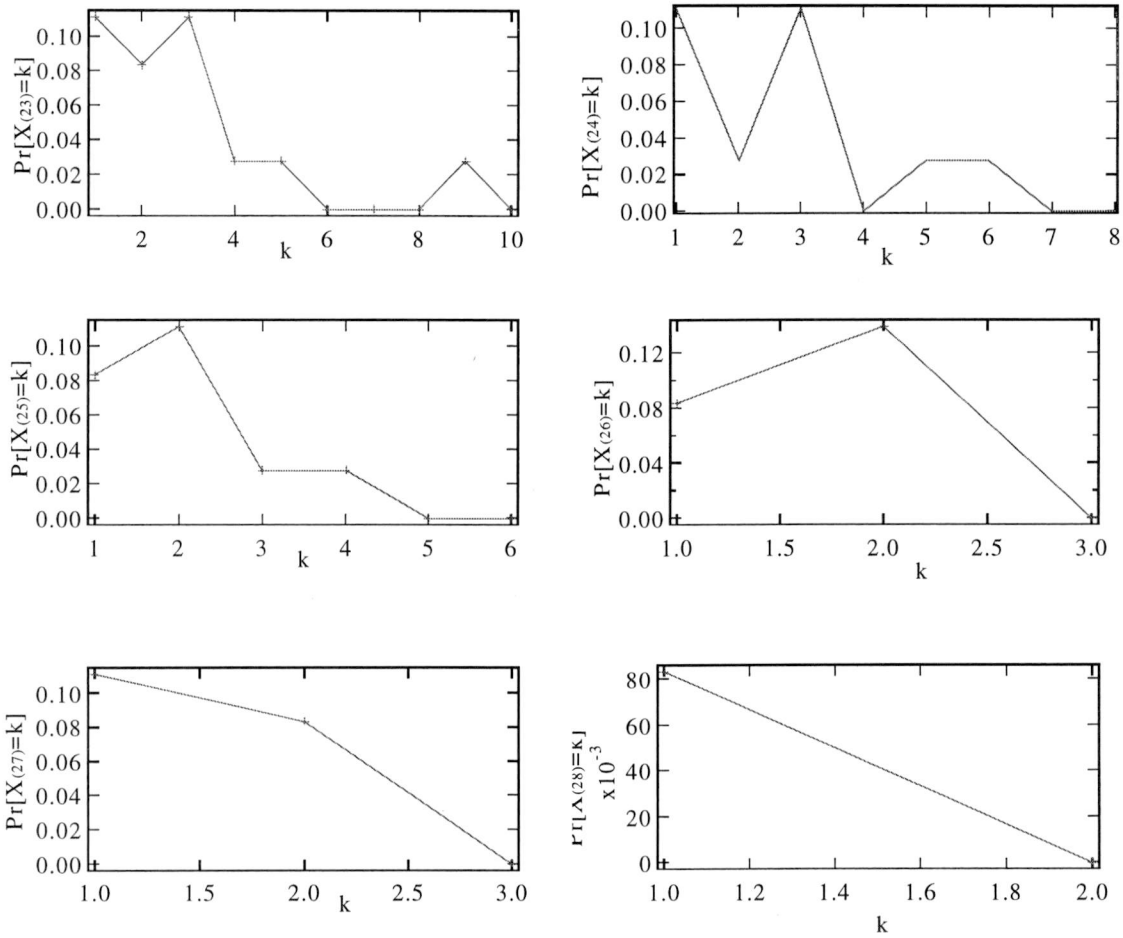


Figure C.1 The degree output of each hierarchy level in RIPE TTM

We cannot make some conclusions about these Figures because of the time limitation of the project, but it is another interesting topic for the future research.